# ABSTRACT


Title of Dissertation: METAL-MEDIATED ACTIVATION OF HYDROGEN PEROXIDE AND DIOXYGEN BY COPPER COMPLEXES IN AQUEOUS SOLUTION

Qing Zhu, Doctor of Philosophy, 2007

Dissertation Directed By: Professor Neil V. Blough
Department of Chemistry and Biochemistry

Dinuclear Cu(II) complexes $[Cu^{II}_2(\mathbf{N_n})Y_2]^{2+}$ (n=4, $Y = ClO_4^-$; n = 5, $Y = NO_3^-$) ($\mathbf{N_n}$ = $-(CH_2)_n-$ (n = 3-5) linked bis[2-(2-pyridyl)ethyl]amine) were recently found to cleave DNA specifically in the presence of a reducing thiol and $O_2$ or in the presence of $H_2O_2$ alone. However, a closely-related $[Cu^{II}_2(\mathbf{N_3})Y]^{2+}$ (n = 3, $Y = ClO_4^-$) and their mononuclear analogue, $[Cu^{II}(MePY_2)(CH_3CN)(ClO_4^-)]^{1+}$ ($MePY_2$ = bis[2-(2-pyridyl)ethyl]methylamine), exhibited no selective cleavage under either condition. To clarify the nature of the intermediate(s) involved in cleavage, the reactivity of these copper complexes was investigated in aqueous solutions.

Spectroscopic studies indicated that an intermediate with an absorption band at 376 nm was generated either from $[Cu^{II}_2(\mathbf{N_{4,5}})Y_2]^{2+}$ in the presence of $H_2O_2$ or from its corresponding Cu(I) complexes in the presence of $O_2$. Formation of this intermediate was pH, phosphate and temperature dependent. This intermediate decayed exponentially at room temperature with concomitant degradation of ligand. Its decay was temperature dependent, but was independent of $H_2O_2$ concentration and a series of added electron donors. This intermediate was not formed with $[Cu^{II}_2(\mathbf{N_3})Y_2]^{2+}$ and its corresponding

Cu(I) complex, and only formed with mononuclear Cu(II) complex under high concentrations of $H_2O_2$ and the copper complex. A highly sensitive method was employed to test for the formation of reactive species produced during the intermediate decay. Methyl radical was detected in the presence of either DMSO or methane. The relative yield of methyl radical from DMSO and methane confirmed unequivocally the involvement of hydroxyl radical. The stoichiometry of hydroxyl radical production with respect to the concentration of the intermediate was 1:1 for both $[Cu^{II}_2(\mathbf{N_{4,5}})Y_2]^{2+}$ and mononuclear Cu(II) complex.

Our results suggested that this intermediate is most likely a Cu(II)(hydro)peroxo complex, of as yet, unknown structure, which decays through a rate-limiting intramolecular electron transfer from the ligand to the metal peroxo center thereby producing a hydroxyl radical and a ligand-based radical. The results also imply that DNA cleavage does not result from direct reaction with a metal-peroxo intermediate, but instead arises from reaction with either the hydroxyl radical or ligand-based radicals.

# METAL-MEDIATED ACTIVATION OF HYDROGEN PEROXIDE AND DIOXYGEN BY COPPER COMPLEXES IN AQUEOUS SOLUTION

By

Qing Zhu

Dissertation submitted to the Faculty and the Graduate School of the
University of Maryland, College Park, in partial fulfillment
of the requirements for the degree of
Doctor of Philosophy
2007

Advisory Committee:
Professor Neil V. Blough, Chair/Advisor
Professor Michael A. Coplan
Professor Steven Rokita
Professor Kenneth D. Karlin
Professor Douglas English

## DEDICATION

To my family

# ACKNOWLEDGEMENTS

First of all, I sincerely thank my advisor Dr. Neil V. Blough for his guidance, patience, encouragement, and support throughout this period of study. I have learned not only a lot of knowledge but also methods of solving problems from him, which is greatly helpful for my future research career.

I sincerely thank Dr. Micheal A. Coplan for his continual advice, encouragement and support. His kindness, consideration and help always make me feel warm. I would like to thank Dr. Steven Rokita for his advice and help in this work. I also want to thank Dr. Kenneth D. Karlin and Dr. Douglas English for their guidance and assistance.

I would like to thank the Blough group members, Rossana, Nixon, Daqing, Yu, Marjan, Pramila, Min and Lynne, for their friendship and help during my graduate study.

I would like to thank Yuxiang, Lian and Lei Li for their help in this work.

I sincerely thank my family. Thank you, my beloved parents, for taking care of my daughter and letting me concentrate on my study over these years. Your endless love and encouragement kept me going. Thank you, my dear sister and brother in law, for your love and help. Finally, a lot of thanks go to my lovely daughter, Qianqian Zhou, and my husband, Shenghu Zhou. Thank you for always loving, understanding and supporting me.

# Table of Contents

# List of Schemes

# List of Tables

# List of Figures

## List of Abbreviations

| | |
|---|---|
| 3-ap | 3-amino-2,2,5,5-teramethyl-1-pyrrolidinyloxy |
| BLM | bleomycins |
| CAT | catalase |
| $D^1$ | dinucleating ligand with two tris(2-pyridylmethyl)amine units covalently linked in their 5-pyridyl positions by $–CH_2CH_2-$ bridge |
| DMA | N,N-dimethyl aniline |
| DMPO | 5,5-dimethyl-pyrroline N-oxide |
| DMSO | dimethyl sulfoxide |
| DTNB | 5,5'-dithiobis(2-nitrobenzoic acid) |
| EDTA | ethylenediamine tetraacetic acid |
| EPR | electron paramagnetic resonance spectroscopy |
| GSH | reduced glutathione |
| HPLC | high performance liquid chromatography |
| L | 2,2',2''-tris(dipicolylamino)triethylamine |
| $MePY_2$ | bis[2-(2-pyridyl)ethyl]methylamine |
| 3-MPA | 3-mercaptopropionic acid |
| NADH | reduced nicotinamide adenine dinucleotide |
| NADPH | reduced nicotinamide adenine dinucleotide phosphate |
| $N_n$ | $-(CH_2)_n-$ (n = 3-5) linked bis[2-(2-pyridyl)ethyl]amine |
| OH | hydroxyl radical |
| 2-OH-BA | 2-hydroxy benzoic acid |

| | |
|---|---|
| 3-OH-BA | 3-hydroxy benzoic acid |
| 4-OH-BA | 4-hydroxy benzoic acid |
| OP | 1.10-phenanthroline |
| ROS | Reactive oxygen species |
| RSH | alkyl thiol |
| TMPA | tris(2-pyridylmethyl)amine |

# Chapter I Introduction

## 1.1 Introduction

Over the past several decades, numerous studies have indicated that the DNA damage initiated by oxidative reactions may contribute to mutagenesis, carcinogenesis, aging, inherited diseases, and cell death. Oxidative damage to DNA can occur to the purine/pyrimidine bases and/or to the deoxyribose sugar through ionizing radiation,[1-3] photooxidation, [4-6] hydroperoxide activation by transition metals,[7, 8] hydroxyl radicals[9, 10] or various other oxidizing species. Oxidative base modification is believed to cause mutations in DNA, and many base modification products resulting from DNA oxidation have been identified. [11] Damage to deoxyribose via hydrogen atom abstraction often leads to breaks in single or double strand DNA, potentially inducing lethal lesions.

During the past two decades, DNA cleavage mediated by transition metal complexes has received significant attention, with a great deal of effort devoted to this area due to its enormous potential applications in biology and in the development of pharmaceuticals.[12-16] One goal of this research is to design and synthesize transition metal complexes that can specifically recognize and cleave DNA so that they can be developed as therapeutic agents or tools for probing the structure of these macromolecules. Obviously, a thorough understanding of the mechanism of DNA cleavage is essential for the rational design and synthesis of the transition metal complexes endowed with appropriate redox properties and DNA affinity. In addition, knowledge of the mechanism is important for interpreting cleavage patterns, and thus the structures of biomolecules. One of the key aspects is characterization of the intermediate(s) responsible for DNA cleavage. Studies on the

nature of the intermediate(s) can provide important information about the specificity of the DNA cleavage and the distribution of the degradation products that are produced.

DNA cleavage by transition metal complexes usually requires 1) a redox-active coordination complex 2) a reducing agent such as ascorbate or thiols and 3) the presence of dioxygen or hydrogen peroxide. The variable oxidation state of transition metals enables them to be efficient catalysts of reactions involving oxidation and reduction. It is commonly believed that DNA strand breakage is initiated by a DNA radical generated by a hydrogen atom abstraction, characteristic of radical reactions. Reactive oxygen species (ROS), a collective term including not only the oxygen radicals ( $O_2^{-\bullet}$ and •OH) but also some non-radical derivatives of $O_2$ ($H_2O_2$ and singlet $O_2$), have been proposed as reactive intermediate responsible for DNA strand breakage. Since $O_2^{-\bullet}$ and $H_2O_2$ have been shown not to directly produce strand cleavage or base modification at physiological concentrations,[17] the more reactive and oxidizing species, hydroxyl radical, is believed to be responsible for the oxidative cleavage of DNA. The possible reactions and radical intermediates produced upon the reaction of dioxygen with the reduced transition metal complexes in aqueous solutions are summarized in Scheme 1.1.[18]

$M^{n+1} + RSH \longrightarrow M^{n+1}\text{-}SR + H^+$ 1.1

$M^{n+1}\text{-}SR \longrightarrow M^{n+} + RS\bullet$ 1.2

$M^{n+} + O_2 \longrightarrow M^{n+1} + O_2^{-\bullet}$ 1.3

$2O_2^{-\bullet} + 2H^+ \longrightarrow H_2O_2 + O_2$ 1.4

$H_2O_2 + M^{n+} \longrightarrow \bullet OH + OH^- + M^{n+1}$ Fenton or Fenton-like Reaction 1.5

$RS\bullet + RS\bullet \longrightarrow RSSR$ 1.6

$\bullet OH + DNA \longrightarrow$ Strand Scission 1.7

**Scheme 1.1 Basic free radical mechanism for metal-mediated DNA cleavage**

As shown in Scheme 1.1, the metal ion in its higher oxidation state is first reduced by a reductant, such as an alkyl thiol (RSH). Superoxide ($O_2^{-\bullet}$) is then generated by one electron transfer from the reduced metal ion to $O_2$. Rapid disproportionation of superoxide in the presence of a proton source thus yields hydrogen peroxide ($H_2O_2$) and $O_2$. The reduced metal ion then reacts with hydrogen peroxide to produce the hydroxyl radical via the Fenton or a Fenton-like reaction (Equation 1.5). Hydroxyl radicals react with DNA and can lead to DNA chain scission and base oxidation.

Although a number of studies have implicated hydroxyl radical in the initial oxidation,[19-21] other work suggests the involvement of metal-based oxidants.[22-26] Considerable debate regarding the nature of the reactive intermediate(s) responsible for DNA cleavage still exists. In fact, many factors can affect the formation and nature of the intermediates. The disagreement on the nature of the reactive intermediates is a reflection of the complexity of the possible reaction pathways as in the following sections.

Oxidizing species generated via the Fenton or Fenton-like reactions are commonly believed to initiate oxidative damage of DNA, but the exact nature of the predominant oxidizing species is still an open question. In fact, the Fenton or Fenton-like reactions are much more complicated than that represented by the Equation 1.5. Both radical and non-radical pathways may be operative depending on the reaction conditions (Scheme 1.2).[27-30] The Fenton or Fenton-like reactions are believed to be initiated through an inner sphere coordination of peroxide to the reduced metal, thereby producing metal-peroxo complexes ($Fe^{II}$-OOH [30, 31] and $Cu^{I}$-OOH [24]), potentially leading to hydroxyl radical formation or formation of high-valent metal species (($Fe^{IV}O)^{2+}$ [32-35] and ($Cu^{III}O)^{+}$ [36, 37]). However, demonstrating the involvement of high-valent metal-based oxidants is often very difficult. Unequivocal evidence for their existence in aqueous solutions has not been found except for Fe-porphyrins. The presence of these oxidants is usually deduced indirectly by a reactivity profile that differs from the hydroxyl radical.

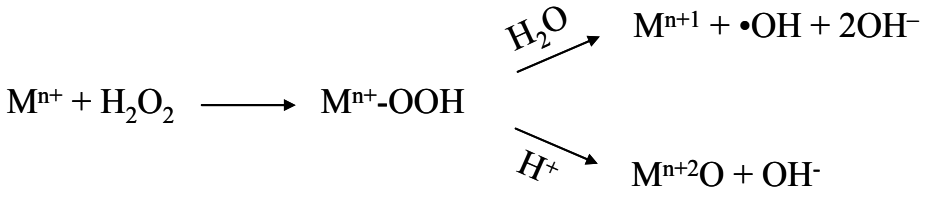


**Scheme 1.2 Radical pathway and non-radical pathway of Fenton-like reactions**

Although little direct evidence for the involvement of metal-based oxidants has been obtained for aqueous systems, some observations do suggest their existence. Many studies have indicated that hydroxyl radical scavengers do not always protect DNA from the damage. Studies also indicate that there is little correlation between the inhibitory effect of hydroxyl radical scavengers and the rate constants for their reactions with the

hydroxyl radical.[38] In addition, high site specificity exhibited by some DNA cleavage reactions is not expected from the reaction between DNA and the hydroxyl radical, a well-known indiscriminate oxidizing species.[39-41] Therefore, the metal-based oxidants responsible for DNA cleavage seem to be a more reasonable explanation for the afore-mentioned observations. However, some workers proposed that site-specific reaction between hydroxyl radical and DNA may also result in the inability of the scavengers to protect DNA.[42-44] Metal ions can efficiently bind to DNA due to the electrostatic interaction between positively charged metal ions and negatively charged phosphate groups in DNA. The binding of metal ion to DNA leads to the local generation of the hydroxyl radical, producing site specific DNA damage prior to diffusion of the hydroxyl radical into bulk solution. Further, scavenger-derived radicals can themselves cause DNA damage and make the protection inefficient. Radicals derived from formate, 2-propanol and glycerol were also found to cause single-strand breaks in DNA.[45] The inconsistency between the inhibitory effect and the rate constants of reactions between free hydroxyl radical and scavengers also can be explained as due to the different affinities of the scavengers to DNA. Unfortunately, the detection methods currently employed cannot differentiate free hydroxyl radicals from the metal-based oxidants unequivocally.

The nature of the intermediate that is generated is often dependent upon the ligands coordinating the central metal ion. The electron donating properties of ligands can alter the reduction potential of the metal and thus change the reactivity with DNA. For example, the standard reduction potential ($E^0$) of iron varies from -0.4 V to 0.12 V depending on the nature of the ligand which binds the iron.[46] An appropriate ligand may effectively stabilize the intermediate and favor its formation. For example, evidence for

the formation of Fe(IV) species in aqueous solution has been very difficult to obtain, but the formation of haem-associated ferry species are well established.[47] Moreover, the coordination geometry in some complexes may also favor the formation of a metal based oxidant by limiting the sites on the metal to which $O_2$ or $H_2O_2$ might coordinate. Coordination to metal by ligands can also alter the interaction between metal and DNA. Many studies have indicated that both coordination geometry and the ligand donor atom type play a key role in determining the mode and extent of binding of complexes to DNA.[20] Some metal coordination complexes undergo specific binding interaction with DNA. Therefore, site specificity of DNA cleavage does not necessarily mean that the intermediate is a selective oxidant. It might also be an overall reflection of the oxidizing properties of the intermediate and the interaction between the metal complex and DNA. Because metal complexes, reaction conditions and detection methods are different from study to study, it is often very difficult to reach an accordant conclusion on the nature of the oxidizing species.

The reducing agent employed may be another important factor in the DNA cleavage reactions. Commonly-used reducing agents in DNA cleavage experiments, such as ascorbate, thiols and reduced nicotinamide adenine dinucleotide (NADH), might also coordinate with the metal centers in the complexes. Although many studies have indicated that DNA cleavage patterns are independent of the type of the reductant, suggesting that common reactive intermediates are formed in the presence of different types of the reductant,[48, 49] the ratio of the reducing agent to the metal complex and binding constants of the reducing agent to metal ion are critical in some cases. When the reductant concentration is high or when a reductant with high affinity for the metal center

is employed, competitive binding between the ligand and the reductant may alter the speciation of the metal complex.[50, 51] Further, other reaction conditions, such as type of buffer, concentration of buffer and pH, may also affect the speciation of the metal complex, altering the nature of the oxidizing intermediate.

Several studies have shown that dioxygen or reductants are not necessary for DNA degradation for some systems. For example, DNA cleavage was detected in a Cu(II)-glutathione system under anaerobic conditions, and both superoxide dismutase and catalase could not inhibit the damage.[52] Although no direct evidence was provided to verify that DNA cleavage resulted from the thiyl radicals, this work indicates that DNA degradation may be even more complicated than expected under some circumstances, because different mechanisms of cleavage may ensue under different experimental conditions.

The study of the mechanism and of intermediates involved in metal-mediated DNA cleavage is not a simple task, not only because of the complexity of some of the systems studied but also because of the difficulty of detecting short-lived intermediates. Current detection methods for radical intermediates, such as spin trapping with electron paramagnetic resonance spectroscopy (EPR), are subject to some limitations, for example low sensitivity[53] and the formation of artifactual products.[54-56] Although product analysis is widely employed and can often be used to deduce the nature of the reactive species responsible for DNA cleavage, the results strongly depend on type of DNA used, reaction conditions, sensitivity of the product detection method and post-reaction treatment. In addition, similarities in the chemical structures of degradation products often make them difficult to separate and identify. Therefore, to obtain a clear picture of the reactive

intermediates, an appropriate model system, carefully controlled experimental conditions and sensitive and reliable detection methods are required.

Many transition metals are capable of cleaving DNA, such as Fe(II), Cu(I), Rh(III), Mn(II), Ni(II) and Co(III). Among them, Fe and Cu complexes are widely studied due to their significance in biological systems. A substantial body of work on DNA cleavage by iron or copper complexes has been published, thus providing a helpful background to the study of other DNA-degrading complexes.

## 1.2 Roles of Iron and Copper in Biological Systems

Iron and copper are essential in the human body because they are key components of a wide range of enzymes participating in redox reactions, respiration and $O_2$ transport. Yet iron and copper are potentially dangerous in biological systems due to their ability to initiate damaging oxidative reactions. Iron and copper can undergo one-electron transfer reactions and act to catalyze autoxidation reactions, the conversion of $H_2O_2$ to •OH and the decomposition of lipid peroxides to reactive peroxyl and alkoxyl radicals[36, 57] (Equation 1.8, 1.9).

$$ROOH + Fe^{3+}/Cu^{2+} \longrightarrow Fe^{2+}/Cu^{+} + RO_2\bullet + H^{+} \qquad 1.8$$

$$ROOH + Fe^{2+}/Cu^{+} \longrightarrow Fe^{3+}/Cu^{2+} + RO\bullet + OH^{-} \qquad 1.9$$

A variety of diseases, such as cardiac malfunctions, liver cancer, diabetes and Wilson's disease,[58] are related to overload of iron or copper which initiates free radical reactions in human body. Although it is not rigorously proven that free radical reactions are the major cause of these diseases, evidence suggests a strong correlation between them. For example, elevated lipid peroxidation end-products and subnormal level of

vitamins E and C have been detected in iron overloaded patients.[59] The hydroxyl radical has been detected in the bile of iron overloaded rats.[60] It is thought that the production of free radicals stimulated by the presence of copper or iron causes damage to biomolecules, thus resulting in diseases mentioned above.

Iron and copper present in biological systems are not usually in a form that produces free radicals. Free radical generation by protein-bound iron or the iron in the ferritin cores is not so efficient as low molecular weight chelates of iron. Evidence shows that a pool of reactive iron or copper species exists in biological systems,[61] making efficient free-radical reactions possible. These low molecular chelates of iron or copper are thought to result from malfunctioning of the complex mechanisms of uptake, storage and utilization of these ions. Oxidative stress may also mobilize iron and copper ions from its unreactive forms and thus raise the levels of free metal ions. For example, superoxide can release iron from ferritin and iron-sulphur proteins. Copper ions can be released by the degradation of caeruloplasmin[57] or homogenization of tissues.

In addition, reductants commonly used in vitro, such as ascorbate, vitamin E, reduced glutathione (GSH) and reduced nicotinamide adenine dinucleotide (NADH), are available in vivo. The free copper or iron ions combined with the availability of these reductants can make free radical reactions possible in vivo. Damage to DNA, lipid and proteins caused by reactive iron or copper species in vivo likely follows similar mechanisms as in vitro. Therefore, mechanistic studies on DNA damage in vitro can be very helpful for understanding the damage that may occur in the more complex biological systems.

## 1.3 Oxidation of DNA by Iron Complexes

Many synthetic iron complexes such as Fe-EDTA (Scheme 1.3) and iron complexes coordinated by natural products such as Fe-bleomycin (Scheme 1.3) have been employed to initiate DNA cleavage in the presence of $O_2$ or $H_2O_2$. Fe-EDTA and its derivatives and Fe-bleomycin are representative complexes employed in past DNA cleavage studies and have been investigated in detail. The intermediates involved have been proposed based on these studies.

### 1.3.1 Fe-EDTA and its Derivatives

$Fe^{II}$-EDTA (Scheme 1.3) is a well-known Fenton reagent and has been used as a footprinting reagent for DNA.[62-64] Since it is a negatively charged complex at physiological pH, $Fe^{II}$-EDTA does not interact with DNA due to electrostatic repulsion. Because of its small molecular size, $Fe^{II}$-EDTA does not affect the structure of substrates studied. DNA cleavage reactions initiated by $Fe^{II}$-EDTA exhibit almost no sequence specificity, leading to the conclusion that the reactive species is probably hydroxyl radicals. It is commonly accepted that hydroxyl radical generated by the reaction of $Fe^{II}$-EDTA with $H_2O_2$ escapes scavenging by the $Fe^{II}$-EDTA itself, diffuses to bulk solution and indiscriminately breaks DNA strands (Equation 1.10).

$$[Fe^{II}(EDTA)]^{2-} + H_2O_2 \longrightarrow [Fe^{III}(EDTA)]^{1-} + \bullet OH + OH^- \qquad 1.10$$

$Fe^{III}$-EDTA causes DNA cleavage only after it is reduced to $Fe^{II}$-EDTA by reductants. Substantial evidence based on the use of spin trapping with detection by electron paramagnetic resonance spectroscopy (EPR), as well as other chemical trapping methods supports a mechanism involving the hydroxyl radical.[65, 66] Studies also show that

the DNA strand break patterns by ionizing radiation, a well-known free hydroxyl radical source, are essentially identical to those caused by the reaction of $Fe^{II}$-EDTA with $H_2O_2$, providing exceedingly strong evidence for the involvement of hydroxyl radicals.[67]

Similar studies have been carried out with derivatives of $Fe^{II}$-EDTA. Methidiumpropyl-$Fe^{II}$-EDTA (Fe-MPE), a derivative of $Fe^{II}$-EDTA, can intercalate non-specifically to DNA through the methidium moiety.[68, 69] Fe-MPE cleaves plasmid DNA at a concentration ($10^{-6}$ M) two orders of magnitude lower than Fe-EDTA ($10^{-4}$ M) in a relatively sequence-independent manner, and is thus believed to involve hydroxyl radical generation.[68, 70] The level of cleavage decreases with the distance from the position of intercalation of the DNA consistent with the decrease in the concentration of the hydroxyl radical species with the distance from the site of its formation.[71]

Fe-EDTA has also been covalently attached to other sequence-specific DNA binding molecules such as distamycin,[72, 73] oligopeptides,[74, 75] or oligonucleotides to achieve site specific DNA cleavage. For example, a hybrid molecule of Fe-EDTA and distamycin results in DNA strand breakage at the sites to which distamycin binds.[76] The hydroxyl radical is also assumed to be the reactive species in these cases.

In contrast, Koppenol and his coworkers reported that ferryl ion (Equation 1.11), presumably ($FeO^{2+}$)-EDTA, is formed by the reaction of $Fe^{II}$-EDTA with $H_2O_2$ based on a kinetic and stoichiometric analysis of this reaction.[32] Their experimental results indicated that the oxidizing intermediate is significantly less reactive than hydroxyl radical toward benzoate and t-butyl alcohol, typical hydroxyl radical scavengers. Moreover, the oxidizing intermediate might further react with hydrogen peroxide to generate the hydroxyl radicals.

$$Fe^{2+} + H_2O_2 \rightleftharpoons [Fe^{IV}OH]^{3+} + H_2O \rightleftharpoons [(Fe^{IV}O)]^{2+} \qquad 1.11$$

Other types of oxidizing species such as bound, complexed, caged or crypto •OH have also been suggested to be the reactive species. In some circumstances, both hydroxyl radicals and ferryl ions might be formed.[31] In the presence of different scavengers and the spin-trapping reagent for hydroxyl radical, 5,5-dimethyl-pyrroline N-oxide (DMPO), EPR studies indicate that the ratio of rate constants for the reaction of hydroxyl radical with scavengers as compared with DMPO in $Fe^{II}$-EDTA/ $H_2O_2$ systems is not always consistent with that obtained from pulsed radiolysis. These studies thus suggest that both the hydroxyl radical and the ferryl ion may be produced in $Fe^{II}$-EDTA/$H_2O_2$ reactions. According to these studies, the major oxidizing intermediate changes from the ferryl ion to free hydroxyl radical with increasing the concentration of hydrogen peroxide.[31] Thus, although the preponderance of evidence indicates that the hydroxyl radical is the primary species that initiates the DNA cleavage, the ferryl ion might also play some role.

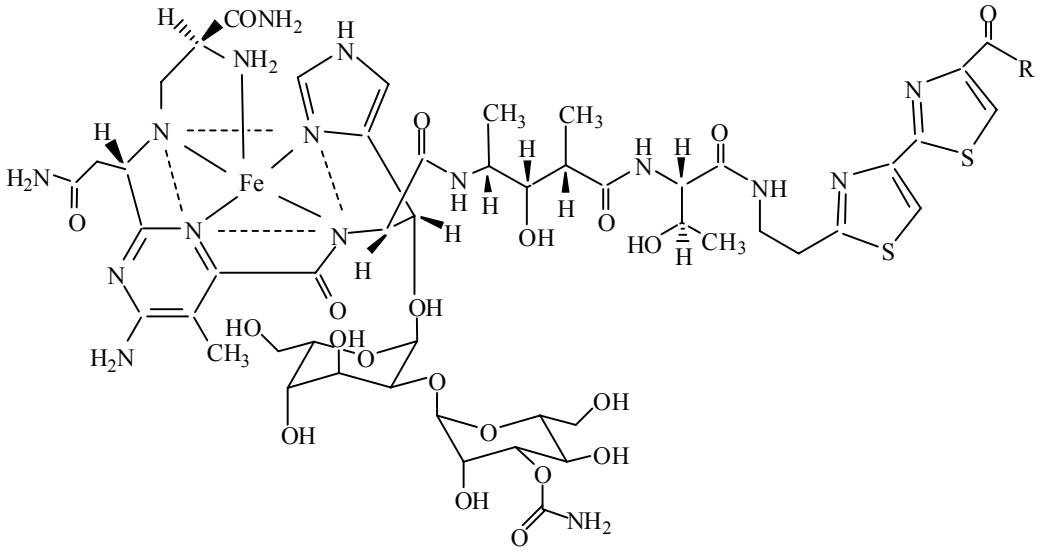

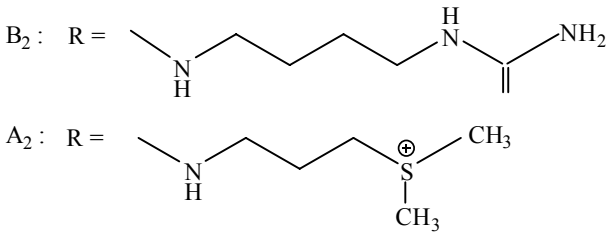


Bleomycins $A_2$ and $B_2$ and Fe-BLM

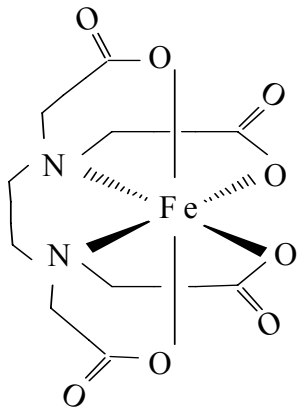

Fe-EDTA

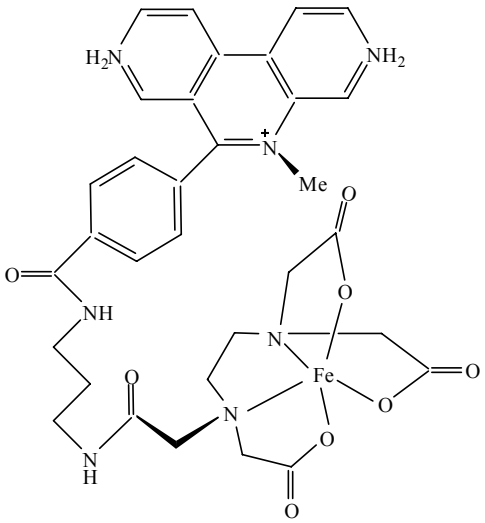

Fe-MPE

**Scheme 1.3 Structures of Fe complexes**

### 1.3.2 Fe-bleomycin

The bleomycins (BLM), discovered by Umezawa and co-workers in 1966,[77, 78] are a family of the glycopeptide-derived antibiotics clinically employed for the treatment of non-Hodgkin lymphomas, squamous cell carcinomas, and testicular tumors.[79-81] The therapeutic activity of the bleomycins is generally assumed to be related to their ability to degrade DNA in vivo.[82] Their pharmaceutical application triggered numerous studies of their mechanism of action.

As in other metal-mediated DNA cleavage systems, bleomycin-induced DNA degradation in vitro requires Fe(II) and dioxygen[83, 84] or Fe(III), reductants and dioxygen,[85] suggesting the production of hydroxyl radicals through the Fenton reaction. However, a mechanism involving a hydroxyl radical intermediate is challenged by several observations. First, the strand breakage patterns by $Fe^{II}$-BLM systems differ from that produced by radiation or by $Fe^{II}$-EDTA systems. A narrower spectrum of products is produced and sequence specificity is observed.[86, 87] Second, accumulation of $H_2O_2$ is negligible and little $O_2^{-\bullet}$ is detected, inconsistent with the requirements for hydroxyl radical generation by Fenton reactions. Third, DNA damage initiated by $Fe^{II}$-BLM can not be completely inhibited by hydroxyl radical scavengers.[88] Although these observations do not completely exclude hydroxyl radical involvement, they at least suggest that the hydroxyl radical is not the major reactive species responsible for Fe-BLM-mediated DNA cleavage.

A relatively clear picture of the Fe-BLM-mediated degradation of DNA, involving a high-valent bleomycin iron-oxo complex, BLM-$Fe^{V}$=O species, was first proposed by

Burger *et al*[89] based on a combination of biophysical techniques such as stopped-flow, EPR and Mossbauer spectroscopy (Scheme 1.4). [90]

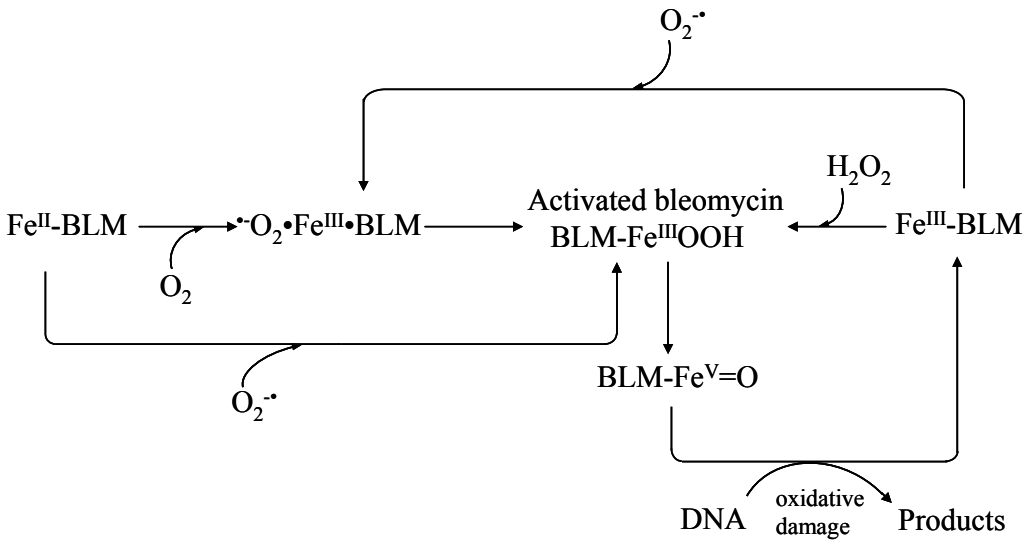


**Scheme 1.4 Proposed mechanism of DNA cleavage caused by Fe-BLM**

Several intermediates involved were observed and characterized optically. As shown in Scheme 1.4, upon addition of $O_2$ to $Fe^{II}$-BLM aqueous solutions, a ternary ferric superoxide complex, $^{\bullet-}O_2$•$Fe^{III}$•bleomycin, is generated, assigned on the basis of information produced by Mossbauer spectroscopy.[91] This intermediate is even-spin and EPR silent. The rate of its formation is first order with respect to both $Fe^{II}$-BLM and dioxygen concentrations, with a formation rate constant of $k = 6.1 \times 10^3$ $M^{-1}s^{-1}$ at 2 $^oC$. [92] $O_2^{-\bullet}$•$Fe^{III}$•bleomycin is converted to activated bleomycin through disproportionation of two $^{\bullet-}O_2$•$Fe^{III}$•bleomycin.[93] One $^{\bullet-}O_2$•$Fe^{III}$•bleomycin molecule is oxidized to produce $O_2$ and unreactive $Fe^{III}$-BLM. The other is reduced to a transient species named "activated bleomycin" which can be trapped by rapid freezing.[94] $^{\bullet-}O_2$•$Fe^{III}$•bleomycin consumption exhibited first order kinetics with the rate constant of $k = 0.11$ $s^{-1}$ at 2 $^oC$ .[92] suggesting

that a bimolecular step, such as dimerization of $^{\cdot}O_2$•$Fe^{III}$•bleomycin might occur prior to the subsequent redox reaction, although this dimer has not been observed.

Several plausible structures of activated bleomycin have been proposed (Scheme 1.5).[89] Most of the evidence supports the existence of a ferric peroxide complex. EPR experiments with $^{57}Fe$ and $^{17}O$-labeled $O_2$ demonstrate that this complex must have odd electron spin localized on the iron and that oxygen is retained as an iron ligand.[89] Electro-spray ionization mass spectrometry confirmed that this species contains two oxygen atoms and that the mass to charge ratio is consistent with HOO-$Fe^{III}$-BLM.[95]

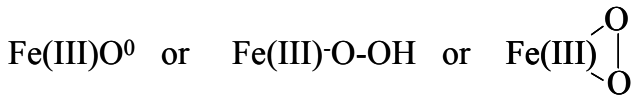


**Scheme 1.5 Proposed structures of activated BLM**

In addition to the reaction of $Fe^{II}$-BLM with $O_2$, activated bleomycin can also be generated via several other routes. The direct reaction of $Fe^{III}$-BLM with peroxide, such as $H_2O_2$ or ethyl hydroperoxide, produces activated bleomycin under anaerobic conditions.[89] In addition, superoxide can also participate in the formation of activated bleomycin.[96-98] Superoxide may react with $Fe^{III}$-BLM to form $^{\cdot}O$•$Fe^{III}$•bleomycin, further producing the activated bleomycin through disproportionation or directly through reaction with $Fe^{II}$-BLM.

The activated bleomycin, HOO-$Fe^{III}$-BLM, decays unimolecular through peroxide cleavage.[99] Since the activated bleomycin decay is not affected by the presence or absence of DNA, the proximate DNA-reactive intermediate is believed to be generated during the decay of the activated bleomycin intermediate. The rate-limiting reaction is the

O-O rupture in the activated bleomycin complex. Some attempts have been made to determine whether the O-O cleavage is homolytic or heterolytic. An activated bleomycin analogue generated by the reaction of $Fe^{III}$-BLM with 10-hydroperoxy-8,12-octadecadienoic acid is known to undergo homolytic O-O cleavage, but its product, the alkoxyl radical, is not capable of cleaving DNA[100] probably due to its big size which disfavors it to access DNA. These studies suggest an intermediate, such as BLM-$Fe^{V}$=O, generated by a heterolytic splitting of the O-O bond, is responsible for oxidizing DNA to yield the final product $Fe^{III}$-BLM. A redox titration showed that the DNA-reactive intermediate has two additional oxidizing equivalents as compared with $Fe^{III}$-BLM, also consistent with the formation of a BLM-$Fe^{V}$=O species,[94] although no direct spectroscopic evidence for this intermediate has yet been provided.

## 1.4 Oxidation of DNA by Copper Complexes

Copper complexes employed as synthetic chemical nucleases have been the subject of continued interest over the past several decades. Since copper can exist in mononuclear and coupled multinuclear configurations in biological systems, a large number of mononuclear and multinuclear copper complexes have been examined. Their nucleolytic activities on single or double stranded DNA have been extensively studied. The nature of the reactive intermediates involved in this process has also been investigated extensively.

### 1.4.1 Bis(1,10-phenanthroline) Copper Complex

Currently, bis(1,10-phenanthroline) copper complex (Scheme 1.6), $Cu(OP)_2$, is the best characterized DNA cleavage agent based on copper. Its chemical nuclease activity was first reported by Sigman and co-workers in 1979,[101] stimulating considerable interest in synthetic chemical nucleases. This complex has been widely applied as a footprinting agent for both proteins and DNA, as a probe of the dimensions of the minor groove of DNA, and to identify transcription start sites.[102-105]

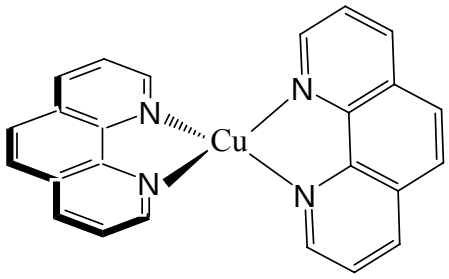


**Scheme 1.6 Structure of $Cu(OP)_2$**

The degradation of DNA by $Cu(OP)_2$ requires Cu(II), $O_2$ and a reducing agent such as ascorbate, reduced nicotinamide adenine dinucleotide phosphate (NADPH) or thiols such as 3-mercaptopropionic acid and 2-mercaptoethanol. The striking characteristic of this system is the absolute requirement for copper. Other metal ions such as Co(II), Cd(II), Ni(II) or Zn(II) cannot initiate the DNA degradation under similar conditions.[106] Moreover, the degradation of DNA is also found to be completely inhibited by the chelators that strongly coordinate copper, such as triethylenetetraamine, neocuproine or EDTA.[106] The observation that DNA degradation can be partially inhibited by superoxide dismutase, completely inhibited by catalase and enhanced by externally added $H_2O_2$ suggests $H_2O_2$ (and $O_2^{-\bullet}$) is necessary for the degradation of DNA.

$H_2O_2$ can be added externally or generated by the spontaneous dismutation of the superoxide ion produced during oxidation of Cu(I) complex by dioxygen. Dioxygen acts as an electron acceptor in the $Cu^{II}(OP)_2$-catalyzed oxidation of the reductant (eg. thiol), thereby producing $H_2O_2$, which reacts with the Cu(I) complex to produce a strong oxidant.

$Cu^{II}(OP)_2$ reacts with DNA in a sequence dependent, but not nucleotide specific manner.[107, 108] Since the absolute requirement for Cu(I) and $H_2O_2$ is identical to that for Fenton reaction, it has been assumed that the reactive intermediate is the hydroxyl radical. Some studies have suggested that an oxo-copper complex[38, 109] or a hydroxyl radical-coordinated copper complex[25] is responsible for DNA degradation, although no direct evidence has been provided for their existence. The site specificity and the inability of typical hydroxyl radical scavengers to inhibit the damage completely support the assumption of metal-based oxidant.[21] Kinetics studies have shown that the reaction rate of the oxidizing intermediate with alcohol is four orders of magnitude slower than the rate for reaction with the hydroxyl radical.[25] Product analysis indicates that the ratio of the 3'-phosphomonoester to 3'-phosphoglycolates is 8:1,[110] inconsistent with 1:1 ratio expected from the reaction of the free hydroxyl radical with DNA. In addition, 5-succinamido-1,10 phenanthroline cuprous complex, which is negatively charged and does not bind to DNA, does not cause DNA cleavage even though it is redox active, further suggesting the oxidizing species is not diffusible. Based on their studies, Sigman and co-workers have proposed that the sequence-dependent reactivity of $Cu^{I}(OP)_2$ is a collective result of site specific binding to DNA and the accessibility of the oxo-copper complex to the hydrogen of the deoxyribose moiety (Scheme 1.7).[111]

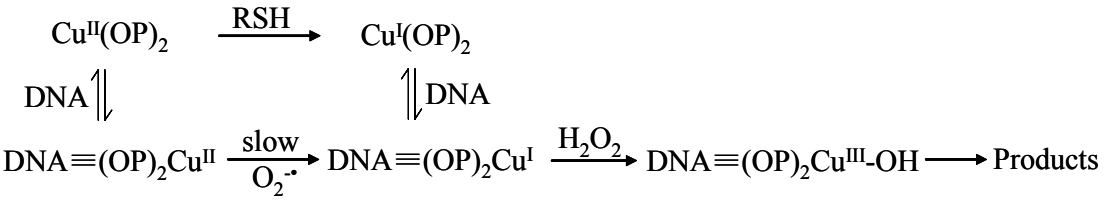


**Scheme 1.7 Proposed mechanism of DNA cleavage caused by $Cu(OP)_2$**[111]

The free $Cu^{II}(OP)_2$ complex is first reduced to $Cu^{I}(OP)_2$ in solution with $Cu^{I}(OP)_2$ then reversibly binding to DNA. The bound complex reacts with $H_2O_2$ to generate an oxo-copper intermediate, which subsequently reacts with DNA to produce strand breakage. Although $Cu^{II}(OP)_2$ complex can also bind with DNA, the reduction reaction between $Cu^{II}(OP)_2$ and superoxide is so slow that it can be neglected.[111]

Although most of the current evidence supports a mechanism involving an oxo-copper intermediate, Williams *et al*[112] pointed out that the oxidizing species diffuses over a limited range from the site where it is produced, suggesting that the oxidizing species is unlikely the oxo-copper complex. Moreover, the evidence does not unequivocally rule out the site-specific cleavage initiated by hydroxyl radicals.

### 1.4.2 Multinuclear Copper Complex

Although considerable progress has been made on the exploration of copper complexes as chemical nucleases, development of highly efficient and selective reagent for DNA cleavage is still a challenging area in the rational design of antitumor and antiviral agents as well as in the field of molecular biology. Multi-nuclear copper complexes offer great potential as efficient and specific DNA cleaving agents because of a number of advantages. First, the copper centers in a multi-nuclear copper complex can

enhance electrostatic interaction between the positively charged copper centers and anionic DNA phosphate backbone, thus facilitating the binding of copper complex to DNA.[39, 113, 114] Second, multiple metal sites favor efficient intramolecular activation of bound $O_2$ through bridging copper centers.[115-117] The multi-nuclear copper complexes can form the reactive intermediate without the need for an extra equivalent of the complex which sometimes is required when the dimer form of a mononuclear copper complex.[12, 118] Third, through an appropriate choice of ligand and coordination geometry, complexes capable of selective binding to particular conformations of nucleic acid may be constructed, producing highly specific DNA strand scission. A large number of multi-nuclear copper complexes have been synthesized and studied in recent years. These studies have demonstrated that certain multinuclear metal complexes do exhibit much more efficient strand scission,[119-121] site specificity[40, 41, 114] or both as compared to mononuclear analogues.[122] For example, a trinuclear copper complex developed by Karlin's group, $[Cu_3^{II}(\mathbf{L})(H_2O)_3(NO_3)_2](NO_3)_4 \cdot 5H_2O$[39] (**L** = 2,2',2''-tris(dipicolylamino)triethylamine) (Scheme 1.8), exhibits a remarkable ability to promote specific strand scission as compared to the action of its mononuclear analogues and $Cu(OP)_2$. Some binuclear copper complexes also exhibit highly efficient and selective properties for DNA cleavage. $[Cu^{II}_2(\mathbf{D^1})(H_2O)_2](ClO_4)_4$ complex[41] (**D$^1$** = dinucleating ligand with two tris(2-pyridylmethyl)amineunits covalently linked in their 5-pyridyl positions by $-CH_2CH_2-$ bridge) (Scheme 1.8) mediates strand scission at junctions between single-stranded and double-helical regions of DNA, while its mononuclear analogue, $[Cu^{II}(\mathbf{TMPA})(H_2O)](ClO_4)_2$ (**TMPA** = tris(2-pyridylmethyl)amine) (Scheme 1.8), is not observed to degrade DNA under similar conditions. $[Cu^{II}_2(\mathbf{D^1})(H_2O)_2](ClO_4)_4$

complex exhibits such a high efficiency that it can initiate strand scission at concentrations where $[Cu(OP)_2]^{2+}$ does not detectably modify DNA. More results showed that a series of binuclear Cu (II) complexes, $[Cu^{II}_2\mathbf{N_n}Y_2]^{2+}$ (n = 4 or 5 and Y = $(ClO_4)^-$ or $(NO_3)^-$)[122] (Scheme 1.8), exhibit very different behavior on DNA cleavage. These complexes were found to specifically cleave DNA at the helix-coil junctions in the presence of a reducing thiol and $O_2$ or in the presence of $H_2O_2$ alone. However, $[Cu^{II}_2\mathbf{N_n}Y_2]^{2+}$ (n = 3) and a closely- related mononuclear Cu(II) complex, $[Cu^{II}(MePY_2)(CH_3CN)(ClO_4^-)]^{1+}$ (Scheme 1.8), exhibited no selective reaction under either condition. The results suggest that the close proximity of the two copper centers as well as coordination geometry are important factors for the efficient and selective cleavage of DNA.

Most of the previous investigations have focused on synthesizing novel copper complexes and testing their DNA cleavage properties. Although mechanisms of DNA cleavage have been discussed in these studies, these have been centered on the reactivity of Cu(I) complexes with $O_2$ in non-aqueous solutions. Further, copper-peroxo species have been assumed to be responsible for DNA cleavage because the hydroxyl radical scavengers can not completely protect DNA from damage. However, no comprehensive studies have yet been performed to investigate the nature of the intermediate(s) generated in aqueous solutions. The high site specificity achieved by some multinuclear copper complexes is thought to be the result of not only the site-selective binding but also the selective oxidation properties of copper-peroxo complex. Many copper-peroxo complexes with different structures have therefore been proposed (Scheme 1.9).[123, 124] Although some of these copper-peroxo complexes shown in Scheme 1.9 have been well

characterized in organic solvents at very low temperature,[125, 126] there is no evidence for their existence in aqueous solutions at room temperature. The nature of the oxidizing intermediate(s) generated by these multinuclear copper complexes in aqueous solution remains unclear, and thus more work is needed to understand the exact nature of the reactive species responsible for DNA strand scission by multinucear copper complexes.

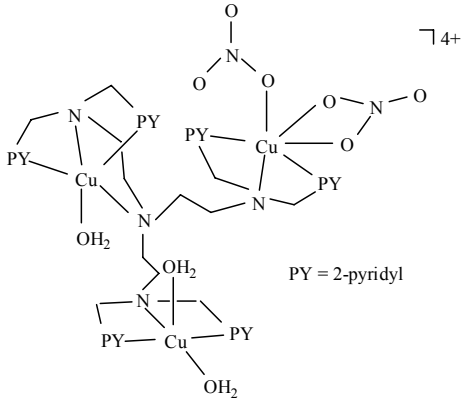


$[Cu^{II}_3(\mathbf{L})(H_2O)_3(NO_3)_2](NO_3)_4 \cdot 5H_2O$

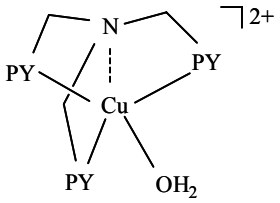


$[Cu^{II}(\mathbf{TMPA})(H_2O)](ClO_4)_2$

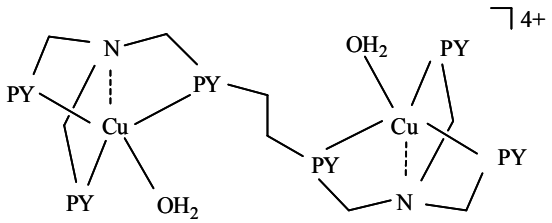


$[Cu^{II}_2(\mathbf{D^1})(H_2O)_2](ClO_4)_4$

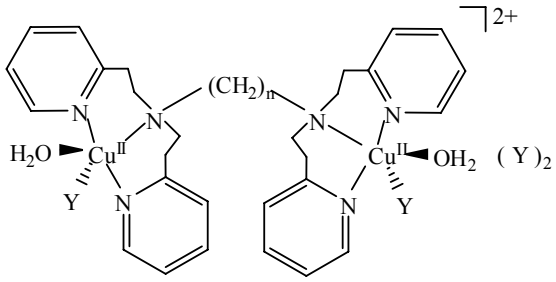


$[Cu^{II}_2(\mathbf{N_n})(Y_2)]^{2+}$, n = 3, Y = $ClO_4^-$
n = 4, Y = $ClO_4^-$
n = 5, Y = $NO_3^-$

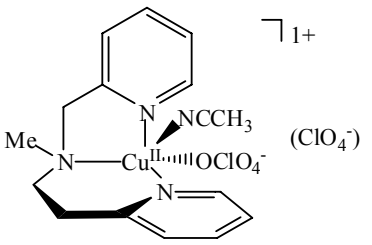


$[Cu^{II}(MePY_2)(CH_3CN)(ClO_4)]^{1+}$

**Scheme 1.8 Structures of Cu(II) complexes**

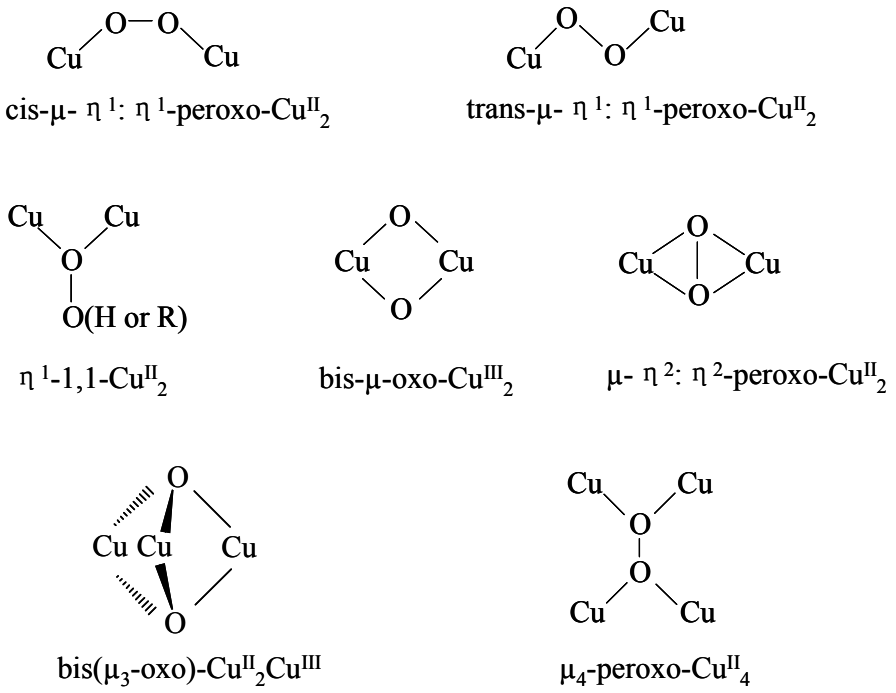


**Scheme 1.9 Structures of Cu-peroxo complexes**

## 1.5 Purpose of the Research

As mentioned above, substantial progress has been made on the mechanism of metal-mediated DNA cleavage. However, the precise nature of the reactive intermediate(s) remains a contentious issue even for the best-characterized and most simple mononuclear Fe and Cu complexes. Although numerous studies provide strong evidence for the generation of hydroxyl radicals by many Fe and Cu complexes[19] in aqueous solutions, claims persist in the literature for the involvement of the metal-based oxidants.[22, 37, 38, 127] Limitations on detection methods make it difficult to reach consistent conclusions about the nature of the reactive intermediates. Although invoking metal-based oxidizing intermediates appears to be unwarranted for many mononuclear copper complexes in aqueous solution, they may well be generated by multinuclear copper

complexes and exhibit novel oxygenation chemistry. In fact, little information about the intermediates generated by multinuclear copper complexes in aqueous solution has been obtained. The purpose of this research is to investigate the nature of the oxidizing intermediates generated from binuclear copper (II) complexes in aqueous solutions and to learn how the copper ligand environment affects the oxidative chemistry, thus providing insights into the mechanism of DNA cleavage mediated by multinuclear copper complexes.

To achieve these objectives, a homologous series of binuclear copper complexes $[Cu^{II}_2\mathbf{N_n}Y_2]^{2+}$ (n = 3-5 and Y = $(ClO_4)^-$ or $(NO_3)^-$) and a mononuclear analogue (Scheme 1.8) were examined in an attempt to identify the intermediate responsible for selective DNA strand scission in aqueous media in the presence of a reductant and dioxygen or in the presence of $H_2O_2$ alone. Recent published results showed that high efficiency and specificity for DNA cleavage were achieved by $[Cu^{II}_2\mathbf{N_n}Y_2]^{2+}$ (n = 4 or 5 and Y = $(ClO_4)^-$ or $(NO_3)^-$) complexes. In contrast, a closely-related binuclear Cu(II) complex, $[Cu^{II}_2\mathbf{N_3}Y_2]^{2+}$ (Y= $ClO_4^-$), and mononuclear Cu(II) complex, $[Cu^{II}(MePY_2)(CH_3CN)(ClO_4)_2]$, exhibited no selective reaction under identical conditions. A $\mu$-$\eta^2$:$\eta^2$ peroxodicopper(II) intermediate generated by $[Cu^{II}_2\mathbf{N_n}Y_2]^{2+}$ (n = 3-5 and Y = $(ClO_4)^-$ or $(NO_3)^-$) has been observed in $CH_2Cl_2$ at -80 $^oC$ and its kinetics and thermodynamics of oxygenation have been determined.[125] The previous studies performed by Karlin group have shown that both ligand properties[128-130] and linker length[131] between the Cu centers influence formation rates of the copper-peroxo intermediates, their structure and their rates of reactivity towards substrates in organic solvents. Therefore binuclear copper complexes, $[Cu^{II}_2\mathbf{N_n}Y_2]^{2+}$ (n = 3-5 and Y = $(ClO_4)^-$

or $(NO_3)^-$) were expected to offer the most definitive information about the nature of the reactive intermediate(s) and the efficiency of oxidative DNA strand scission.

In this study, a copper-based intermediate was spectroscopically observed for the first time in aqueous solutions. This intermediate was generated either by $[Cu^{II}_2\mathbf{N_{4,5}}Y_2]^{2+}$ in the presence of $H_2O_2$ or by $[Cu^{I}_2\mathbf{N_{4,5}}Y_2]^{2+}$ in the presence of dioxygen but was not formed by $[Cu^{II}_2\mathbf{N_3}Y_2]^{2+}$ or $[Cu^{I}_2\mathbf{N_3}Y_2]^{2+}$ complex under identical conditions. This intermediate was generated by mononuclear Cu(II) complex only when high concentrations of $H_2O_2$ and Cu(II) complex were employed and was not generated by the mononuclear Cu(I) complex with dioxygen. This intermediate decayed over time at room temperature and simultaneously produced an oxidizing species, identified as the hydroxyl radical. Based on this study, a correlation among the formation of the copper-based intermediate, hydroxyl radical generation and the efficiency of DNA cleavage has been established.

This study employed a highly sensitive technique (Scheme 1.10), previously developed by Blough and coworkers.[53, 132, 133] to discriminate between the formation of the hydroxyl radical or a metal-based oxidizing species. In this method, the hydroxyl radical or other oxidizing species reacts with DMSO to produce a methyl radical,[134] which is then quantitatively trapped by a stable nitroxide radical, 3-amino-2,2,5,5-tetramethyl-1-pyrrolidinyloxy (3-ap) to form a methyl adduct (I). I is then derivatized with fluorescamine (II) in pH 8.2 borate buffer to produce a highly fluorescent product, Me-3apf (III), which can be separated by reverse-phase HPLC and detected fluorimetrically.

Since DMSO is not necessary a specific scavenger for the hydroxyl radical, the detection of III indicates the presence of either a hydroxyl radical or an oxidant sufficiently strong to oxidize DMSO. To test further for the presence of hydroxyl radical, methane was used in place of DMSO. Because of the high valence energy of C-H bonds in methane, only very strongly oxidizing species can abstract a H atom to generate the methyl radical. The formation of III in the presence of methane qualitatively demonstrates hydroxyl radical involvement. By comparing the ratio of Me-3apf yields obtained for DMSO and methane with that calculated based on rate constants for reactions of the hydroxyl radical with DMSO and methane, hydroxyl radical and metal-based oxidants can be unequivocally differentiated.

Reaction of the hydroxyl radical with benzoic acid is another independent means to test for the formation of the hydroxyl radical. The hydroxyl radical first reacts with benzoic acid to form an intermediate radical. In the presence of $O_2$ or other electron acceptors, three isomers, 4-OH-BA, 3-OH-BA and 2-OH-BA, are generated subsequently with the ratio close to 1:1:1.[135] The hydroxylated products shown in Scheme 1.11 can be separated by reverse-phase HPLC and quantified fluorimetrically or spectrophotometrically.

In this thesis, chapter II examines the nature of the intermediate generated by the reaction of $[Cu^{II}_2\mathbf{N_n}Y_2]^{2+}$ (n = 3-5 and Y = $(ClO_4)^-$ or $(NO_3)^-$) complexes with $H_2O_2$ in aqueous solution. The results show that 1) an intermediate with an absorption maximum at 376 nm is generated by the reaction of the $[Cu^{II}_2(\mathbf{N_4})(ClO_4^-)_2]^{2+}$ or $[Cu^{II}_2(\mathbf{N_5})(NO_3^-)_2]^{2+}$ complexes with $H_2O_2$ under both anaerobic conditions and aerobic conditions, 2) this intermediate is not formed with the $[Cu^{II}_2(\mathbf{N_3})\ (ClO_4^-)_2]^{2+}$ complex, 3) this intermediate

decays over time at room temperature to form the hydroxyl radical at a stoichiometric ratio of 1:1 between the intermediate and hydroxyl radical, 4) the decay of the intermediate is not accelerated in the presence of the externally added electron donors. These results indicate that the hydroxyl radical is generated by an intramolecular electron transfer from ligand to a metal-peroxo center. For comparison, the reactions of a closely-related mononuclear Cu (II) complex, $[Cu^{II}(MePY_2)(CH_3CN)(ClO_4^-)]^{1+}$, with $H_2O_2$ are also examined in chapter II. Chapter III provides preliminary evidence that the same intermediate can be formed from the Cu(I) complexes ($Cu^{I}_2\mathbf{N_{4,5}}$) through reaction with dioxygen. In chapter IV, the conclusions of this study are presented and future research pertaining to this study is provided.

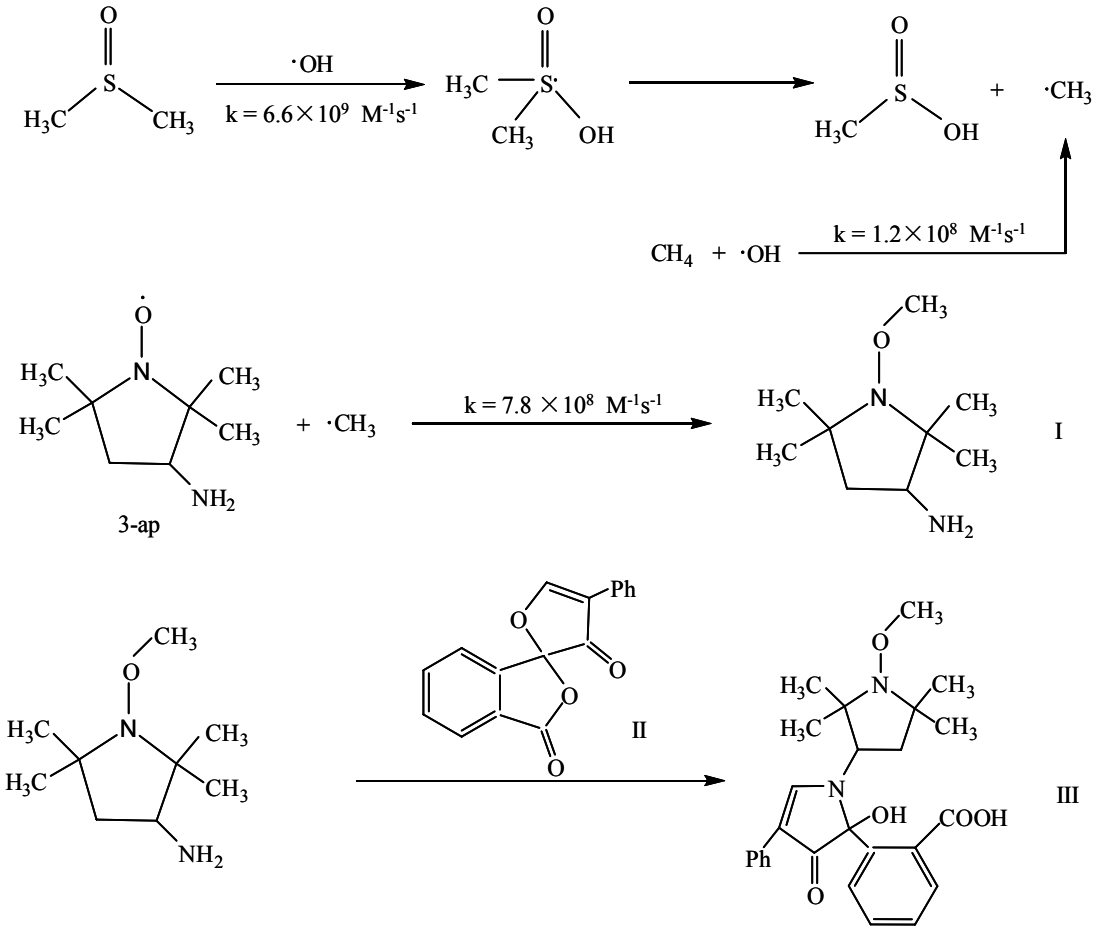


**Scheme 1.10 Radical trapping experiment in the presence of DMSO or methane**[53, 132]

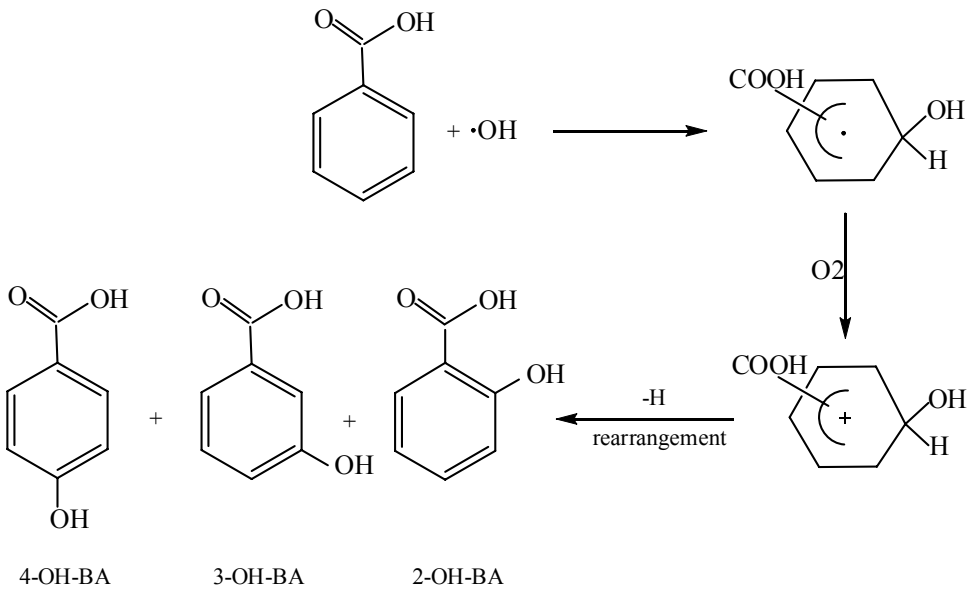


**Scheme 1.11 Radical trapping experiment in the presence of benzoic acid**[135]

# Charpter II Metal- mediated Activation of $H_2O_2$ by Copper(II) Complexes in Aqueous Solution

## 2.1 Introduction

Copper complexes as chemical nucleases have been extensively studied because they possess biologically accessible redox potentials and relatively high nucleobase affinity.[13, 120, 136-138] However, the nature of the intermediates responsible for copper complex-mediated DNA damage is still being debated. Even for the most well-known and best studied complex, $Cu^{II}(OP)_2$, which has been widely used as a footprinting agent for DNA, the exact nature of the reactive species involved in DNA cleavage is still unknown.[12] A popular concept is that the Cu(I) complex, generated in the presence of reducing agents such as alkyl thiols (RSH), reacts with molecular oxygen to form $O_2^{-\cdot}$ and $H_2O_2$, subsequently producing the hydroxyl radical through the reaction of $H_2O_2$ with Cu(I). The hydroxyl radical thus leads to the DNA degradation.[19-21] However, this concept is often challenged by experimental observations that suggest the involvement of metal-based oxidants.[23-26]

Multinuclear copper complexes are capable of cleaving DNA efficiently and specifically, thus making them potentially valuable tools for investigating intermolecular interactions between large biological molecules. A number of multinuclear copper complexes exhibit much higher efficiency and specificity of DNA strand scission than the mononuclear analogues. Based on these studies, the high nucleolytic efficiency and selectivity of the multinuclear copper complexes may be due to 1) a synergistic effect due

to multiple metal centers that promote intramolecular activation of $O_2$ through the bridging of copper atoms [115-117] 2) enhanced electrostatic interaction between the two copper centers in the dinuclear Cu(II) complex and the anionic DNA backbone [39,113] 3) favored binding to particular conformations of nucleic acid or favored the reactive intermediate generation depending on the coordination geometry of multinuclear copper complexes. Although metal-based reactive intermediate(s) have been proposed for DNA cleavage by the multinuclear copper complexes, this assignment was based on the reactivity of multinuclear Cu(I) complexes with $O_2$ in non-aqueous solutions. Currently little is known about the nature of the reactive intermediates generated by multinuclear copper complexes in aqueous solution.

Recent results have shown that binuclear Cu(II) complexes, $[Cu^{II}_2(\mathbf{N_4})(ClO_4^-)_2]^{2+}$ ($Cu^{II}_2\mathbf{N_4}$) and $[Cu^{II}_2(\mathbf{N_5})(NO_3^-)_2]^{2+}$ ($Cu^{II}_2\mathbf{N_5}$), cleave DNA specifically at the helix-coil junctions in the presence of $H_2O_2$ under anaerobic conditions, or alternatively, in the presence of a reductant (3-mercaptopropanoic acid ) under aerobic conditions. However, a closely-related $[Cu^{II}_2(\mathbf{N_3})(ClO_4^-)_2]^{2+}$ ($Cu^{II}_2\mathbf{N_3}$) complex and a mononuclear analogue, $[Cu^{II}(MePY_2)(CH_3CN)(ClO_4^-)]^{1+}$ (mono-$Cu^{II}$) (Scheme 1.8), exhibited no reactivity under identical conditions.[122] Investigation of the intermediates generated from these complexes in aqueous solution is expected to provide information on the nature of the intermediates and on the origin of the selective DNA strand scission. Further, the effects of ligand structure on the formation rate, structure, stability, and reactivity of the intermediate can also be examined.

To achieve these objectives, the reactivity of the binuclear copper(II) complexes $Cu^{II}_2\mathbf{N_n}$ (n = 3-5) and a mononuclear Cu(II) analogue, mono-$Cu^{II}$ with $H_2O_2$ in aqueous

media was examined. A novel approach, described in Scheme 2.1, was employed to discriminate between the generation of metal-based oxidants and free hydroxyl radical.[53] Benzoic acid was used further to test for the presence of hydroxyl radical formation under aerobic conditions (Scheme 1.11).[135]

In this work, a copper-based intermediate was observed for the first time in aqueous solution. This intermediate was generated by the reaction of the $Cu^{II}_2\mathbf{N_4}$ or $Cu^{II}_2\mathbf{N_5}$ complex with $H_2O_2$ to form an absorption band at 376 nm. This intermediate was not formed with $Cu^{II}_2\mathbf{N_3}$ complex but was formed with mono-$Cu^{II}$ at high concentrations of $H_2O_2$ and the copper complex. The intermediate decayed exponentially with time at room temperature. The decay was not accelerated by the addition of a series of externally added electron donors. An oxidizing species produced during the decay of the intermediate was detected and quantified by the approach outlined in Scheme 2.1. The ratio of the yields of Me-3apf (III in scheme 2.1) obtained in the presence of DMSO and methane was consistent with that calculated using the rate constants for hydroxyl radical reaction with these compounds, providing unequivocal evidence for hydroxyl radical formation during intermediate decay. The results from experiments with benzoic addition provided independent evidence for the hydroxyl radical generation. Chemical trapping studies also indicated that mono-$Cu^{II}$ generated the hydroxyl radical at a much lower rate than the $Cu^{II}_2\mathbf{N_4}$ and $Cu^{II}_2\mathbf{N_5}$ under similar $H_2O_2$ and copper complex concentrations, due to limited formation of the intermediate from mono-$Cu^{II}$ under these conditions. Based on these studies, we attribute the hydroxyl radical formation to a rate-limiting intramolecular electron transfer from the ligand to a metal-peroxo center. These results thus suggest that

either the hydroxyl radical or a ligand-based radical acts as the reactive intermediate initiating DNA cleavage in these complexes.

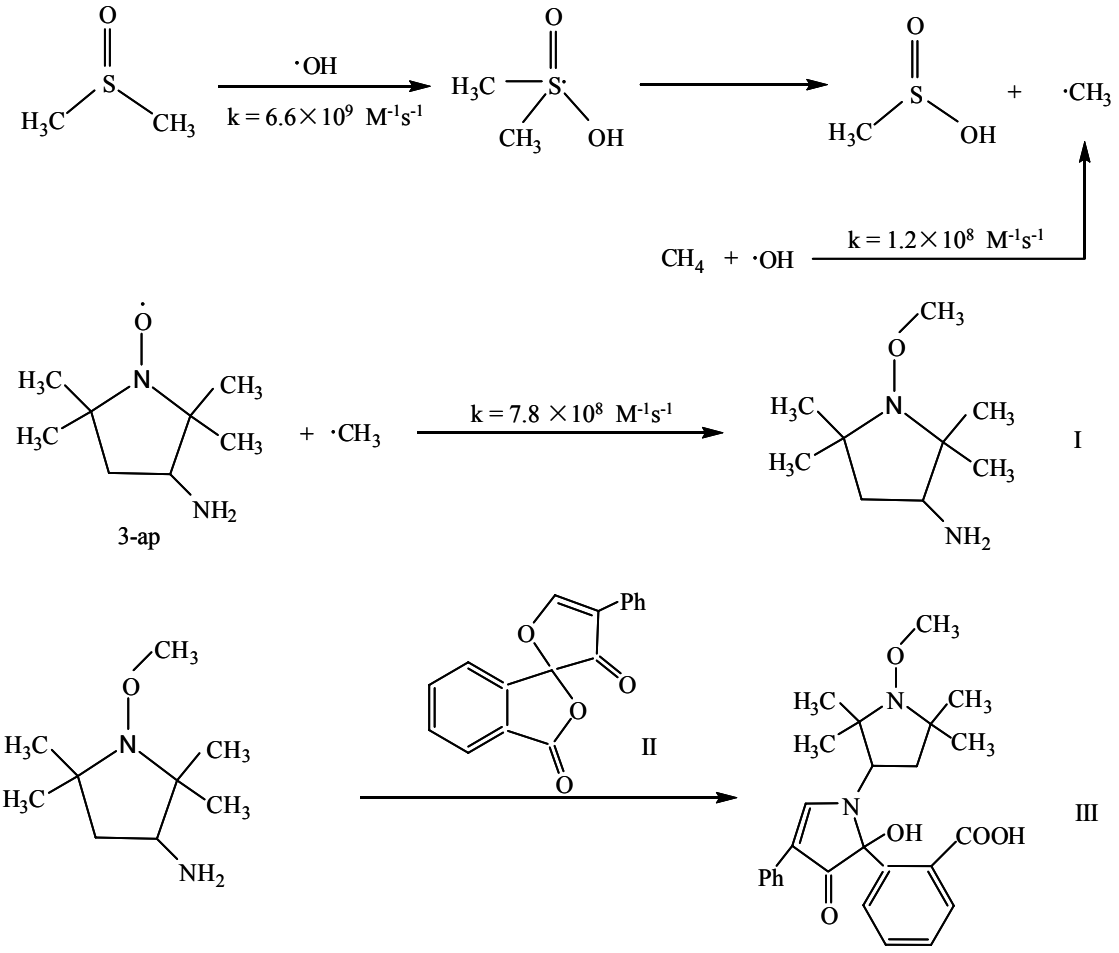


**Scheme 2.1 Radical trapping experiments in the presence of DMSO or methane**

## 2.2 Experimental Sections

### 2.2.1 Reagents and Materials

Fluorescamine, guanine and catalase (CAT) were obtained from Sigma. Boric acid (99.99%), sodium hydroxide (99.998%), sodium hydrogen phosphate (99.995%), sodium dihydrogen phosphate (99.999%), benzoic acid (99+%), dimethylaniline (DMA) (99.5+%), salicylic acid (99+%), 3-hydroxybenzoic acid (99%), 4-hydroxybenzoic acid (99%), ferrous sulfate pentahydrate and L(-) glucose (99+%) were purchased from Aldrich. Dimethyl sulfoxide (DMSO) (99.9%, HPLC grade), acetonitrile (99.93%, HPLC grade), methanol (HPLC grade) and hydrogen peroxide (30%) were obtained from Fisher. Glacial acetic acid (99.9%), hydrochloric acid (36.5%-38%), resublimed iodine and ammonium hydroxide (30%) were obtained from J.T.Baker. 3-Amino-2,2,5,5-tetramethyl-1-pyrrolidinyloxy (3-ap) (99%) was obtained from Acros. 3-mercaptopropionic acid (3-MPA) (99+%) and ethylenediamine tetraacetic acid di-sodium salt ( EDTA, 99%) were obtained from Sigma-Aldrich. Compressed nitrogen (ultra pure carrier grade), compressed air (ultra zero grade) and methane (ultra high purity) were obtained from Airgas. $[Cu^{II}_2(\mathbf{N_n})(Y_2)]^{2+}$ (n = 3-5, Y = $ClO_4^-$ or $NO_3^-$) and $[Cu^{II}(MePY_2)(CH_3CN)(ClO_4^-)]^{1+}$ complexes (structures shown in scheme 1.8) were synthesized, characterized and supplied by Dr Kenneth D. Karlin's group, Department of Chemistry, Johns Hopkins University**.** All chemicals were used as received. A Millipore MilliQ system provided water for all experiments. The standard buffer used in all experiments was 10 mM sodium phosphate, pH 6.8 unless otherwise stated.

### 2.2.2 Apparatus

Either a 8452 Hewlett Packard diode array or a Shimadzu 2401 UV-PC ultraviolet-visible spectrophotometers with scanning range from 200 nm to 800 nm were used to acquire absorption spectra. These spectrophotometers were also used for determining the concentration of the following compounds: hydrogen peroxide ( 240 nm, $\varepsilon_{240}$ = 56.4 $M^{-1}cm^{-1}$), 3-amino-2,2,5,5-tetramethyl-1-pyrrolidinlyoxy (396 nm, $\varepsilon_{396}$ = 2850 $M^{-1}cm^{-1}$), $Cu^{II}_2\mathbf{N_4}$ complex ( 260 nm, $\varepsilon_{260}$ = 18700 $M^{-1}$ $cm^{-1}$), $Cu^{II}_2\mathbf{N_5}$ complex ( 260 nm, $\varepsilon_{260}$ = 22000 $M^{-1}cm^{-1}$), $Cu^{II}_2\mathbf{N_3}$ complex (262 nm, $\varepsilon_{262}$ = 23100 $M^{-1}cm^{-1}$) and mono-$Cu^{II}$ (260 nm, $\varepsilon_{260}$ = 14100 $M^{-1}$ $cm^{-1}$) . A 1.0-cm quartz cuvette was used for all optical measurements.

The extinction coefficients of the $Cu^{II}_2\mathbf{N_n}$ (n = 3-5) and mono-$Cu^{II}$ complexes were acquired by dissolving a carefully weighed amount of the complexes into water at pH 5.8; a series of dilutions of the complex were then prepared from the stock solution by transferring an appropriate volume of the stock into 2 ml water. The absorption spectra of the resulting solutions were recorded. Molar extinction coefficients were obtained from the slopes of the plots of absorption versus concentration at selected wavelengths.

The high-performance liquid chromatograph (HPLC) has been described in previous studies.[53] It consists of an Eldex Model B-100-S single piston pump followed by an E-lab gradient controller. A 0-5000 psi pressure gauge, a Valco Model C 10W injection valve and a 0.5 × 10 cm Nova-Pak water column with 4 μM reversed-phase ($C_{18}$) packing housed by a RMC 8 × 10 cm Waters radial compression module were connected by lines. 0.5-μm filters were placed before the pump and after the column. A Spectroflow Model 757 absorbance detector was used in series with a Hitachi Model L-7485

fluorescence detector. ELAB software was used for data collection and analysis. Loop size was 50 µl. The flow rate was 1 ml/min. Chromatographic separations were performed isocratically at room temperature. For separation and quantification of Me-3apf (III), the mobile phase composition was 35% sodium acetate buffer (50 mM, pH 4.0)/ 65% methanol (v/v). The excitation and emission wavelengths on the fluorometric detection were set to 390 nm and 490 nm, respectively. For separation and identification of salicylic acid, the mobile phase composition was 65% phosphate buffer (25 mM, pH 2.0)/ 35% methanol (v/v). The excitation wavelength and emission wavelength was set to 305 nm and 410 nm respectively.

A ORION model 720 A pH meter was used to measure the pH of all solutions.

### 2.2.3 Experiment Protocols

#### 2.2.3.1 Optical Absorption

The standard reaction was carried out in a cuvette with total reaction volume of 3 ml. A given volume of phosphate buffer (10 mM, pH 6.8) and an appropriate volume of a stock solution of the Cu(II) complex were added to the cuvette. The resulting mixture was then purged with $N_2$ for 20 minutes. $H_2O_2$ which has been degassed with $N_2$ for 20 minutes was transferred from stock solution by using a 100 µl gas-tight syringe. Complete absorption spectra or the absorption at 376 nm was then obtained over time. The reaction solution or head space was purged by $N_2$ during the entire measurement. The concentrations of the Cu(II) complex and $H_2O_2$ were varied systematically and are provided in the figure captions.

To test for the effect of externally added electron donors on the intermediate decay rate, the same protocol as described above was employed to initiate the reaction.

When absorption at 376 nm reached its maximum, an appropriate volume of deaerated stock solution of an electron donor was injected into the reaction mixture. Changes of absorption at 376 nm with time in the presence of electron donors were then monitored. As a control, the same volume of deaerated phosphate buffer (10 mM, pH 6.8) was injected in place of the electron donor solution when maximum absorption at 376 nm was reached.

The experimental protocol was the same for reactions carried out under aerobic conditions except that air was employed in place of $N_2$ for all solutions.

#### 2.2.3.2 Chemical Trapping Studies

The radical trapping experiments were carried out in a 5 ml Micro-Vial with total reaction volume of 3 ml. A sample solution containing Cu(II) complex (10 or 20 μM), DMSO (10 mM) and appropriate concentration of 3-ap (varying between 50 to 500 μM) was prepared in 10 mM phosphate buffer at pH 6.8. The solution was deoxygenated by bubbling with ultra-high purity nitrogen gas for 20 minutes before the reaction was initiated by addition of deoxygenated $H_2O_2$ solution (100 μM). The reaction was terminated at different times by derivatization with fluorescamine under aerobic conditions. The reaction solution was purged with $N_2$ during the entire course of the reaction. Derivatization was performed as follows: 100 μl of the reaction mixture was withdrawn at different times and mixed with 400 μl borate buffer (0.2 M, pH 8.4); 200 μl of fluorescamine (5 mM) in acetonitrile were then added to derivatize the reaction product, Me-3ap (I), to produce Me-3apf (III). The resultant solution was vortexed and

placed in the dark for 3 minutes to complete the reaction before it was loaded onto HPLC for separation and quantification.

To further test for the hydroxyl radical, methane was used in place of DMSO. The sample solution, containing Cu(II) complex (10 μM) and 3-ap (20 μM), was purge with methane for 20 minutes (The solubility of methane in phosphate buffer is 1.5 mM). $H_2O_2$ (100 μM), deaerated by purging with $N_2$ for at least 20 minutes, was then added to sample solution to initiate the reaction. The reaction was terminated at different times by derivatization solution with fluorescamine under aerobic conditions as described above. Methane was used to purge the reaction solutions during the entire reaction course to maintain anaerobic conditions.

Benzoic acid was used to test for the presence of hydroxyl radicals under aerobic conditions. The reaction solution, containing benzoic acid (1.0 mM) and Cu (II) complex (10.0 μM), was prepared in phosphate buffer (10 mM, pH 6.8). This solution was purged with air for 20 minutes before $H_2O_2$ (6.0 mM) was added to initiate the reaction. The reaction was terminated at different times by directly injecting the sample into HPLC and detecting the formation of salicylic acid. Since the ratio of three hydroxylated isomers, 2-OH-BA, 3-OH-BA and 4-OH-BA, is close to 1:1:1, the concentration of hydroxyl radicals generated in reaction systems was approximated as three times the concentration of salicylic acid quantified by HPLC. Conditions for separation and identification of salicylic acid by HPLC have been described in Section 2.2.2.

A calibration curve was obtained for salicylic acid by serial dilution of known concentration of the stock solution. The linear range of calibration curve was from 100 nM to 10 μM.

#### 2.2.3.3 Product Analysis by Thin Layer Chromatography

Thin layer chromatography (TLC) was employed to analyze preliminarily the products produced from the reaction of Cu(II) complex with $H_2O_2$. Cu(II) complex (2 mM) and $H_2O_2$ (7 mM), dissolved in 10 mM phosphate buffer at pH 6.8, were mixed rapidly to initiate the reaction under anaerobic conditions. The resultant solution was allowed to react for 15 minutes at room temperature; concentrated ammonium hydroxide was then added to release the ligands, which were then extracted into a minimum volume of methylene chloride. The extraction was loaded onto a 10×20 cm silica gel thin layer chromatography plate (AnalTech, Inc) and developed using a mobile phase containing methanol and concentrated ammonium hydroxide, 100:5 v/v. After drying, the TLC plate was placed into a container containing iodine vapor for visualization of the products.

To investigate the effect of radical scavengers on products, Cu(II) complex (2 mM) and DMSO (2 M) were prepared in phosphate buffer (10 mM, pH 6.8) prior to addition of $H_2O_2$ (7 mM). The analysis procedure was as same as that in the absence of DMSO.

#### 2.2.3.4 Preparation of Fluorescent Product Me-3apf and Calibration of HPLC

The protocol employed to prepare Me-3apf and to calibrate the HPLC was previously published.[132] Me-3apf (III) (Scheme 2.1) was used as a standard to calibrate the response of fluorescence detector. The method used to synthesize Me-3apf was described previously.[132] 3-ap (3 mM), DMSO (30 mM) and $H_2O_2$ (3 mM) were mixed in 100 mM phosphate buffer at pH 7.5. Fe(II)-EDTA (3 mM) prepared by dissolving 4 mM EDTA and 3 mM ferrous sulfate in deoxygenated 100 mM phosphate buffer at pH 4.2 was added to the mixed solution to initiate reaction. The reaction was allowed to proceed

anaerobically in the dark for 40 minutes. The resulting solution was then derivatized with fluorescamine in borate buffer at pH 8.4. After adjusting the pH from 8.4 to 4, the derivatized sample (~ 10 ml) was then extracted by using a Waters $C_{18}$ Sep-Pak. The Sep-Pek was rinsed first with Milli-Q water, then with methanol several times to activate the stationary phase before use. After the derivatized sample was loaded onto the Sep-Pak, a dark yellow band was observed. This band was then eluted with a minimum volume of acetonitrile which was further reduced by flushing with dry nitrogen.

The yellow solid obtained from above procedure was then dissolved in minimum volume of HPLC mobile phase (65% methanol and 35% acetate buffer). The resultant solution was injected into HPLC and the product Me-3apf (III) was collected directly from the HPLC and extracted into 2 ml chloroform. After evaporation of chloroform by flushing with dry $N_2$, a bright yellow solid was left and stored at -20 $^{o}$C.

To calibrate the fluorescence detector of HPLC, the concentration of Me-3apf stock solution was determined spectrophotometrically (386 nm, $\varepsilon_{386}$ = 5225 $M^{-1}cm^{-1}$).[132] A linear response was obtained from 100 nM to 10 μM. This standard was also employed to confirm the identity of the product by co-elution.

## 2.3 Results and Discussion

### 2.3.1 Intermediate Generation in the Presence of $H_2O_2$

Addition of $H_2O_2$ to an aqueous solution of either $Cu^{II}_2\mathbf{N_4}$ or $Cu^{II}_2\mathbf{N_5}$ complex produced a species within ~ 30 seconds of $H_2O_2$ addition that exhibited a prominent absorption band at 376 nm but decreased absorption at 260 nm (Figure 2.1). This band was not formed upon addition of $H_2O_2$ to $Cu^{II}_2\mathbf{N_3}$ complex under same conditions.

This band was also observed for $Cu^{II}_2\mathbf{N_4}$ and $Cu^{II}_2\mathbf{N_5}$ but not $Cu^{II}_2\mathbf{N_3}$ when 10 mM phosphate buffer (pH 6.8) was used in place of water (Figure 2.2). The similarity of absorption spectra in water and phosphate buffer indicated that the species generated in both cases were the same. Formation of this species was found to be affected by organic solvents such as methanol and acetonitrile. When high concentration of methanol or acetonitrile (>10 M) was present in solution prior to hydrogen peroxide addition, generation of the species was completely inhibited. Further, absorption at 260 nm of the $Cu^{II}_2\mathbf{N_4}$ and $Cu^{II}_2\mathbf{N_5}$ complexes decreased in phosphate buffer (10 mM, pH 6.8) as compared with that in water, suggesting interaction between Cu(II) complex and phosphate (see below).

The absorption band at 376 nm observed for $Cu^{II}_2\mathbf{N_4}$ and $Cu^{II}_2\mathbf{N_5}$ decreased over time, with the decay usually complete by ~ 20 minutes at room temperature. The resultant spectrum was clearly different from the spectrum of the original Cu(II) complexes. In contrast, a slight increase of the absorption at 376 nm was observed for $Cu^{II}_2\mathbf{N_3}$, due to the accumulation of reaction products. The intermediate generated in the presence of $H_2O_2$ for both the $Cu^{II}_2\mathbf{N_4}$ and $Cu^{II}_2\mathbf{N_5}$ exhibited not only very similar absorption spectra but also very similar decay kinetics (see below).

The extinction coefficient of the intermediate absorbing at 376 nm was determined by the addition of increasing $H_2O_2$ concentrations to the complexes in 10 mM phosphate buffer (pH 6.8). Plots of absorption at the 376 nm versus $H_2O_2$ concentration exhibited a plateau above ~500 μM $H_2O_2$ for both $Cu^{II}_2\mathbf{N_4}$ and $Cu^{II}_2\mathbf{N_5}$ complexes (Figure 2.3). This maximum in absorption was used to calculate the extinction coefficient of the intermediate based on the molarity of the copper ion. The values obtained for $Cu^{II}_2\mathbf{N_4}$ and $Cu^{II}_2\mathbf{N_5}$ were very similar, 2630 $M^{-1}cm^{-1}$ and 2900 $M^{-1}cm^{-1}$respectively, also suggesting that the intermediate formed from these two complexes is very similar, if not identical in structure.

Although a species with absorption at 376 nm was also formed with a closely-related mononuclear Cu(II) complex, mono-$Cu^{II}$ (Figure 2.4), much higher concentrations of $H_2O_2$ (several mM) and Cu(II) complex (500 μM) were required as compared with $Cu^{II}_2\mathbf{N_4}$ and $Cu^{II}_2\mathbf{N_5}$. Even under these higher concentrations, the rate of formation was much slower than $Cu^{II}_2\mathbf{N_4}$ and $Cu^{II}_2\mathbf{N_5}$ (Figure 2.4). The increase in absorption at 376 nm with increasing $H_2O_2$ concentration also exhibited a different dependence (Figure 2.5). Instead of a plateau as for $Cu^{II}_2\mathbf{N_4}$ or $Cu^{II}_2\mathbf{N_5}$ complex, an absorption maximum was reached in mono-$Cu^{II}$complex at ~ 50 mM $H_2O_2$, suggesting that a maximum amount of the intermediate was generated at this concentration. At higher concentrations of $H_2O_2$, the absorption at 376 nm decreased with increasing $H_2O_2$ concentration, suggesting that additional $H_2O_2$ was inhibiting the formation of the intermediate. The absorption at the maximum was used to calculate the extinction coefficient of the intermediate formed from mono-Cu(II) complex, based on the molarity of the copper ion. This value ($\varepsilon_{376\ nm}$ = 2690 $M^{-1}cm^{-1}$) was comparable to those obtained from $Cu^{II}_2\mathbf{N_4}$ ($\varepsilon_{376\ nm}$ = 2630 $M^{-1}cm^{-1}$)

and $Cu^{II}_2\mathbf{N_5}$ ($\varepsilon_{376\ nm}$= 2900 $M^{-1}cm^{-1}$). The very similar absorption spectra and extinction coefficients suggest that the intermediates formed from mono-$Cu^{II}$, $Cu^{II}_2\mathbf{N_4}$ and $Cu_2\mathbf{N_5}$ also have very similar structures.

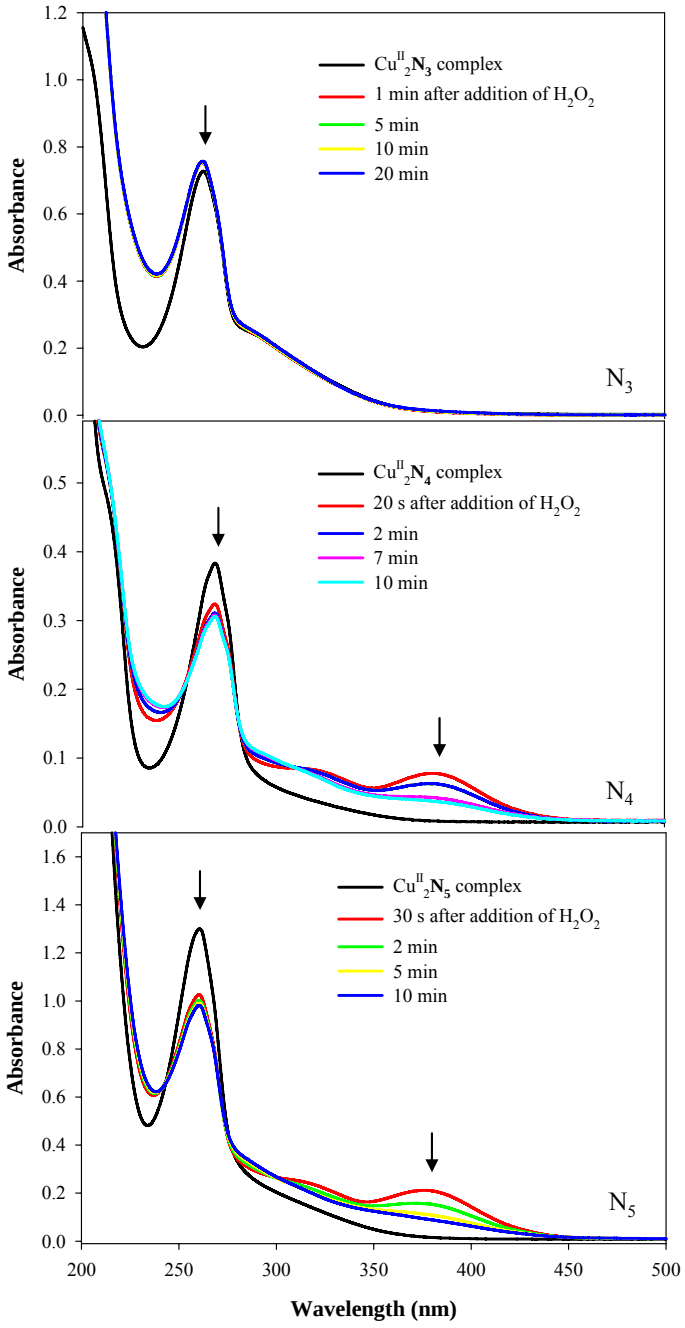


**Figure 2.1 Absorption spectrum of $Cu^{II}N_{3\text{-}5}$ before and after addition of $H_2O_2$ in water**

$Cu^{II}$**N$_3$** (30 μM), $Cu^{II}$**N$_4$** (20 μM) or $Cu^{II}$**N$_5$** (50 μM) was dissolved in water at pH 5.8. $H_2O_2$ (3 mM, 200 μM or 500 μM) was added to the corresponding solution to initiate the reaction under anaerobic conditions. Time dependence of the absorption spectra following $H_2O_2$ addition is shown.

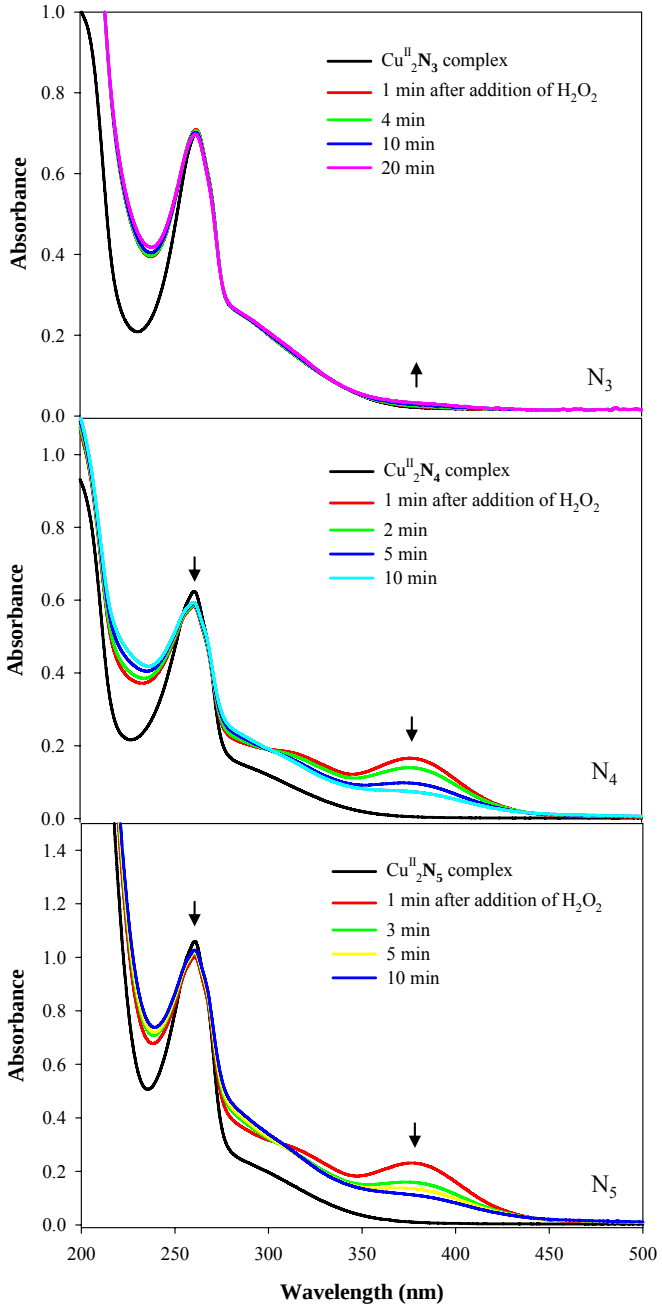


**Figure 2.2 Absorption spectrum of $Cu^{II}N_{3\text{-}5}$ before and after addition of $H_2O_2$ in 10 mM phosphate buffer**

$Cu^{II}\mathbf{N_3}$ ( 30 μM), $Cu^{II}\mathbf{N_4}$ (40 μM) or $Cu^{II}\mathbf{N_5}$ ( 50 μM) was dissolved in 10 mM phosphate buffer at pH 6.8. $H_2O_2$ (3 mM, 530 μM or 500 μM) was added to the corresponding solution to initiate the reaction under anaerobic conditions. Time dependence of the absorption specta following $H_2O_2$ addition is shown.

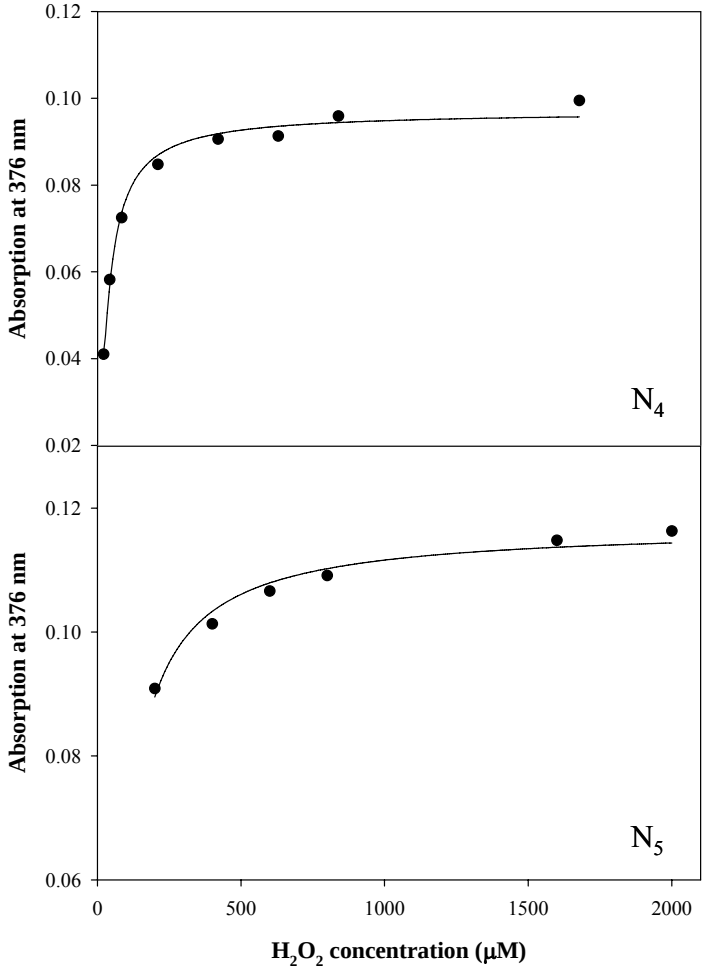


**Figure 2.3 $H_2O_2$ titration experiments of $Cu^{II}_2N_{4,5}$ complexes**

$Cu^{II}_2$**N4** complex (21.0 μM) or $Cu^{II}_2$**N5** complex (20.0 μM) was dissolved in phosphate buffer (10 mM, pH 6.8). Varying concentrations of $H_2O_2$ were added to initiate the reaction under anaerobic conditions. Absorption maximum at 376 nm was then recorded for the different $H_2O_2$ concentration. Lines in this figure were based on a fit to polynomial equation only so that the trend could be shown clearly.

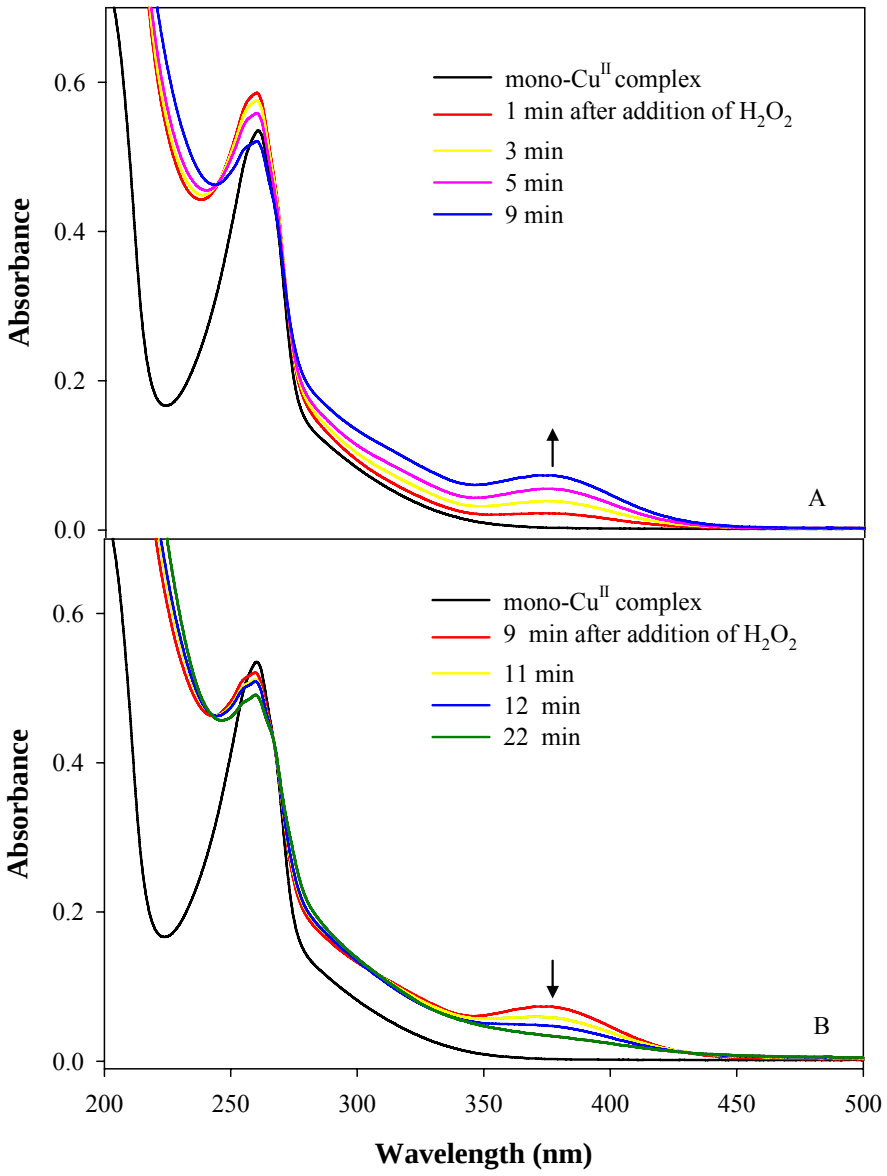


**Figure 2.4 Absorption spectrum of mononuclear Cu(II) complex before and after addition of $H_2O_2$ in 10 mM phosphate buffer**

Mono-Cu$^{II}$ complex (50 µM) was dissolved in phosphate buffer (10 mM, pH 6.8). $H_2O_2$ (3 mM) was added to initiate the reaction under anaerobic conditions. Time dependence of the absorption spectra following $H_2O_2$ addition is shown. Absorption spectra of the formation of the intermediate (panel A) and decay (panel B) were recorded over time.

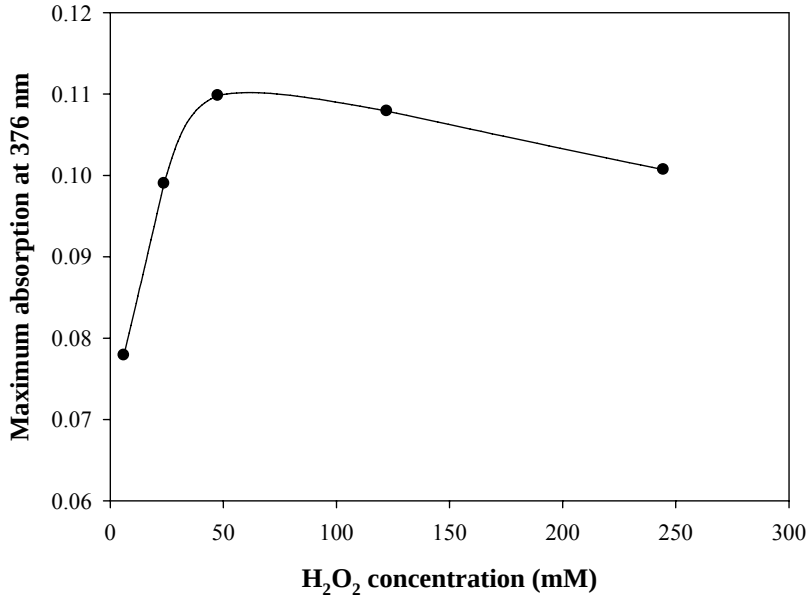


**Figure 2.5 $H_2O_2$ titration experiments of the mononuclear Cu(II) complex**

Mono-$Cu^{II}$ complex (39.4 μM) was dissolved in phosphate buffer (10 mM, pH 6.8). $H_2O_2$ with varying concentrations (6.1 mM, 23.8 mM, 47.6 mM, 122.3 mM or 244.6 mM) was added to initiate the reaction under anaerobic conditions. Absorption maximum at 376 nm was then recorded for the different $H_2O_2$ concentration.

### 2.3.2 Effect of Phosphate and pH on the Absorption Spectra of Cu(II) Complexes and the Formation of the Intermediate

Both pH and phosphate concentration affected the absorption spectra of the Cu(II) complexes themselves, as well as the formation of the intermediate. With increasing phosphate concentrations at pH 7.0, as shown in Figure 2.6, the absorption bands of the Cu(II) complexes at 260 nm, 300 nm and d-d transition band at 750 nm were suppressed, suggesting binding of the phosphate to the copper center. A similar tendency was observed in $Cu^{II}_2\mathbf{N_4}$, $Cu^{II}_2\mathbf{N_5}$ and the mononuclear Cu(II) complex solutions, the effect of phosphate on the absorption spectrum of $Cu^{II}_2\mathbf{N_3}$ complex was much smaller, suggesting that the geometry of $Cu^{II}_2\mathbf{N_3}$ does not favor the binding of the phosphate to the copper centers.

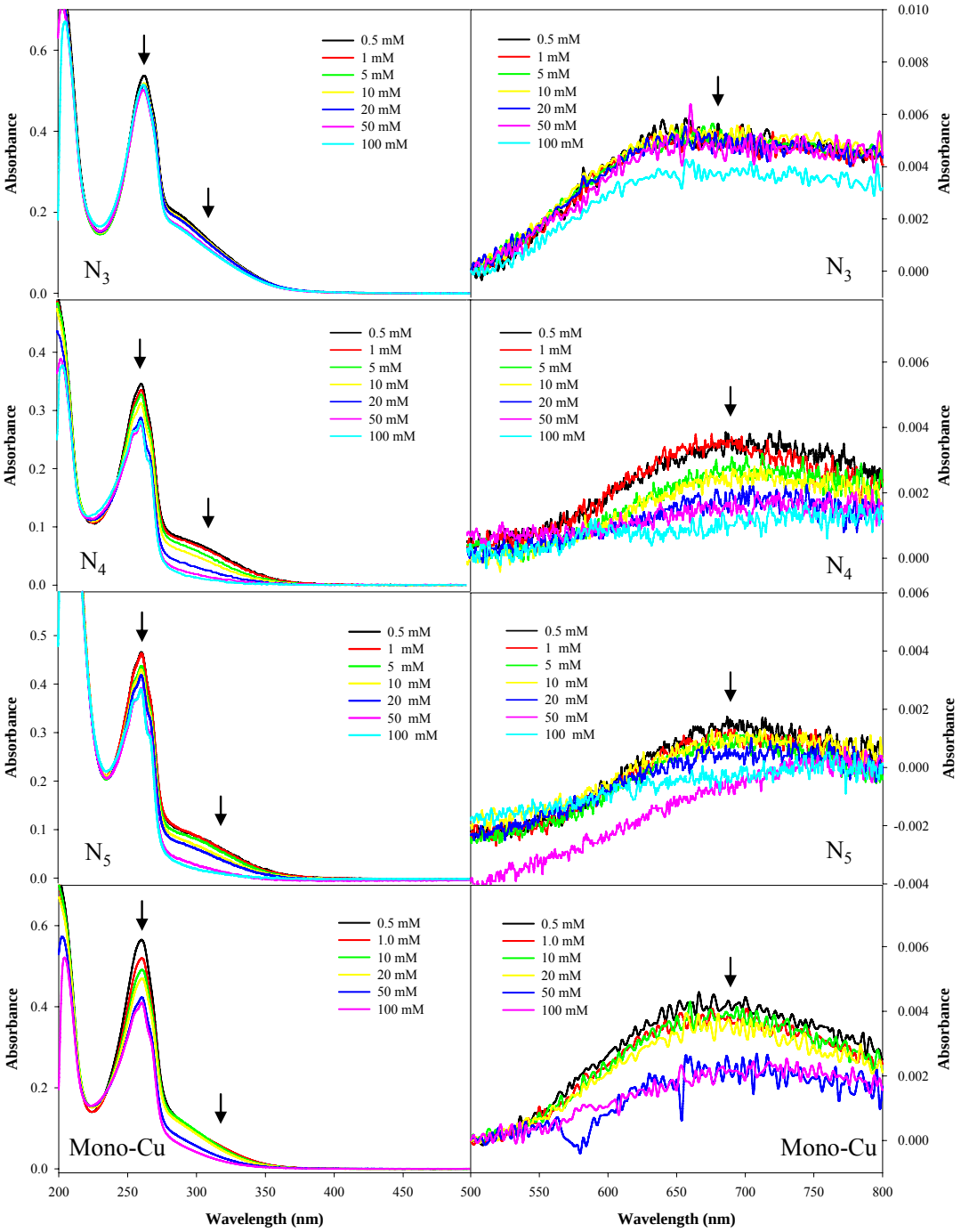


**Figure 2.6 Phosphate dependence of the absorption spectra of Cu(II) complexes**

$Cu^{II}_2$**N3-5** (20 μM) complexes or mono-Cu(II) complex (39 μM) were dissolved in phosphate buffer at concentrations ranging from 0.5 mM to 100 mM at pH 7.0.

With increasing phosphate concentration, formation of the intermediate generated by $Cu^{II}_2\mathbf{N_4}$ and $Cu^{II}_2\mathbf{N_5}$ was suppressed (Figure 2.7, 2.9). Moreover, high concentration of phosphate (50 or 100 mM) obviously altered the absorption spectra of $Cu^{II}_2\mathbf{N_4}$ and $Cu^{II}_2\mathbf{N_5}$ in the presence of $H_2O_2$, suggesting that speciation was changed and new reaction pathways were thus created. The shift of the isosbestic point from ~300 nm to ~350 nm with increasing phosphate concentration suggested that reactions proceeded through different pathways, thus leading to different products (Figure 2.7). The change in speciation by high concentrations of phosphate in $Cu^{II}_2\mathbf{N_4}$ and $Cu^{II}_2\mathbf{N_5}$ systems was probably due to coordination of phosphate to copper centers.

However, phosphate concentration did not alter substantially the absorption spectra of $Cu^{II}_2\mathbf{N_3}$ in the presence of $H_2O_2$ as shown in Figure 2.8. The increase of absorption at 376 nm over time might be due to the accumulation of product(s) which had slight absorption at this wavelength. These results suggested that the reaction of $Cu^{II}_2\mathbf{N_3}$ with $H_2O_2$ did not proceed through the intermediate, and that phosphate did not substantially alter the speciation of $Cu^{II}_2\mathbf{N_3}$ in the presence of $H_2O_2$.

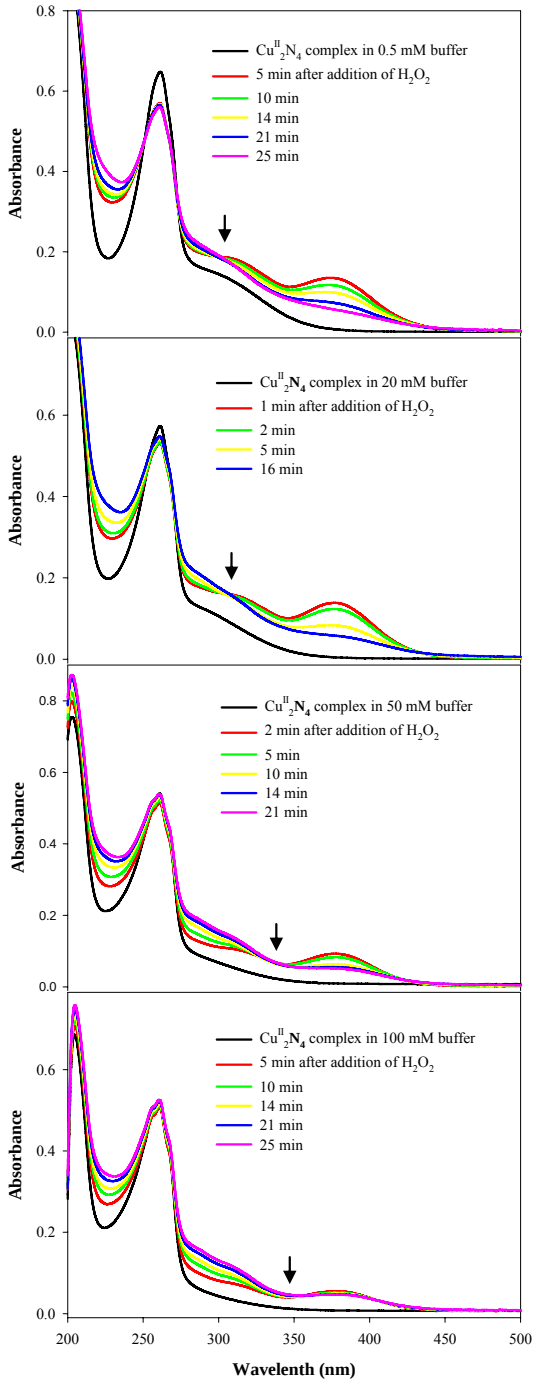


**Figure 2.7 Effect of phosphate concentration on the absorption spectrum of $Cu^{II}_2N_4$ in the presence of $H_2O_2$**

$Cu^{II}_2$**$N_4$** complex (40 μM) was dissolved in phosphate buffer with varying concentrations (0.5 mM, 20 mM, 50 mM or 100 mM) at pH 7.0. $H_2O_2$ (200 μM) was added to initiate the reaction under anaerobic conditions.

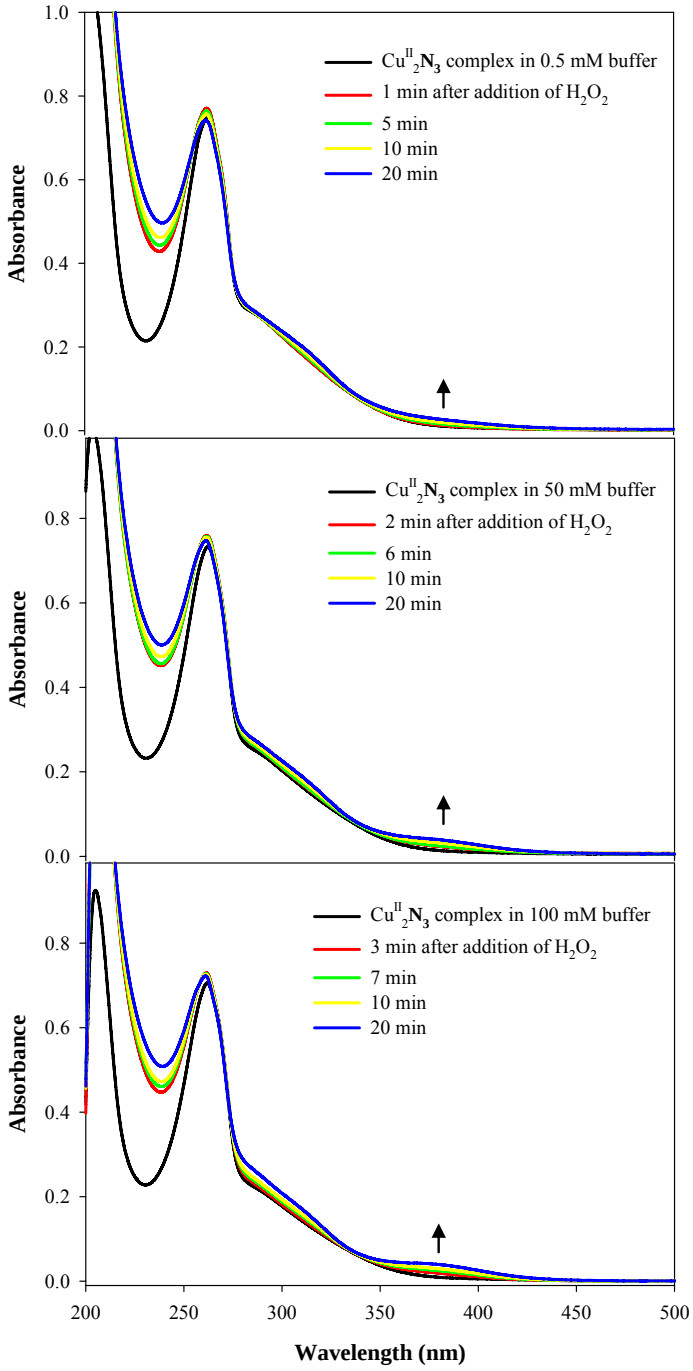


**Figure 2.8 Effect of phosphate concentration on the absorption spectrum of $Cu^{II}_2N_3$ in the presence of $H_2O_2$**

$Cu^{II}_2$**N$_3$** complex (30 μM) was dissolved in phosphate buffer with varying concentrations (0.5 mM, 50 mM or 100 mM) at pH 7.0. $H_2O_2$ (3.0 mM) was added to initiate the reaction under anaerobic conditions.

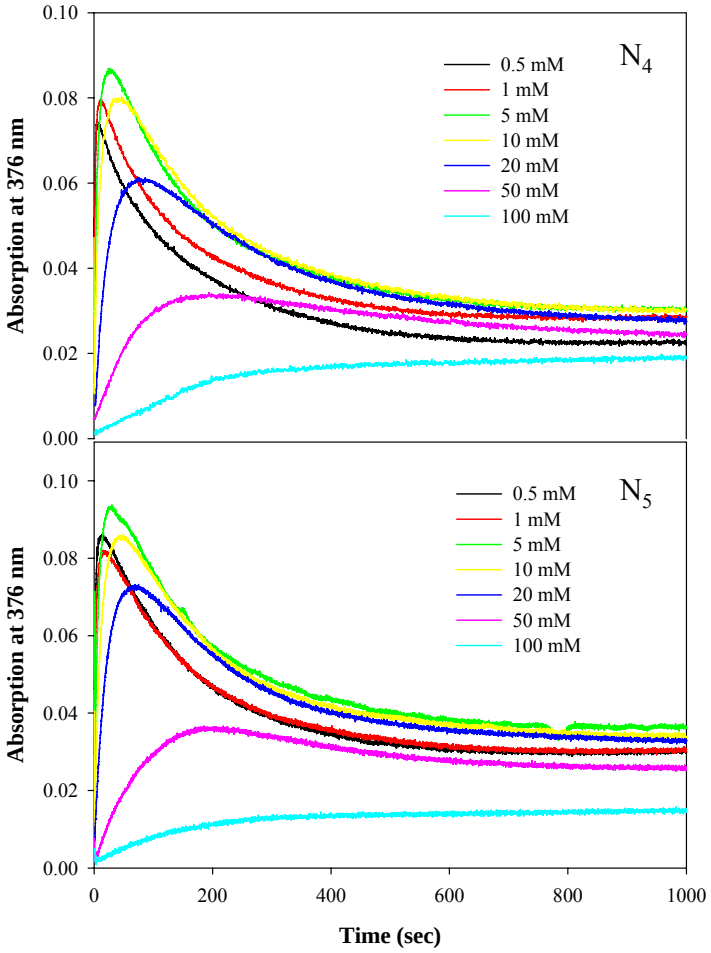


**Figure 2.9 Effect of phosphate concentration on absorption at 376 nm for $Cu^{II}_2N_{4,5}$ complexes in the presence of $H_2O_2$**

$Cu^{II}_2\mathbf{N_{4,5}}$ complex (20 μM) was dissolved in phosphate buffer at concentrations ranging from 0.5 mM to 100 mM at pH 7.0. $H_2O_2$ (200 μM) was added to initiate the reaction under anaerobic conditions. Absorption at 376 nm was then recorded over time.

As shown in Figure 2.10, $Cu^{II}_2\mathbf{N_4}$, $Cu^{II}_2\mathbf{N_5}$ and mono-$Cu^{II}$ complexes were sensitive to pH of solutions and exhibited similar changes in their absorption spectra. With decreasing pH, the absorption bands at 260 nm, 300 nm and 700 nm were obviously suppressed, probably due to the protonation of ligand weakening the binding of the ligand to the copper centers. The decrease of the absorption band at 300 nm and d-d transition band at high pH (eg. pH 10.0) might be due to hydrolysis of Cu(II) complex at this pH.

By contrast, the absorption spectrum of $Cu^{II}_2\mathbf{N_3}$ was reactively insensitive to pH change. Only small changes in absorption spectra of $Cu^{II}_2\mathbf{N_3}$ were observed when pH ranged from 5 to 10.

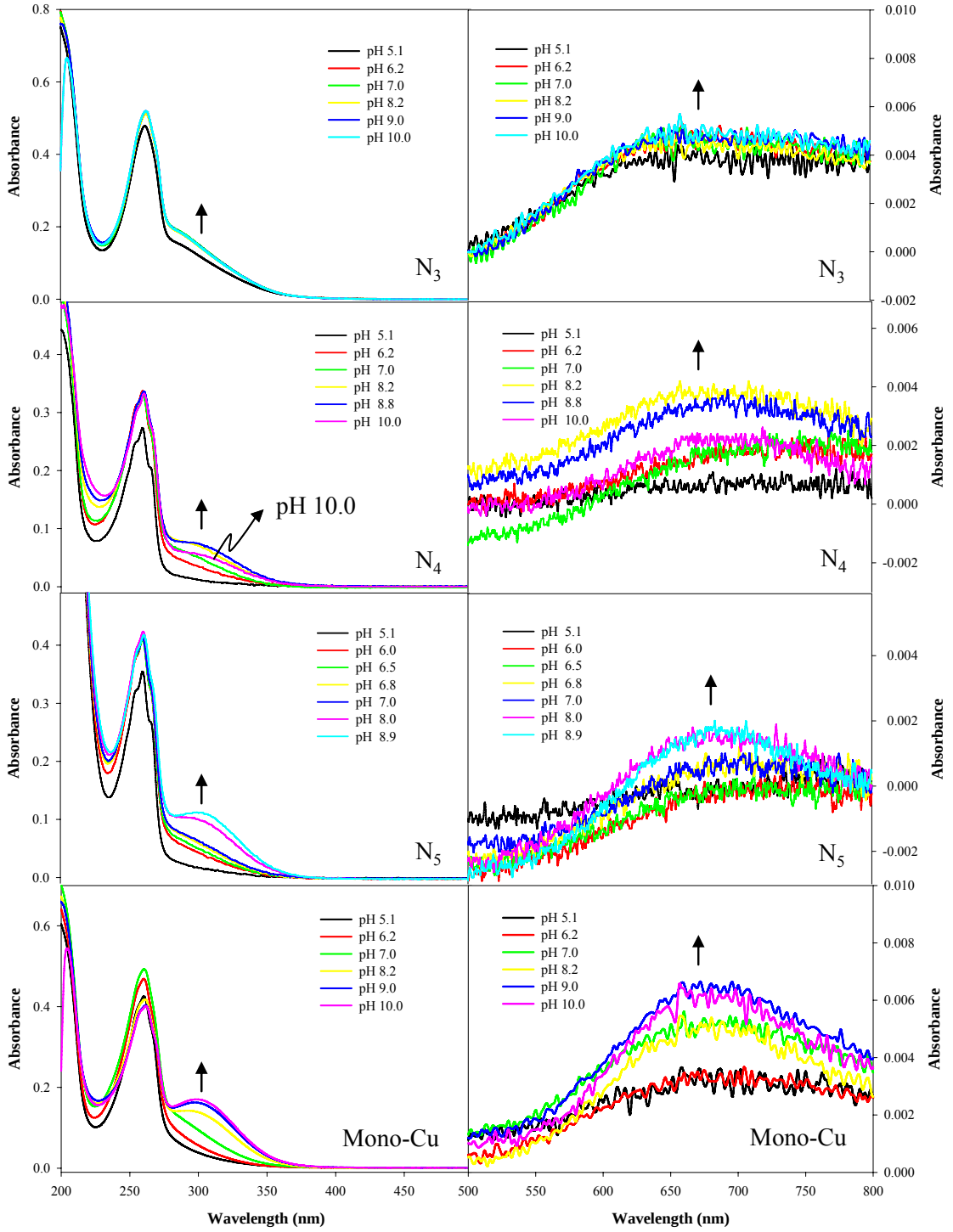


**Figure 2.10 pH dependence of the absorption spectra of Cu(II) complexes**

$Cu^{II}_2$**N3-5** (20 μM) complexes or mono-Cu(II) complex (39 μM) were dissolved in 10 mM phosphate buffer at pH ranging from 5 to 10.

The formation of the intermediate generated by $Cu^{II}_2\mathbf{N_4}$ and $Cu^{II}_2\mathbf{N_5}$ was strongly pH dependent. Both full absorption spectra (Figure 2.11) and change of absorption at 376 nm (Figure 2.13) at different pH indicated that the intermediate was only generated at near neutral pH (6-8). The intermediate generation was eliminated at pH $\leq$ 5 and pH $\geq$ 9. The obvious alterations in absorption spectra at either low or high pH suggested changes in speciation, which is probably due to either complete protonation of the ligand (at low pH) or strong hydrolysis of Cu(II) complexes (at high pH). Although a very similar pH dependence was observed in both $Cu^{II}_2\mathbf{N_4}$ and $Cu^{II}_2\mathbf{N_5}$ systems (Figure 2.13), the intermediate generated from $Cu^{II}_2\mathbf{N_5}$ was more sensitive to pH than that formed with $Cu^{II}_2\mathbf{N_4}$. For $Cu^{II}_2\mathbf{N_4}$ complex, when the pH of solution was increased from 7.0 to 8.2, the decay rate was almost constant. By contrast, the intermediate decay rate doubled when the pH was changed from 7.0 to 8.1 for $Cu^{II}_2\mathbf{N_5}$ system, implying that intermediate generated from $Cu^{II}_2\mathbf{N_5}$ complex is not as stable as that generated from $Cu^{II}_2\mathbf{N_4}$ complex.

Although some changes in the absorption spectra of $Cu^{II}_2\mathbf{N_3}$ in the presence of $H_2O_2$ were observed at different pH, the overall effect was small (Figure 2.12).

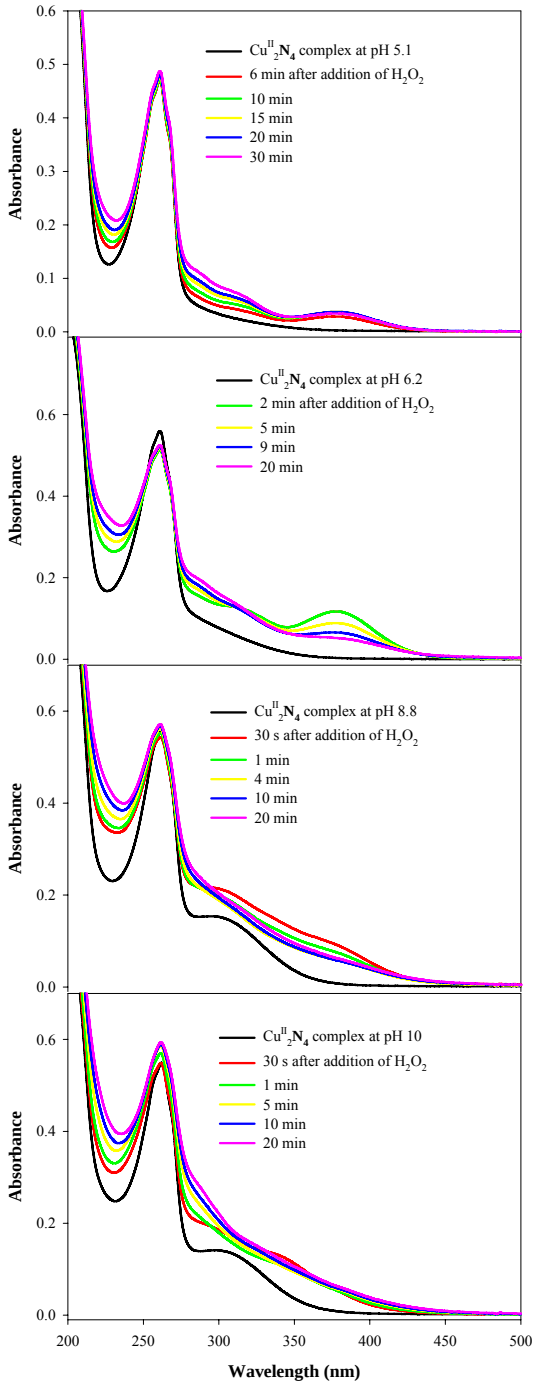


**Figure 2.11 Effect of pH on the absorption spectrum of the $Cu^{II}_2N_4$ complex in the presence of $H_2O_2$**

$Cu^{II}_2$**N$_4$** complex (40 µM) was dissolved in 10 mM phosphate buffer at different pH (5.1, 6.2, 8.8 or 10.0). $H_2O_2$ (200 µM) was added to initiate the reaction under anaerobic conditions.

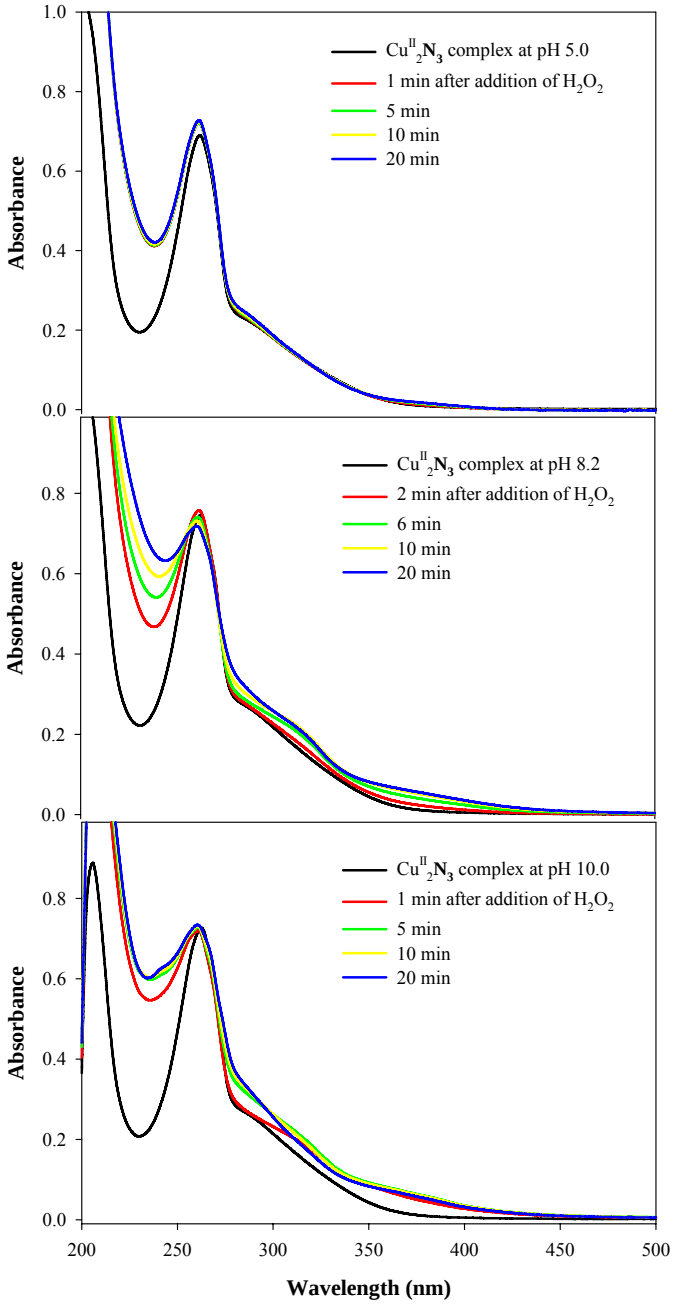


**Figure 2.12 Effect of pH on the absorption spectrum of $Cu^{II}_2N_3$ complex in the presence of $H_2O_2$**

$Cu^{II}_2$**N$_3$** complex (30 μM) was dissolved in 10 mM phosphate buffer at different pH (5.1, 8.2 or 10.0). $H_2O_2$ (3.0 mM) was added to initiate the reaction under anaerobic conditions.

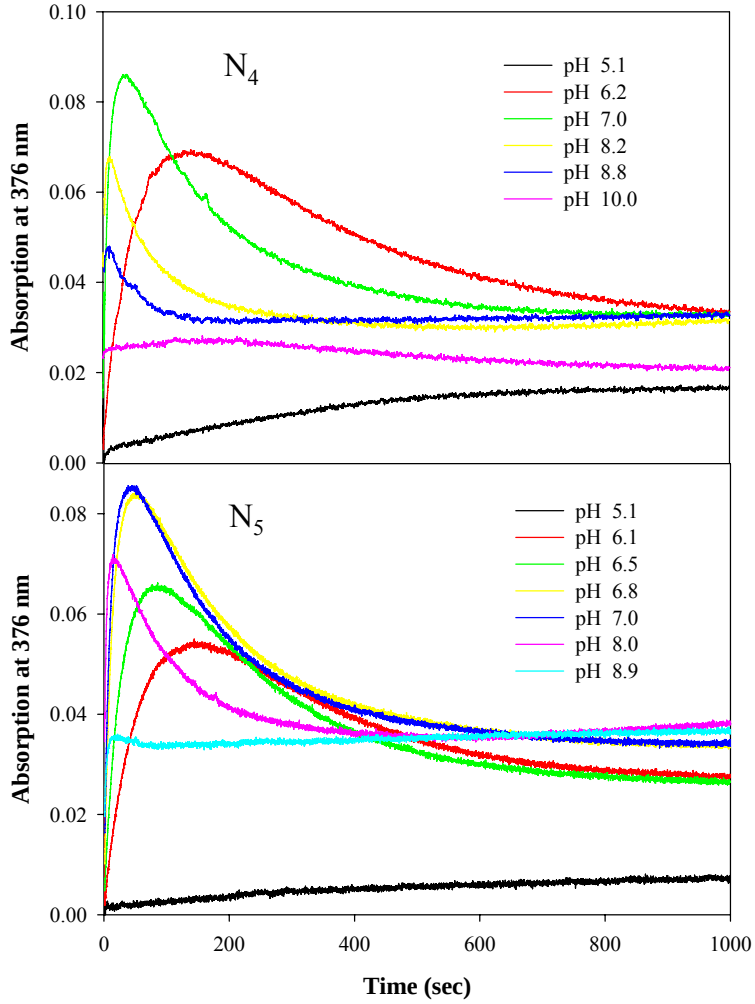


**Figure 2.13 Effect of pH on absorption at 376 nm for $Cu^{II}_2N_{4,5}$ complexes in the presence of $H_2O_2$**

$Cu^{II}_2$**N**$_{4,\ 5}$ complex (20 µM ) was dissolved in 10 mM phosphate buffer at pH ranging from 5.1 to 10.0. $H_2O_2$ (200 µM) was added to initiate the reaction under anaerobic conditions. Absorption at 376 nm was then measured as a function of time.

### 2.3.3 Kinetics of Intermediate Formation and Decay

Kinetics of the formation and decay of the intermediate generated by $Cu^{II}_2\mathbf{N_4}$ and $Cu^{II}_2\mathbf{N_5}$ was examined spectrophotometrically at 376 nm in 10 mM phosphate buffer at pH 6.8. Cu (II) complex concentration was kept constant, with $H_2O_2$ concentration (at least ten fold excess) varied to initiate the reaction under anaerobic conditions. Although the decay of the intermediate was independent of the $H_2O_2$ concentration in both $Cu^{II}_2\mathbf{N_4}$ and $Cu^{II}_2\mathbf{N_5}$ systems, its formation was accelerated with increasing $H_2O_2$ concentration, consistent with the following reaction scheme 2.2.

$$Cu^{II}_2N_{4,5} + H_2O_2 \xrightarrow{k_1} \text{Intermediate} \xrightarrow{k_2} \text{Product}$$

**Scheme 2.2 Reaction scheme of $Cu^{II}_2N_{4,5}$ with $H_2O_2$**

An analytical solution for this reaction scheme was obtained from Rodigun and Rodiguina[139] shown in Equation 2.1.

$$A = \left( X\frac{k_1}{k_2 - k_1} + Y \right) e^{-k_1 \cdot t} - X\frac{k_1}{k_2 - k_1} e^{-k_2 \cdot t} + Z \qquad 2.1$$

$$X = C_0^0(\varepsilon_1 - \varepsilon_2)b \;, \quad Y = C_0^0(\varepsilon_0 - \varepsilon_2)b \;, \quad Z = C_0^0\,\varepsilon_2 b$$

In Equation 2.1, A is absorption at 376 nm, $k_1$ is the pseudo-first order rate constant for the formation of the intermediate, $k_2$ is decay rate constant of the intermediate, $C_0^0$ is initial concentration of Cu(II) complex, $\varepsilon_0$, $\varepsilon_1$ and $\varepsilon_2$ are extinction coefficients of Cu(II) complex, intermediate and product at 376 nm, respectively and b is the length of cuvette. Some of examples of curve fitting are shown in Figure 2.15. Values of X, Y, Z, $k_1$, $k_2$ were obtained from curve fittings. Based on fittings to a family of curves (see for example, Figure 2.14), X, Y, Z and $k_2$ were found to be constant in agreement with the

kinetic model. The values of these parameters and the uncertainties derived from the curve fittings to a family of curves are shown in Table 2.1.

**Table 2.1 Values of parameters obtained from curve fitting**

| | $k_2$ | X | Y | Z |
|---|---|---|---|---|
| $Cu^{II}_2N_4$ | 0.0081±0.0004 | 0.066±0.003 | -0.0011±0.0007 | 0.038±0.001 |
| $Cu^{II}_2N_5$ | 0.0079±0.0001 | 0.078±0.003 | -0.0021±0.001 | 0.045±0.002 |

As shown in Table 2.2 and Figure 2.14, a linear relation was obtained between the pseudo first order rate constants for formation ($k_1$) and $H_2O_2$ concentration for both $Cu^{II}_2N_4$ and $Cu^{II}_2N_5$ systems, indicating that the intermediate formation is first order with respect to $H_2O_2$. The excellent fitting of the experiment data to Equation 2.1 is also consistent with the intermediate formation being first order with respect to the Cu (II) complex concentration.

**Table 2.2 $H_2O_2$ dependence of $k_1$ obtained from curve fitting**

| $Cu^{II}_2N_4$ | | $Cu^{II}_2N_5$ | |
|---|---|---|---|
| $H_2O_2$ (M) | $K_1$ ($s^{-1}$) | $H_2O_2$ (M) | $K_1$ ($s^{-1}$) |
| $2.1 \times 10^{-4}$ | $6.1 \times 10^{-2}$ | $2.0 \times 10^{-4}$ | $3.0 \times 10^{-2}$ |
| $4.2 \times 10^{-4}$ | $1.1 \times 10^{-1}$ | $4.0 \times 10^{-4}$ | $5.2 \times 10^{-2}$ |
| $6.3 \times 10^{-4}$ | $1.6 \times 10^{-1}$ | $6.0 \times 10^{-4}$ | $7.4 \times 10^{-2}$ |
| $8.4 \times 10^{-4}$ | $2.1 \times 10^{-1}$ | $8.0 \times 10^{-4}$ | $1.0 \times 10^{-1}$ |
| $1.7 \times 10^{-3}$ | $4.1 \times 10^{-1}$ | $1.6 \times 10^{-3}$ | $1.7 \times 10^{-1}$ |
| / | / | $2.0 \times 10^{-3}$ | $2.2 \times 10^{-1}$ |

However, to further test this, the dependence of the intermediate formation on the concentration of Cu(II) complex was examined (Figure 2.16). Since, at early times, the absorption at 376 nm is proportional to the intermediate concentration, the change of absorption at 376 nm with time was used to calculate the initial rate of the intermediate

formation. As shown in Figure 2.16, the plot of the initial formation rate versus the Cu (II) complex concentration increased linearly, confirming that formation of the intermediate is first order with respect to Cu (II) complex. Further, intermediate decay was independent of the Cu(II) complex concentration, indicating that decay of the intermediate does not occur through a bimolecular reaction of two molecules of the intermediate.

The formation rate constants of the intermediate generated from the $Cu^{II}_2\mathbf{N_4}$ and $Cu^{II}_2\mathbf{N_5}$ complexes were 250 ± 2 $M^{-1}s^{-1}$ and 110 ± 4 $M^{-1}s^{-1}$, respectively, at 26.5 $^oC$. The errors were obtained from the standard error of the slope of the plot of the pseudo first order formation rate constant ($k_1$) versus $H_2O_2$ concentration. The rate constant of the intermediate formation obtained from $Cu^{II}_2\mathbf{N_4}$ complex system is almost double of that obtained from $Cu^{II}_2\mathbf{N_5}$ complex system, suggesting that the structures of complexes (length of the bridge in this case) may play an important role on the intermediate formation. The decay rate constants were comparable, 0.0083 $s^{-1}$ for $Cu^{II}_2\mathbf{N_4}$ complex and 0.0079 $s^{-1}$ for $Cu^{II}_2\mathbf{N_5}$ complex, respectively, at 26.5$^oC$.

Decay of the intermediate was found not to be affected by externally added catalase as long as the intermediate formation was complete prior to catalase addition. In the presence of 1.5 units/ml catalase, the rate coefficients of intermediate decay were 0.34 $min^{-1}$ for $Cu^{II}_2\mathbf{N_4}$ system and 0.35 $min^{-1}$ for $Cu^{II}_2\mathbf{N_5}$ system, which were comparable to those obtained from the experiments in the absence of catalase , 0.29 $\pm$0.05 $min^{-1}$ for $Cu^{II}_2\mathbf{N_4}$ system and 0.32 $\pm$0.05 $min^{-1}$ for $Cu^{II}_2\mathbf{N_5}$ system. The uncertainties represent $\pm$ one standard deviation from the average of at least three independent experiments. This result indicates that the formation reaction of the intermediate is irreversible.

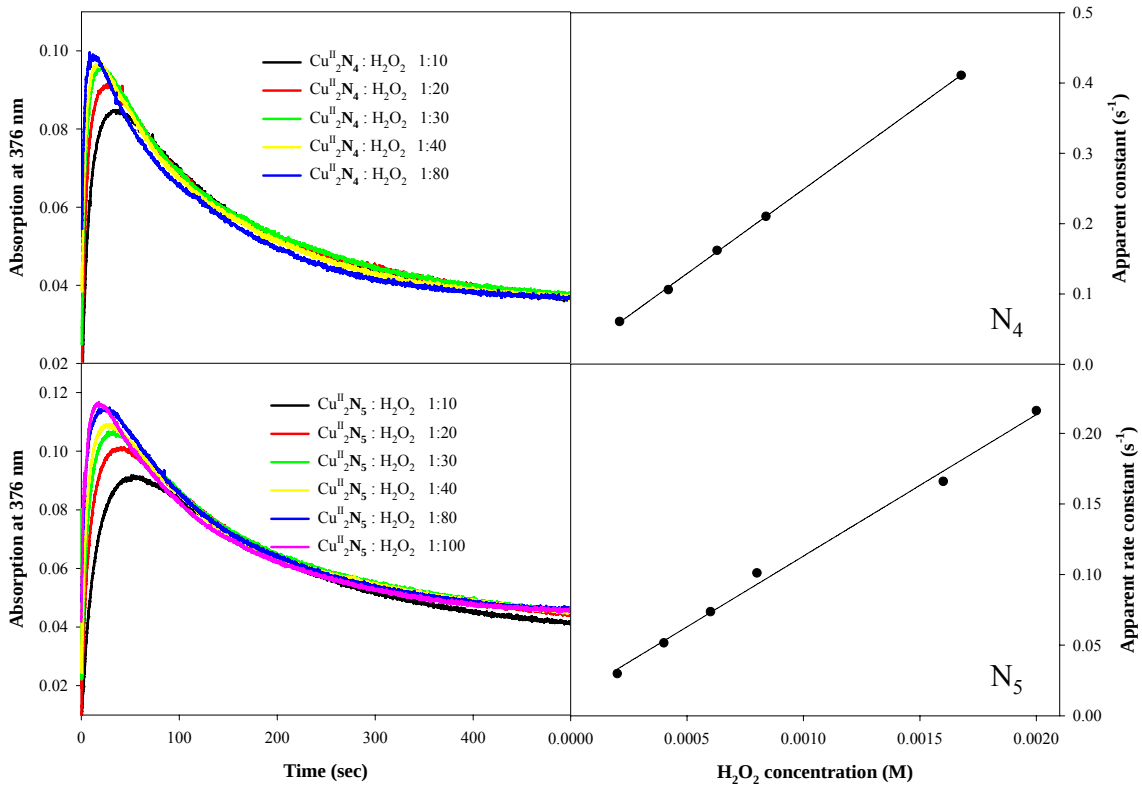


**Figure 2.14 Dependence of the formation and decay of the intermediate on $H_2O_2$ concentration for $Cu^{II}_2N_{4,5}$ complexes**

$Cu^{II}_2\mathbf{N_4}$ (21 μM) or $Cu^{II}_2\mathbf{N_5}$ (20 μM ) was dissolved in phosphate buffer (10 mM, pH 6.8) at 26.5 $^oC$. $H_2O_2$ with varying concentration (210 μM, 420 μM, 630 μM, 840 μM and 1680 μM for $Cu^{II}_2\mathbf{N_4}$ system or 200 μM, 400 μM, 600 μM, 800 μM, 1.6 mM and 2.0 mM for $Cu^{II}_2\mathbf{N_5}$ system) was added to initiate the reaction under anaerobic conditions. Absorption at 376 nm was then recorded as a function of time (left panels). The molar ratios of $Cu^{II}_2\mathbf{N_{4,5}}$ complex to $H_2O_2$ are shown in legend. The plot of the apparent formation rate constant versus $H_2O_2$ concentration is also shown (right panels).

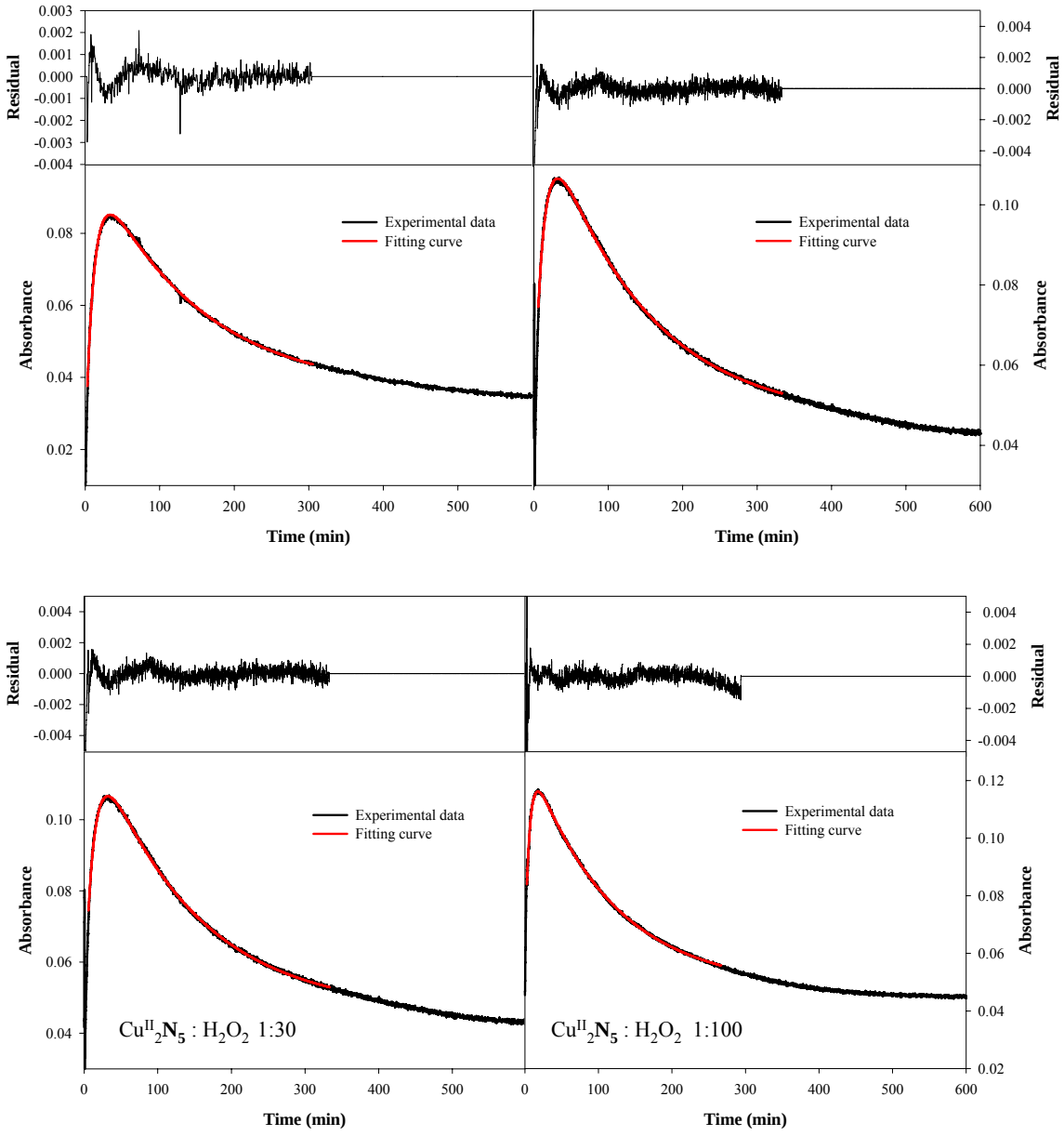


**Figure 2.15 Fits to the formation and decay of the intermediate for $Cu^{II}_2N_{4,5}$ complexes at 376 nm**

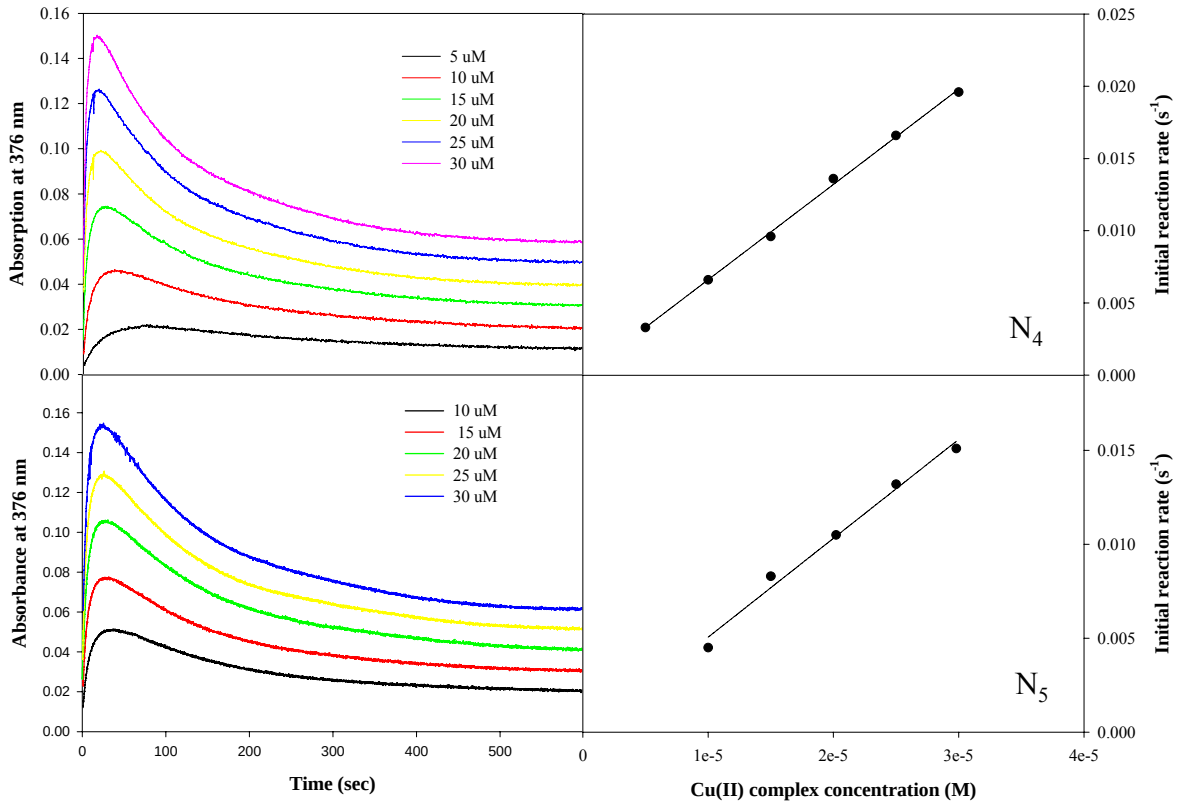


**Figure 2.16 Dependence of the formation and decay of the intermediate on the concentration of $Cu^{II}_2N_{4,5}$ complexes.**

$Cu^{II}_2$**N4,5** complex with varying concentrations (shown in legend) was dissolved in phosphate buffer (10 mM, pH 6.8). $H_2O_2$ (600 μM) was added to initiate reaction under anaerobic conditions. Absorption at 376 nm was then recorded over time (left panels). The plot of initial formation rate of the intermediate versus Cu(II) complex concentration is also shown (right panels).

The kinetics of formation and decay of the intermediate generated by mono-$Cu^{II}$ complex was also investigated (Figure 2.17). The results clearly showed that the intermediate generation in mono-$Cu^{II}$ system was slow although the $H_2O_2$ concentration was at least 30 times higher than that used in $Cu^{II}_2\mathbf{N_4}$ and $Cu^{II}_2\mathbf{N_5}$ systems. Further, the kinetics of formation of the intermediate could not be fit to Equation 2.1 (Figure 2.18), suggesting a more complicated mechanism for its formation. As with $Cu^{II}_2\mathbf{N_4}$ and $Cu^{II}_2\mathbf{N_5}$, the decay of the intermediate formed from mono-$Cu^{II}$ complex was independent of $H_2O_2$ concentration. The rate constant for decay was acquired from data collected at long times. When the formation of the intermediate was complete, at these long times, plots of ln(absorption) versus time were linear with the slope producing rate constant for decay of 0.0077 $s^{-1}$ at 26.5 $^{o}$C. This value was comparable to those obtained from $Cu^{II}_2\mathbf{N_4}$ (0.0081 $s^{-1}$) and $Cu^{II}_2\mathbf{N_5}$ (0.0079 $s^{-1}$) at same temperature, further suggesting that the intermediates generated from $Cu^{II}_2\mathbf{N_4}$, $Cu^{II}_2\mathbf{N_5}$ and mono-$Cu^{II}$ complexes possess similar structures.

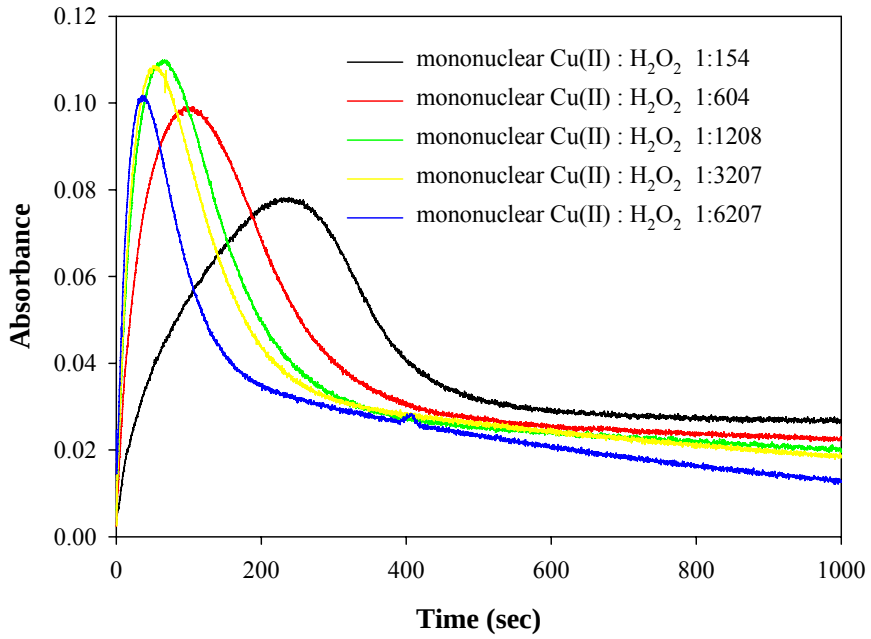


**Figure 2.17 Dependence of the formation and decay of the intermediate on $H_2O_2$ concentration for mono-$Cu^{II}$ complex**

Mono-$Cu^{II}$ complex (39 μM) was dissolved in phosphate buffer (10 mM, pH 6.8). $H_2O_2$ with varying concentrations (6.1 mM, 23.8 mM, 47.6 mM, 122.3 mM or 244.6 mM) was added to initiate the reaction under anaerobic conditions. Absorption at 376 nm was then recorded over time. The molar ratios of mono-$Cu^{II}$ complex to $H_2O_2$ are shown in legend.

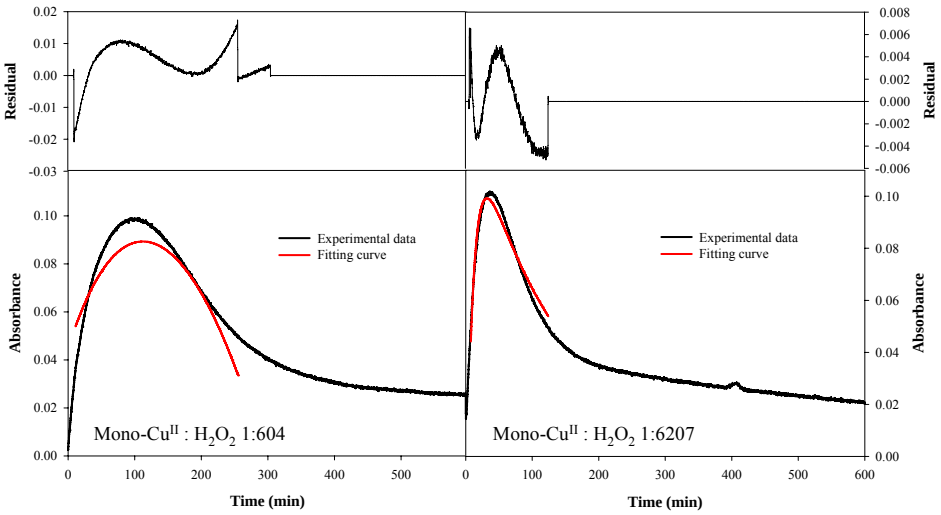


**Figure 2.18 Fits to the formation and decay of the intermediate for mono-$Cu^{II}$ complex at 376 nm**

The kinetics of formation and decay of the intermediate formed from $Cu^{II}_2\mathbf{N_4}$ and $Cu^{II}_2\mathbf{N_5}$ complexes depended strongly on temperature. The half-life of the intermediate formed from the $Cu^{II}_2\mathbf{N_4}$ complex was almost 30 minutes at 3 $^{o}$C, approximately eight times longer than that at 20 $^{o}$C (Figure 2.19). The temperature dependence of the rate constants for decay was employed to calculate activation energy for the decay of the intermediate. The activation energies of the intermediate decay are 78 ± 5 kJ/mol for $Cu^{II}_2\mathbf{N_4}$ complex and 74 ± 4 kJ/mol for $Cu^{II}_2\mathbf{N_5}$ complex, respectively. The errors were derived from the standard error of the slope of the plot of ln(rate constant for decay) versus (1/temperature) shown in insets of Figure 2.19. The similar activation energies is consistent with the kinetic results described above, which indicate that the decay rate constants for these binuclear Cu(II) complexes are also similar. Since formation of the intermediate was too fast to obtain sufficient data points at higher temperature, the activation energy for the intermediate formation was not acquired from these experiments. A more rapid kinetic method, such as stopped-flow, is needed to obtain these data.

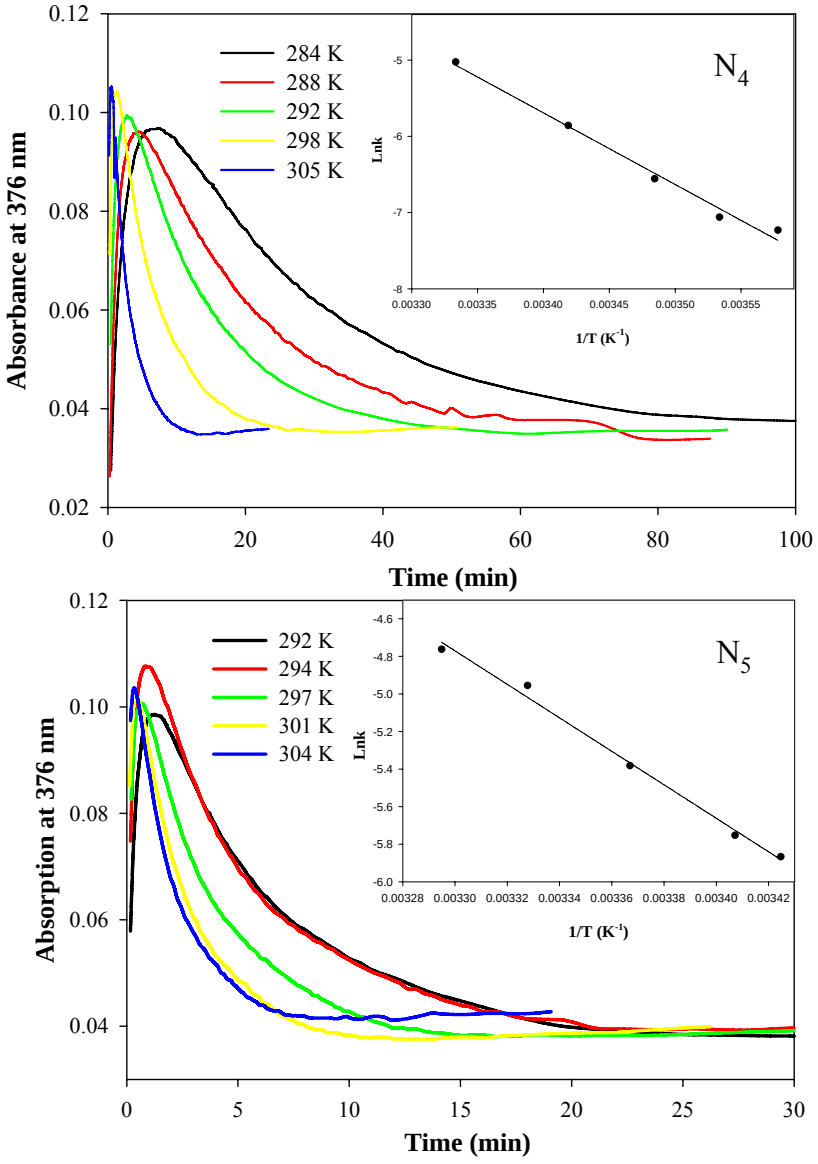


**Figure 2.19 Temperature dependence of the formation and decay of the intermediate formed with $Cu^{II}_2N_{4,5}$ complexes.**

$Cu^{II}_2$**N4** complex (23 μM) or $Cu^{II}_2$**N5** complex (20 μM) was dissolved in phosphate buffer ( 10 mM, pH 6.8). Both Cu(II) complex and $H_2O_2$ solutions were equilibrated at certain temperature for 30 minutes before $H_2O_2$ (230 μM for $Cu^{II}_2$**N4** system or 600 μM for $Cu^{II}_2$**N5** system) was added to initiate the reaction under anaerobic conditions. Absorption at 376 nm was then recorded over time at different temperatures shown in the legend.

### 2.3.4 Effect of Added Electron Donors

To examine the reactivity of this intermediate, a series of electron donors, such as dimethyl sulfoxide (DMSO), glucose, 3-amino-2,2,5,5-tetramethyl-1-pyrrolidinyloxy (3-ap), dimethylaniline (DMA), 3-mercaptopropionic acid (3-MPA), benzoic acid and guanine, were added following completion of the intermediate formation. The decay of the intermediate in the presence of these electron donors was then monitored and compared with that obtained from experiments in the absence of added electron donors.

For $Cu^{II}_2\mathbf{N_4}$ complex system, experiments indicated that the decay of the intermediate was not accelerated by any of these electron donors, suggesting that this intermediate was unreactive with these compounds (Table 2.3). Results also showed that the rate coefficients in the absence of electron donors under anaerobic conditions ($0.29 \pm 0.05$ $min^{-1}$) and under aerobic conditions ($0.26 \pm 0.04$ $min^{-1}$) were comparable, indicating that the intermediate decay was also dioxygen-independent.

Compared with the intermediate generated from $Cu^{II}_2\mathbf{N_4}$ complex, the decay of the intermediate generated by $Cu^{II}_2\mathbf{N_5}$ complex was affected by some of the electron donors, but the overall effect was very small. As shown in Table 2.4, the decay of the intermediate was not accelerated by glucose, benzoic acid, DMSO and guanine, but was slightly accelerated by 3-ap, 3-MPA and DMA at relatively high concentration. When guanine was used as an electron donor, the intermediate decay observed in $Cu^{II}_2\mathbf{N_5}$ system was obviously higher than that observed in $Cu^{II}_2\mathbf{N_4}$ system, owing to the more rapid decay of $Cu^{II}_2\mathbf{N_5}$ complex at higher pH (See section 2.3.2). Overall, the intermediate generated from the $Cu^{II}_2\mathbf{N_4}$ and $Cu^{II}_2\mathbf{N_5}$ complexes was not highly reactive

with added electron donors, suggesting that this intermediate is unlikely to be the reactive species responsible for the DNA cleavage, particularly in the case of $Cu^{II}_2\mathbf{N_4}$.

**Table 2.3 Effect of added electron donors on the decay of the intermediate formed from $Cu^{II}_2N_4$ complex**

| External electron donors | Electron donor concentration | Decay of intermediate in the presence of electron donor | Decay of intermediate in the absence of electron donor (control experiment) |
|---|---|---|---|
| Glucose * | 40 mM | 0.25 $min^{-1}$ | 0.26 ± 0.04 $min^{-1}$ |
| Benzoic acid | 1.3 mM | 0.29 $min^{-1}$ | 0.29 ± 0.05 $min^{-1}$ |
| 3-ap | 1.4 mM | 0.29 $min^{-1}$ | 0.29 ± 0.05 $min^{-1}$ |
| Guanine ** | 300 uM | 0.33 ± 0.02 $min^{-1}$ | 0.32 ± 0.01 $min^{-1}$ |
| DMSO | 39 mM | 0.24 $min^{-1}$ | 0.29 ± 0.05 $min^{-1}$ |
| N,N-dimethyl-aniline *** | 8.9 mM | 0.33 $min^{-1}$ | 0.34 $min^{-1}$ |
| 3-mercaptopropionic acid | 1.5 mM | 0.33 $min^{-1}$ | 0.29 ± 0.05 $min^{-1}$ |

$Cu^{II}_2\mathbf{N_4}$ complex was dissolved in phosphate buffer (10 mM, pH 6.8). $H_2O_2$ was added to initiate the reaction under anaerobic conditions at room temperature. Solutions of different electron donors were added when the maximum absorption at 376 nm was reached. Control experiments were performed in the same manner except that phosphate buffer was injected instead of electron donor solutions. The uncertainties represent ± one standard deviation from the average of at least three independent experiments. Concentrations of DMSO and 3-ap were chosen so that the indicated concentrations could be safely used in chemical trapping experiments (see section 2.3.5 below). High concentration of 3-mercaptopropionic acid changes the speciation of the complexes. Benzoic acid and guanine with concentrations higher than those indicated in this table were not examined because of the difficulties of maintaining the pH of the solutions.

* Both control experiment and the experiment in the presence of glucose were carried out under aerobic conditions.

** Stock solution of guanine was prepared by dissolving an appropriate amount of guanine in 100 mM sodium hydroxide solution. 100 mM sodium hydroxide solution was injected instead of guanine stock solution in the control experiment. pH of reaction solution was 7.1.

*** Stock solution of N,N-dimethyl-aniline was prepared by dissolving an appropriate amount of N,N-dimethylaniline in methanol. The same volume of methanol was added instead of stock solution in the control experiment.

**Table 2.4 Effect of added electron donors on the decay of the intermediate formed from $Cu^{II}_2N_5$ complex**

| External electron donors | Electron donor concentration | Decay of intermediate in the presence of electron donor | Decay of intermediate in the absence of electron donor (control experiment) |
|---|---|---|---|
| Glucose | 40 mM | $0.37 \pm 0.02$ $min^{-1}$ | $0.32 \pm 0.05$ $min^{-1}$ |
| Benzoic acid | 1.1 mM | $0.36 \pm 0.06$ $min^{-1}$ | $0.32 \pm 0.05$ $min^{-1}$ |
| 3-ap | 1.5 mM | $0.55 \pm 0.03$ $min^{-1}$ | $0.32 \pm 0.05$ $min^{-1}$ |
| Guanine * | 310 uM | $0.52 \pm 0.06$ $min^{-1}$ | $0.50 \pm 0.02$ $min^{-1}$ |
| DMSO | 40 mM | $0.28 \pm 0.02$ $min^{-1}$ | $0.32 \pm 0.05$ $min^{-1}$ |
| N,N-dimethyl-aniline ** | 9.0 mM | $0.56 \pm 0.01$ $min^{-1}$ | $0.35 \pm 0.02$ $min^{-1}$ |
| 3-mercaptopropionic acid | 1.5 mM | $0.45 \pm 0.01$ $min^{-1}$ | $0.32 \pm 0.05$ $min^{-1}$ |

$Cu^{II}_2\mathbf{N_5}$ complex was dissolved in phosphate buffer (10 mM, pH 6.8). $H_2O_2$ was added to initiate the reaction under anaerobic conditions at room temperature. Solutions of different electron donors were added when the maximum absorption at 376 nm was reached. Control experiments were done in the same way except that same volume of phosphate buffer was injected instead of electron donor solutions The uncertainties represent ± one standard deviation from the average of at least three independent experiments. The reasons about selection of concentration of electron donors are the same as those described in Table 2.2.

* Stock solution of guanine was prepared by dissolving an appropriate amount of guanine in 100 mM sodium hydroxide solution. 100 mM sodium hydroxide solution was injected instead of guanine stock solution in the control experiment. pH of reaction solution was 7.3.

** Stock solution of N,N-dimethyl-aniline was prepared by dissolving certain amount of N,N-dimethyl-aniline in methanol. The same volume of methanol was added instead of stock solution in the control experiment.

### 2.3.5 Detection of Oxidizing Species and Preliminary Product Analysis

#### 2.3.5.1 Reaction with DMSO

To determine whether reactive species such as OH radicals were generated during the decay of the intermediate, a reaction mixture containing the $Cu^{II}_2\mathbf{N_4}$ or $Cu^{II}_2\mathbf{N_5}$ complex, 3-ap, DMSO and $H_2O_2$ under anaerobic conditions was examined for the formation of Me-3apf (III) (Scheme 2.1). In the presence of these compounds, a substantial amount of Me-3apf (retention time ~9 minutes) was observed by HPLC (Figure 2.20). No Me-3apf was produced when the Cu(II) complex, 3-ap, DMSO or $H_2O_2$ was omitted (Figure 2.20). To establish the conditions under which this reactive species could be quantitatively scavenged, the dependence of Me-3apf yield on DMSO and 3-ap was examined (Figure 2.21). At DMSO concentration above 5 mM and 3-ap concentration above 100 μM, Me-3apf yields were found to be independent of the concentration of DMSO and 3-ap. Concentrations above these values were thus employed in all subsequent studies. The observation of Me-3apf formation indicated that an oxidizing species was generated during intermediate decay, possibly the hydroxyl radical or a metal-based oxidant.

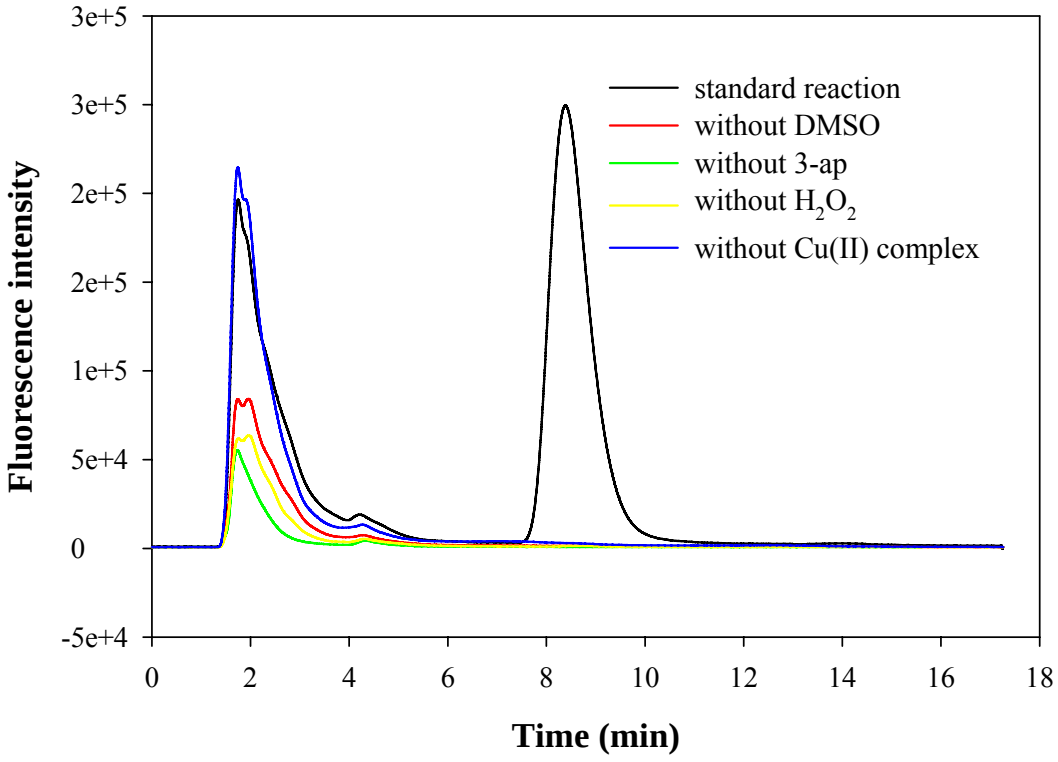


**Figure 2.20 Chromotogram of the formation of Me-3apf**

Standard reaction contained $Cu^{II}_2\mathbf{N_4}$ complex (19.6 μM), DMSO (10 mM), 3-ap (510 μM) and $H_2O_2$ (80 μM) in phosphate buffer (10 mM, pH 6.8) under anaerobic conditions. The other reactions were carried out in the absence of one of reactants shown in legend.

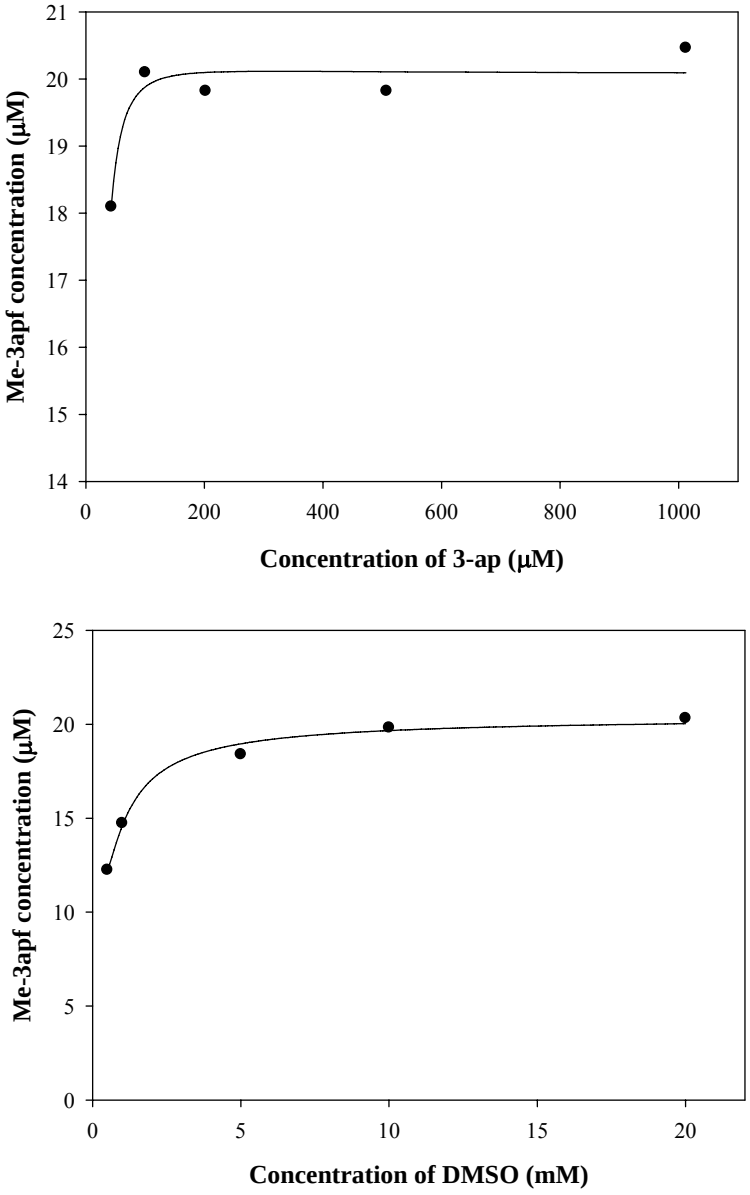


**Figure 2.21 3-ap and DMSO titration experiments**

Reaction mixture contained $Cu^{II}_2\mathbf{N_4}$ complex (20 μM), DMSO, 3-ap and $H_2O_2$ (100 μM) in phosphate buffer (10 mM, pH 6.8) under anaerobic conditions. In 3-ap titration experiments (upper panel), DMSO (10 mM) concentration was constant. In DMSO titration experiments, 3-ap (500 μM) concentration was constant. After a 20 minute reaction, an aliquot was withdrawn and immediately derivatized by fluorescamine under aerobic conditions. The derivatized sample was then analyzed by HPLC. Lines in this figure were obtained based on a fit to polynomial equation only so that the trend could be shown clearly.

The kinetics of Me-3apf formation obtained from both $Cu^{II}_2\mathbf{N_4}$ and $Cu^{II}_2\mathbf{N_5}$ systems were very similar (Figure 2.22, 2.23) and consistent with the kinetics of the intermediate decay. The continued slower formation of Me-3apf after intermediate decay was attributed to the secondary reaction of the excess hydrogen peroxide with the decomposition product(s) of the intermediate (Figure 2.22, 2.23 inner panels).

To test this possibility, catalase was added following the formation of the intermediate to remove excess $H_2O_2$ (Note that it was previously established that catalase did not affect the decay of the intermediate once formed (See section 2.3.3)). In the presence of catalase, no Me-3apf was formed at times longer than the intermediate decay, consistent with this conclusion. Based on the data (Figure 2.24), the stoichiometry between the intermediate decay and the formation of this reactive intermediate was found to be close to 1:1 for both $Cu^{II}\mathbf{N_4}$ and $Cu^{II}_2\mathbf{N_5}$.

For comparison, Me-3apf generation by $Cu^{II}_2\mathbf{N_3}$ complex and mono-$Cu^{II}$ was also investigated under identical solution conditions at low $H_2O_2$ concentration (Figure 2.25). At low $H_2O_2$ concentration, neither the mono-$Cu^{II}$ nor $Cu^{II}_2\mathbf{N_3}$ exhibits the formation of the intermediate, and little Me-3apf was formed. In contrast, $Cu^{II}_2\mathbf{N_4}$ and $Cu^{II}_2\mathbf{N_5}$ systems, which form the intermediate at these $H_2O_2$ concentrations, exhibited comparable and high efficiency for the production of Me-3apf. The different behavior of these Cu(II) complexes is consistent with their reactivity in DNA cleavage experiments, exhibiting a relationship between the intermediate formation and the subsequent formation of an oxidizing species responsible for DNA cleavage.

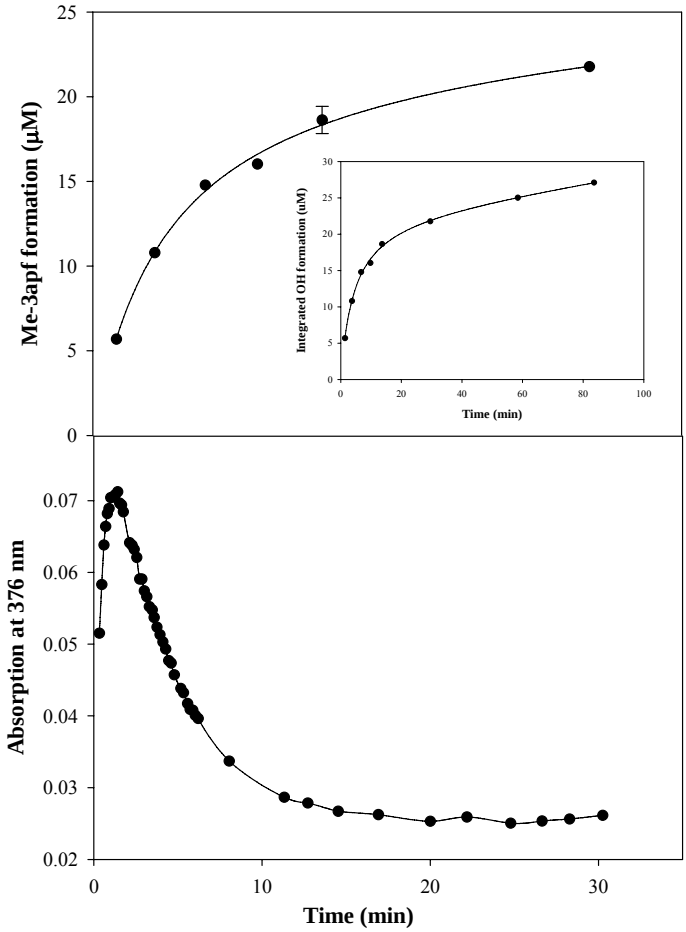


**Figure 2.22 Time course of the formation of Me-3apf and the absorption at 376 nm during decay of the intermediate formed from $Cu^{II}_2N_4$ complex**

$Cu^{II}_2$**N**$_4$ complex (20 μM), DMSO (10 mM) and 3-ap (510 μM) were dissolved in phosphate buffer (10 mM, pH 6.8). $H_2O_2$ (80 μM) was added to initiate the reaction under anaerobic conditions. Reaction was terminated at different times by derivatization with fluorescamime under aerobic conditions. Me-3apf was separated and quantified by HPLC (upper panel). Absorption at 376 nm was also measured over time (lower panel). The line in upper panel was obtained based on a fit to polynomial equation only so that the trend of Me-3apf formation could be shown clearly.

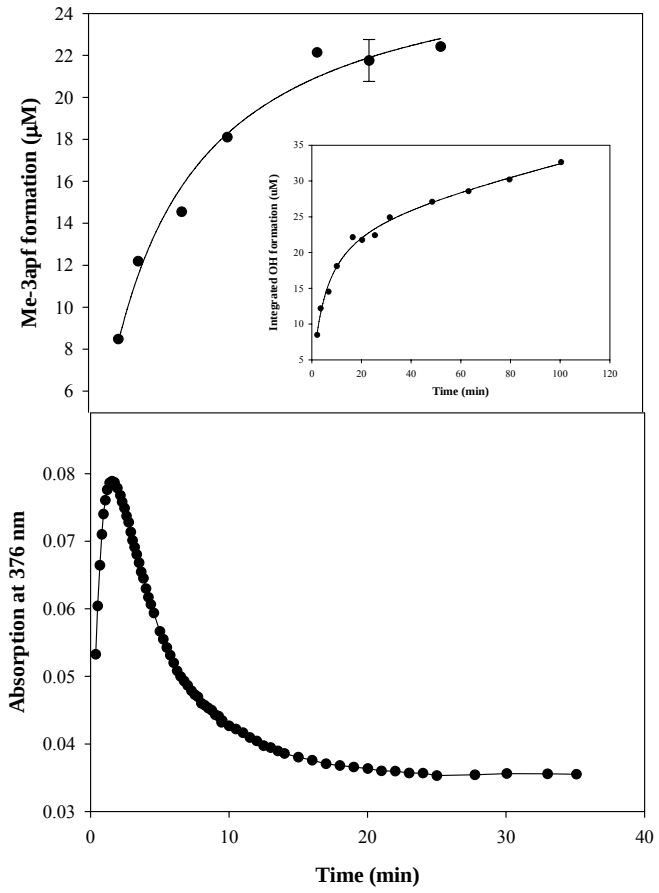


**Figure 2.23 Time course of the formation of Me-3apf and the absorption at 376 nm during decay of the intermediate formed from $Cu^{II}_2N_5$ complex**

$Cu^{II}_2$**N**$_5$ complex (20 μM), DMSO (10 mM) and 3-ap (500 μM) were dissolved in phosphate buffer (10 mM, pH 6.8). $H_2O_2$ (80 μM) was added to initiate the reaction under anaerobic conditions. Reaction was terminated at different times by derivatization with fluorescamine under aerobic conditions. Me-3apf was separated and quantified by HPLC (upper panel). Absorption at 376 nm was also measured over time (lower panel). The line in upper panel was obtained based on a fit to polynomial equation only so that the trend of Me-3apf formation could be shown clearly.

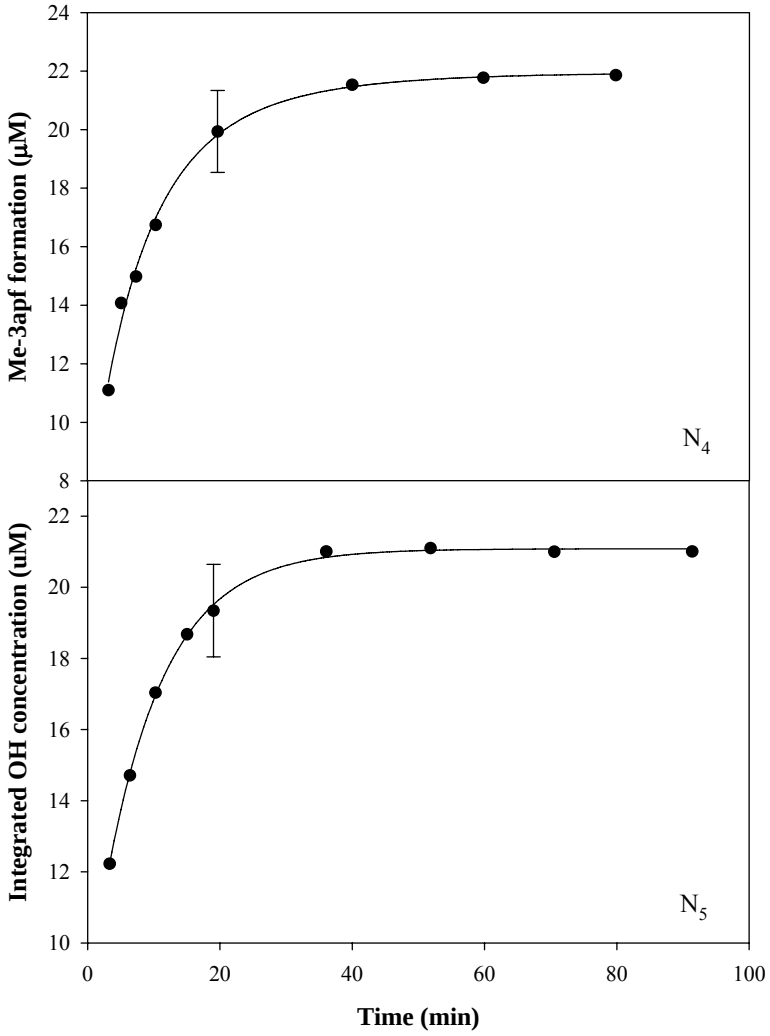


**Figure 2.24 Me-3apf formation in the presence of catalase**

$Cu^{II}_2\mathbf{N_4}$ (upper panel) or $Cu^{II}_2\mathbf{N_5}$ (below panel) complex (20.0 μM), DMSO (10 mM) and 3-ap (500 μM) were dissolved in phosphate buffer (10 mM, pH 6.8). $H_2O_2$ (80 μM) was then added to initiate the reaction under anaerobic conditions. Catalase (1.5 units/ml) was added when the intermediate formation was complete. Reaction was terminated at different times by derivatization with fluorescamine under aerobic conditions. Me-3apf was separated and quantified by HPLC. Lines in this figure were obtained based on a fit to polynomial equation only so that the trend could be shown clearly.

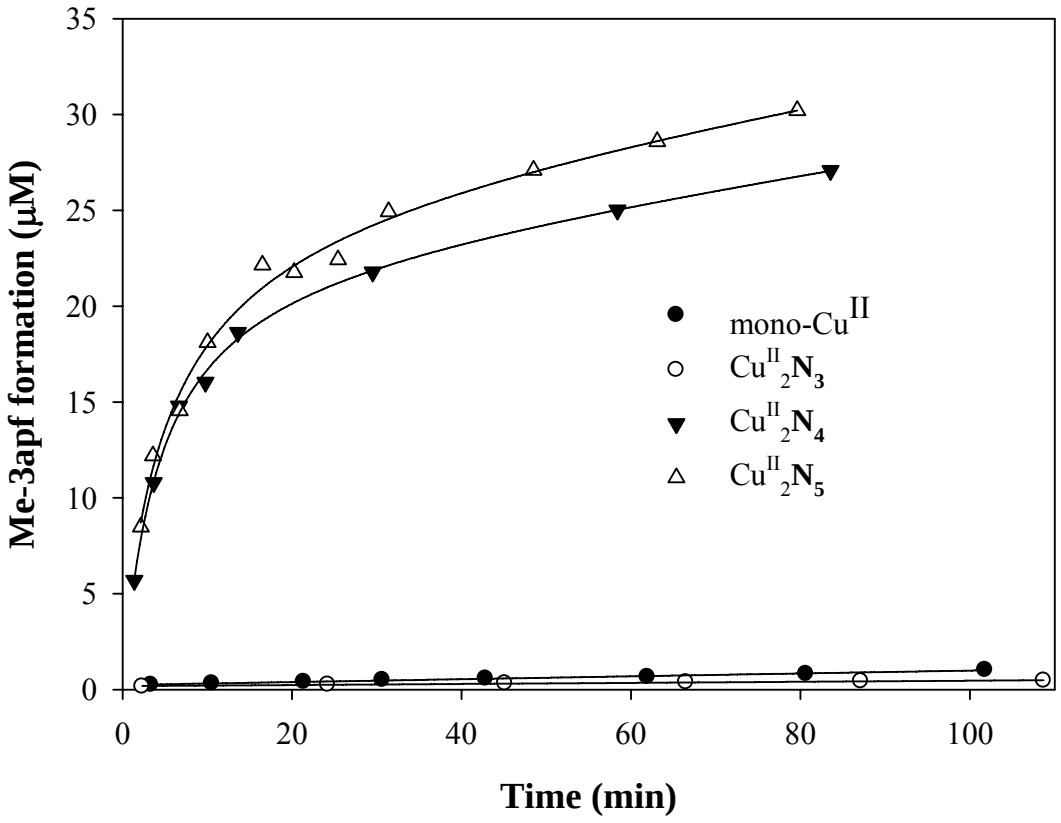


**Figure 2.25 Formation of Me-3apf by different Cu(II) complexes**

Cu(II) complex (20 μM), mono-$Cu^{II}$ ( ● ) or $Cu^{II}_2\mathbf{N_3}$ ( ○ ) or $Cu^{II}_2\mathbf{N_4}$ ( ▼ ) or $Cu^{II}_2\mathbf{N_5}$ ( △ ) , DMSO (10 mM) and 3-ap (510 μM) were dissolved in phosphate buffer (10 mM, pH 6.8). $H_2O_2$ (80 μM) was added to initiate the reaction under anaerobic conditions. Reaction was terminated at different times by derivatization with fluorescamine under aerobic conditions. The derivatized sample was then separated and analyzed by HPLC. Lines in this figure were obtained based on a fit to polynomial equation only so that the trend of Me-3apf formation could be shown clearly.

### 2.3.5.2 Reaction with Methane

To test whether the oxidizing species produced during the intermediate decay was the hydroxyl radical, methane was used in place of DMSO. Since the C-H bonds in methane have high valence bond energy, only very strongly oxidizing species can abstract H atom from it to form the methyl radical, resulting in Me-3apf formation (Scheme 2.1). Therefore, the detection of Me-3apf in the presence of methane can provide qualitative evidence for the hydroxyl radical formation. As shown in Figure 2.26, Me-3apf was detected in the presence of methane when $Cu^{II}_2\mathbf{N_{4,\ 5}}$ was employed to activate $H_2O_2$.

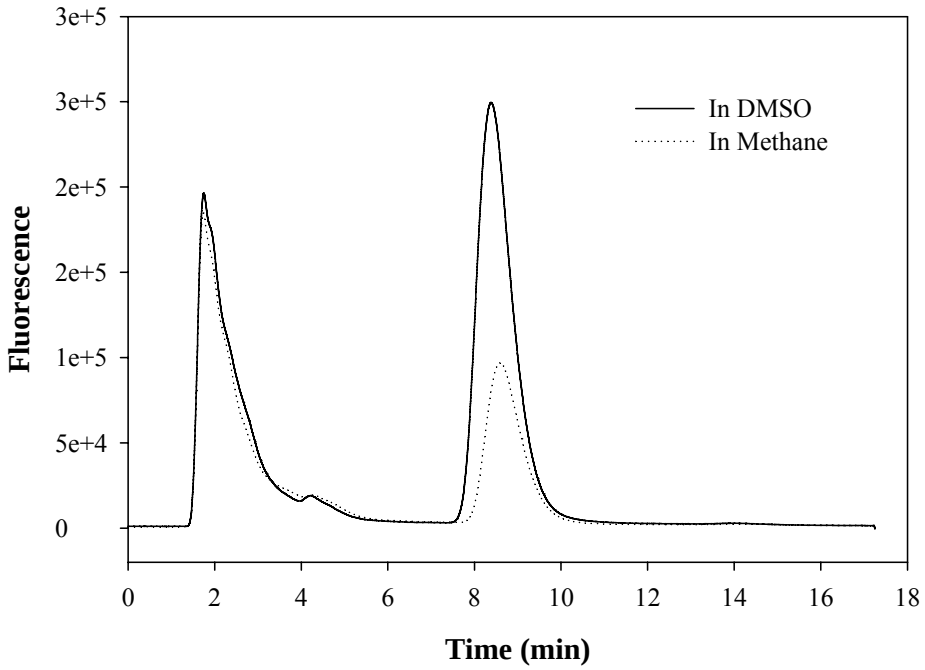


**Figure 2.26 Chromotogram of the formation of Me-3apf in the presence of DMSO and methane**

$Cu^{II}_2\mathbf{N_4}$ complex (10.0 μM), DMSO (1.5 mM) or methane (Solubility in water is 1.5 mM at room temperature.) and 3-ap ( 50 μM in DMSO experiment , 20 μM in methane experiment) were dissolved in phosphate buffer (10 mM, pH 6.8). $H_2O_2$ (100 μM) was added to initiate the reaction under anaerobic conditions.

In the absence of $Cu^{II}_2\mathbf{N_{4,5}}$, 3-ap, $H_2O_2$ or methane, Me-3apf could not be observed. Detection of Me-3apf in the methane experiment indicated that hydroxyl radicals are most likely generated during the intermediate decay. A lower yield of Me-3apf was obtained in methane experiment as compared with that in DMSO experiment under similar conditions, because the second-order rate constant for the reaction of methane with the hydroxyl radical ($k_{CH4} = 1.2\times10^7$ $M^{-1}s^{-1}$)[140] is much smaller than that for the reaction of DMSO with the hydroxyl radical ($k_{DMSO} = 6.6\times0^9$ $M^{-1}s^{-1}$)[141]. Moreover, a competitive reaction between the hydroxyl radical and 3-ap ($k_{3\text{-}ap} = 4.9\times10^9$ $M^{-1}s^{-1}$) (Blough'a group) further reduces the yield of Me-3apf in the methane experiments. A subsequently lower 3-ap concentration was used in the methane experiments because maximum Me-3apf yield could be reached based on 3-ap titration in methane (Figure 2.27). The results indicate that $Cu^{II}_2\mathbf{N_4}$ and $Cu^{II}_2\mathbf{N_5}$ complexes exhibited similar kinetics of hydroxyl radical formation in both the DMSO and methane experiments (Figure 2.28).

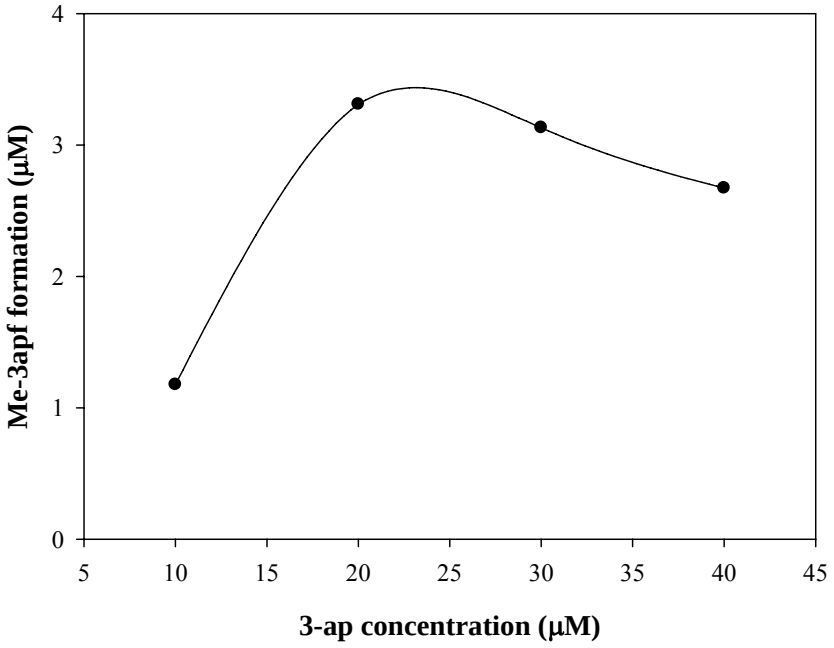


**Figure 2.27 3-ap titration in the presence of methane**

$Cu^{II}_2\mathbf{N_4}$ complex (10.0 μM), methane (Solubility in water is 1.5 mM at room temperature.) and 3-ap with concentration ranging from 10 μM to 40 μM were dissolved in phosphate buffer (10 mM, pH 6.8). $H_2O_2$ (100 μM) was added to initiate the reaction under anaerobic conditions. Reaction was terminated after 20 minutes by derivatization with fluorescamine under aerobic conditions. Me-3apf was then separated and analyzed by HPLC.

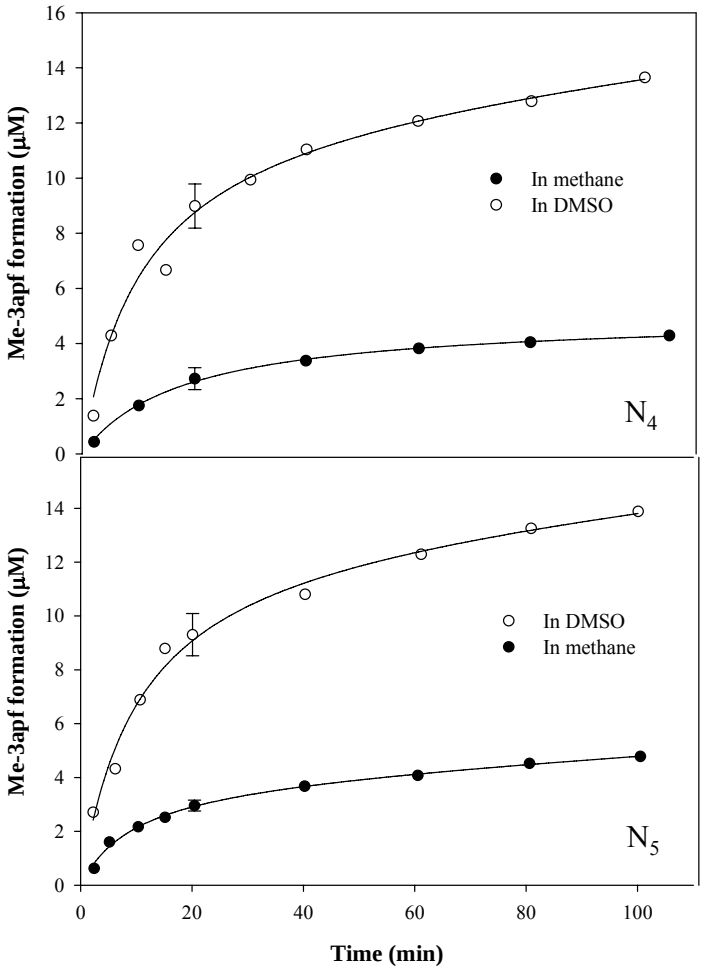


**Figure 2.28 Formation of Me-3apf in the presence of DMSO and methane**

$Cu^{II}_2\mathbf{N_4}$ or $Cu^{II}_2\mathbf{N_5}$ complex (10.0 μM), DMSO (1.5 mM) or mehane (Solubility in water is 1.5 mM at room temperature.) and 3-ap ( 50 μM in DMSO experiment, 20 μM in methane experiment) were dissolved in phosphate buffer (10 mM, pH 6.8). $H_2O_2$ (100 μM) was added to initiate the reaction under anaerobic conditions. In methane experiment, anaerobic condition was maintained by bubbling methane gas during the entire reaction. Reaction was terminated at different times by derivatization with fluorescamine under aerobic conditions. Me-3apf was then separated and analyzed by HPLC. Lines in this figure were obtained based on a fit to polynomial equation only so that the trend of Me-3apf formation could be shown clearly.

The yield ratio of Me-3apf in DMSO and methane experiments was employed to further test for the involvement of hydroxyl radical (Figure 2.28). By comparing the yield ratio of Me-3apf obtained from DMSO and methane experiment with that calculated based on the rate constants for the reaction of the hydroxyl radical with DMSO and methane, we can differentiate unequivocally between the hydroxyl radical and other strong oxidizing species.

The yield of Me-3apf (III) in DMSO experiment can be calculated by Equation 2.2.

$$Y_{DMSO} = \frac{Y_0\, k_{DMSO}[DMSO]}{k_{DMSO}[DMSO] + k_{3\text{-}ap}[3\text{-}ap] + k_{H_2O_2}[H_2O_2] + k_{Cu\ complex}[Cu\ complex]} \qquad 2.2$$

where $Y_{DMSO}$ is Me-3apf yield for a given conditions in the DMSO experiments, $Y_0$ is the maximal yield of hydroxyl radicals in reaction system, $k_{DMSO,}$ $k_{3\text{-}ap}$, $k_{Cu\ complex}$ and $k_{H2O2}$ are rate constants for reactions of OH radical with DMSO, 3-ap, Cu(II) complex and $H_2O_2$ respectively. Because of the high rate constant and concentration of DMSO used, the equation 2.2 can be simplified to $Y_{DMSO} = Y_0$.

Similarly, yield of Me-3apf in methane experiment is given by Equation 2.3.

$$Y_{CH_4} = \frac{Y_0 k_{CH_4}[CH_4]}{k_{CH_4}[CH_4] + k_{3\text{-}ap}[3\text{-}ap] + k_{H_2O_2}[H_2O_2] + k_{Cu\ complex}[Cu\ complex]} \qquad 2.3$$

where $Y_{CH4}$ is Me-3apf yield for a given condition in the methane experiments, $k_{CH4}$ is rate constant for reaction of OH radical with methane, $k_{DMSO,}$ $k_{3\text{-}ap}$, $k_{Cu\ complex}$ and $k_{H2O2}$ are defined as above

After arrangement, the Equation 2.3 can be simplified and given in the form of Equation 2.4.

$$\frac{Y_{CH_4}}{Y_0} = \frac{1}{C + R \bullet \frac{[\text{Cu complex}]}{[CH_4]}} \qquad 2.4$$

where

$$C = \frac{k_{CH_4}[CH_4] + k_{3\text{-ap}}[3\text{-ap}] + k_{H_2O_2}[H_2O_2]}{k_{CH_4}[CH_4]}$$

and

$$R = \frac{k_{\text{Cu complex}}}{k_{CH_4}}$$

The yield ratio of Me-3apf in DMSO and in the methane experiment is given by Equation 2.5.

$$\frac{Y_{DMSO}}{Y_{CH_4}} = 1 + \frac{k_{3\text{-ap}}[3\text{-ap}] + k_{H_2O_2}[H_2O_2] + k_{\text{Cu complex}}[\text{Cu complex}]}{k_{CH_4}[CH_4]} \qquad 2.5$$

The rate constant of the reaction of the Cu (II) complex with the reactive intermediate radical was estimated from experiments. To do so, the experiments were carried out in methane. All the reaction conditions were same except that different Cu (II) complex concentrations were used (Figure 2.29). Different yields of Me-3apf were then obtained. By using equation 2.4, R (ratio of $k_{cu\ complex}$ to $k_{CH4}$ ) was estimated to be ~ 200. $k_{cu\ complex}$ was much larger than $k_{CH4}$, suggesting hydroxyl radical involvement. If we assume that the reactive intermediate was hydroxyl radical, the rate constant of Cu(II)

complex reacting with hydroxyl radical could be roughly estimated, $2.8 \times 10^{10}$ $M^{-1}s^{-1}$, based on R and rate constant of $CH_4$ with the OH radical.

The yield ratio of Me-3apf calculated by using Me-3apf formation after a 20 minute reaction in the DMSO and methane experiments produced a value of $Y_{DMSO}/Y_{methane} = 2.8 \pm 0.4$ for $Cu^{II}_2\mathbf{N_4}$ complex system or $Y_{DMSO}/Y_{methane} = 2.9 \pm 0.2$ for $Cu^{II}_2\mathbf{N_5}$ complex system (Figure 2.28), which was very close to 2.7, the calculated value using known rate constants for the reactions of OH radical with 3-ap, methane and DMSO. The close agreement between the experimental yield ratio and the calculated yield ratio is further consistent with OH radical being produced during the intermediate decay. The concentrations of reactants and Me-3apf used for calculation mentioned above were shown in Table 2.5.

**Table 2.5 Concentrations of reactants and formation of Me-3apf in the presence of DMSO and methane**

| | Cu(II) complex (μM) | DMSO (mM) | Methane (mM) | $H_2O_2$ (μM) | 3-ap (μM) | Me-3apf (μM) |
|---|---|---|---|---|---|---|
| $\mathbf{Cu^{II}_2N_4}$ | 10.0 | 1.5 | 1.5 | 100 | 50 * | 8.7±0.7 |
| | | | | | 20 ** | 3.2±0.4 |
| $\mathbf{Cu^{II}_2N_5}$ | 10.0 | 1.5 | 1.5 | 100 | 50 * | 9.6±0.8 |
| | | | | | 20 ** | 3.2±0.2 |

* in the presence of DMSO
** in the presence of methane
The uncertainties represent ± one standard deviation from the average of three independent experiments.

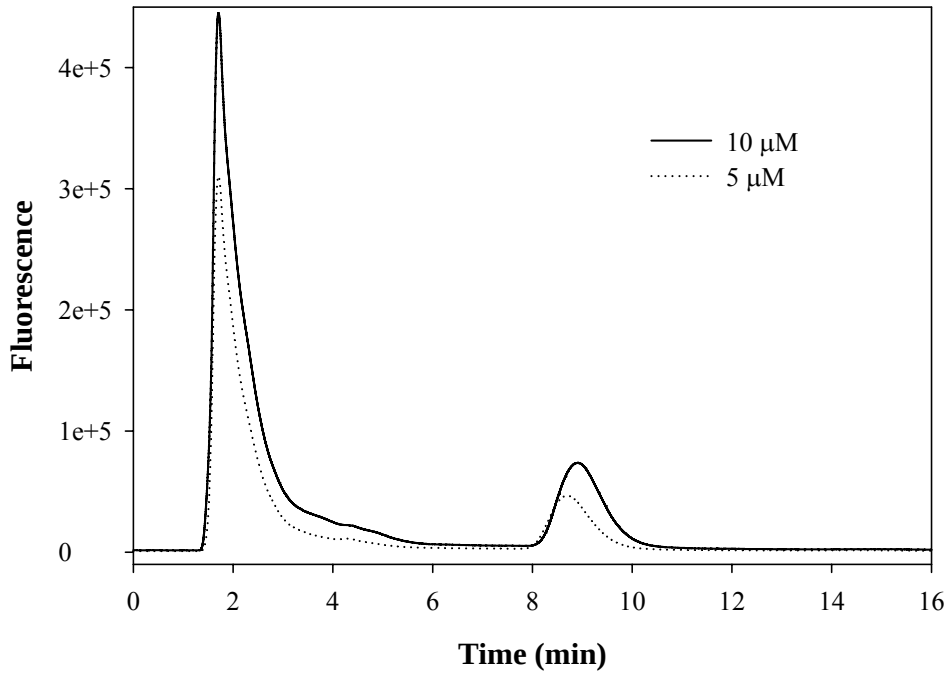


**Figure 2.29 Chromotogram of the formation of Me-3apf at different concentration of $Cu^{II}_2N_4$ in the presence of methane**

$Cu^{II}_2\mathbf{N_4}$ complex (5.0 or 10.0 μM), methane (Solubility in water is 1.5 mM at room temperature.) and 3-ap (20 μM) were dissolved in phosphate buffer (10 mM, pH 6.8). $H_2O_2$ (100 μM) was added to initiate the reaction under anaerobic conditions. After a 20 minute reaction, an aliquot was withdrawn and derivatized by fluorescamine under aerobic conditions. Me-3apf was then separated and analyzed by HPLC.

### 2.3.5.3 Hydroxyl Radical Generation by $Cu^{II}_2N_4$ and Mono-$Cu^{II}$ in the Presence of High Concentration of $H_2O_2$

Although the intermediate was not generated by mono-$Cu^{II}$ complex at low $H_2O_2$ concentrations, it was observed to be formed at high concentration of $H_2O_2$. Hydroxyl radical generation in the presence of high concentration of $H_2O_2$ was therefore investigated. In this experiment, benzoic acid was used to determine hydroxyl radical

generation under aerobic conditions (Scheme 1.11). As shown in Figure 2.30, the kinetics of hydroxyl radical formation in the presence of a high concentration of $H_2O_2$ under aerobic conditions was the same as that obtained at low $H_2O_2$ concentration under anaerobic conditions in $Cu^{II}_2\mathbf{N_4}$ complex system. The inflection point at about 20 minutes indicated the intermediate decay was complete and the secondary decomposition became predominant. Under these experimental conditions, ~10 μM hydroxyl radicals were produced by ~10 μM $Cu^{II}_2\mathbf{N_4}$ complex, indicating that the stoichiometry of hydroxyl radical generation with respect to the concentration of the intermediate was 1:1. As compared with $Cu^{II}_2\mathbf{N_4}$ system, only ~5 μM hydroxyl radicals were generated from ~10 μM mononuclear Cu(II) complex, indicating that the hydroxyl radical arises from a dimer. The stoichiometry of OH radical generation with respect to Cu(II) complex concentration strongly suggests that the intermediate generated from $Cu^{II}_2\mathbf{N_4}$ and mono-$Cu^{II}$ complexes possesses very similar structures, and is probably a (hydro)peroxo-bridged binuclear copper(II) complex, of as yet, unknown structure.

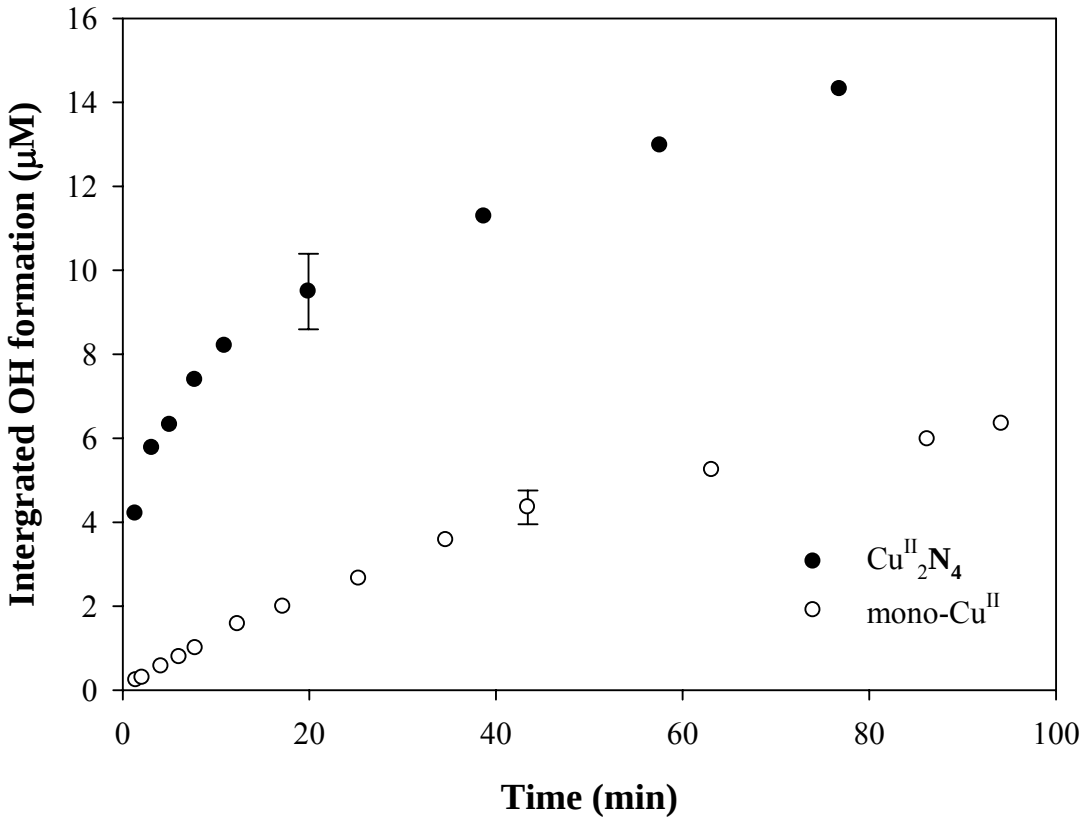


**Figure 2.30 Formation of the hydroxyl radical in the presence of high concentration of $H_2O_2$**

$Cu^{II}_2$**N$_4$** (10 μM) or mono-$Cu^{II}$ (10 μM) and benzoic acid (1.0 mM) were dissolved in phosphate buffer (pH 6.8, 10 mM). $H_2O_2$ (6.1 mM) was added to initiate reaction under aerobic conditions. Reaction was terminated at different times when sample was directly injected into HPLC. Formation of the hydroxyl radical was approximated as 3 times of the concentration of salicylic acid analyzed by HPLC.

### 2.3.5.4 Preliminary Product Analysis

As shown above, the intermediates generated from $Cu^{II}_2\mathbf{N_4}$ or $Cu^{II}_2\mathbf{N_5}$ complexes did not react with externally added electron donors and the stoichiometry of the hydroxyl radical formation with respect to the loss of the intermediate was 1:1. Hydroxyl radical generation during the decay of the intermediate is therefore attributed to a rate-limiting intramolecular electron transfer from ligand to the metal peroxo center. Ligand-based radicals or oxidation products of ligand were then expected to be produced, concomitant with the hydroxyl radical generation. In the absence of a hydroxyl radical scavenger, the hydroxyl radical was expected to attack further the ligand, the products of the intermediate decay or the intermediate itself to cause further oxidation. To test this possibility, the absorption spectra in the presence and absence of a hydroxyl radical scavenger were investigated. As shown in Figure 2.31, a blue shift of the isosbestic point was observed in the presence of a hydroxyl radical scavenger in both $Cu^{II}_2\mathbf{N_4}$ and $Cu^{II}_2\mathbf{N_5}$ systems, although the shift in $Cu^{II}_2\mathbf{N_5}$ system was not as obvious as that in $Cu^{II}_2\mathbf{N_4}$ system. The shift of the isosbestic point suggested that different products were generated in the presence and absence of the scavenger. Since the decay of the intermediate was not affected by the presence of the scavenger, the results suggest that the hydroxyl radicals do not directly attack the Cu-peroxo center. The slight difference on the absorption spectra in the presence and absence of a scavenger for $Cu^{II}_2\mathbf{N_5}$ also suggests that products of the intermediate decay generated from $Cu^{II}_2\mathbf{N_5}$ system may not be the same as those produced from $Cu^{II}_2\mathbf{N_4}$ system.

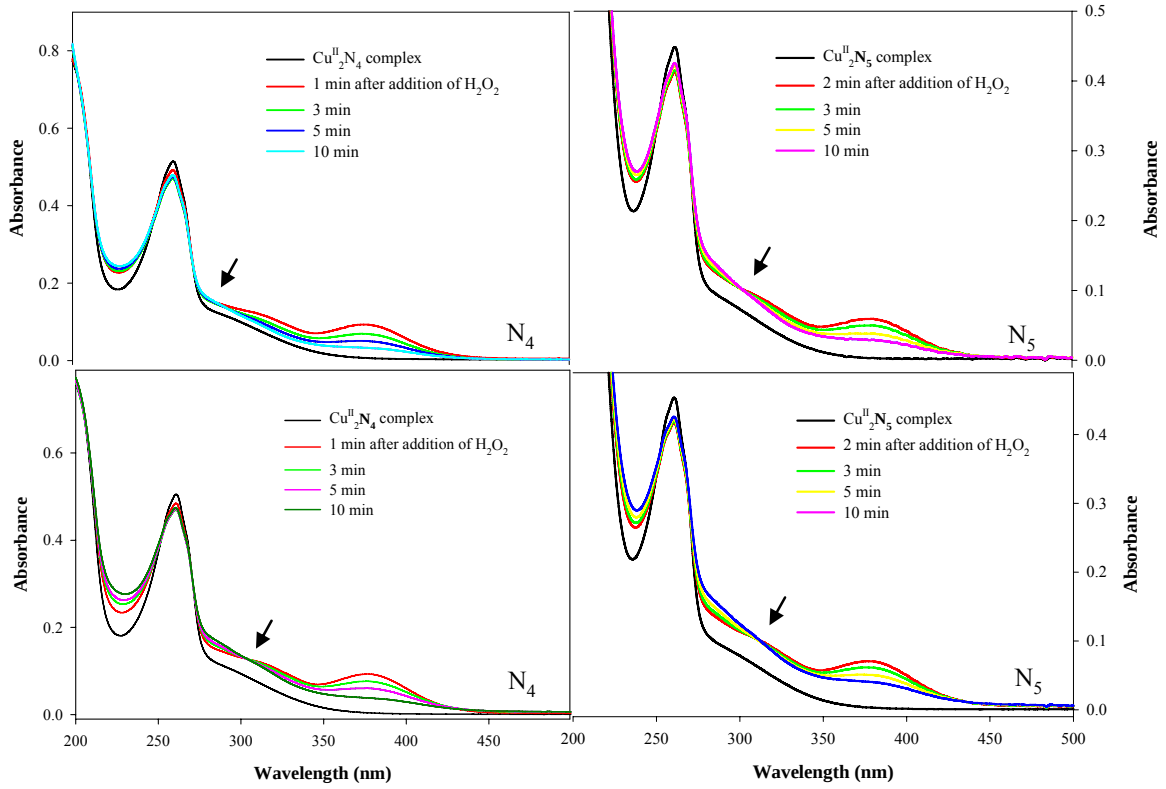


**Figure 2.31 The intermediate decay in the presence or absence of an OH scavenger**

$Cu^{II}_2$**N$_4$** complex (27 μM) or $Cu^{II}_2$**N$_5$** complex (20 μM) was dissolved in phosphate buffer (10 mM, pH 6.8). $H_2O_2$ (40 μM for $Cu^{II}_2$**N$_4$** system or 80 μM for $Cu^{II}_2$**N$_5$** system) was added to initiate the reaction under anaerobic conditions. Glucose (40 mM) (upper panels) or phosphate buffer (control, lower panels) was added to the reaction mixture when the intermediate formation was complete.

Thin layer chromatography (TLC) was employed to investigate the ligand degradation products during intermediate decomposition in the presence and absence of an added OH scavenger. The $Cu^{II}_2\mathbf{N_4}$ complex was studied as a representative and the results are shown in Table 2.6. Silica was used as stationary phase and the mobile phase was a mixture of methanol and concentrated ammonium hydroxide, 100:5 (v/v). In the presence of the OH scavenger, DMSO in this case, two products were observed under these separation conditions, with retention factors ($R_f$) of 0.66 ± 0.05 and 0.53 ± 0.06 respectively. These two products are suggested to arise from an initial internal electron transfer from ligand to metal peroxo center. By contrast, an additional product with an $R_f$ value 0.22 ± 0.04 was detected in the absence of the OH scavenger, which was attributed to the direct reaction of hydroxyl radical with ligand. The results of TLC experiments were consistent with the observations from absorption spectra and provide evidence for an intramolecular electron transfer process from the ligand to the metal-peroxo center, thus producing the hydroxyl radical.

**Table 2.6 Product analysis by TLC in the presence and absence of an added OH scavenger**

| Sample | $R_f$ 1 | $R_f$ 2 | $R_f$ 3 | $R_f$ 4 |
|---|---|---|---|---|
| $Cu^{II}_2N_4$ | / | / | / | 0.88 ±0.03 |
| $Cu^{II}_2N_4 + H_2O_2$ | 0.22±0.04 | 0.53±0. 06 | 0.66±0.05 | 0.88±0.03 |
| $Cu^{II}_2N_4 + H_2O_2 + DMSO$ | / | 0.53±0. 06 | 0.66±0.05 | 0.88 ±0.03 |

$Cu^{II}_2N_4$ complex (2 mM) and $H_2O_2$ (7 mM) dissolved in 10 mM phosphate buffer at pH 6.8 were mixed quickly to initiate the reaction under anaerobic conditions. The resultant solution was allowed to react for 15 miniutes before analyzing by TLC. Silica was used and mobile phase was methanol and concentrated ammonium hydroxide, 100:5 v/v. $R_f$1-$R_3$3 are reference values of degradation products. The uncertainties represent ± one standard deviation from the average of three independent experiments.

Since hydroxyl radical production causes further oxidation of the ligand, the Cu(II) free ion is expected to be released after complete degradation of the ligand in the absence of OH scavengers. To test this possibility, a solution containing $Cu^{II}_2\mathbf{N_4}$ complex and excess $H_2O_2$ was kept at room temperature for 24 hours under aerobic conditions to completely degrade the complex. Benzoic acid was then added to trap hydroxyl radicals. The results showed that after 24 hour degradation, the hydroxyl radical formation rate was of the same magnitude as that produced by $CuCl_2$ system based on molarity of copper ion under similar conditions (Figure 2.32). The hydroxyl radical formation rate in $Cu^{II}_2\mathbf{N_4}$ system was a slightly more than double that of the $CuCl_2$ system, presumably because not all of copper ions existed in the form of free ions. When the ligand of the $Cu^{II}\mathbf{N_4}$ complex was added to the degraded Cu (II) complex system, an absorption band at 376 nm was again observed in the presence of excess hydrogen peroxide and decayed with identical kinetics, suggesting the regeneration of copper complexes in the system (Figure 2.33). These results are consistent with the idea that hydroxyl radical produced during the intermediate decay reacts with the complexes to produce ligand degradation and release the bound copper.

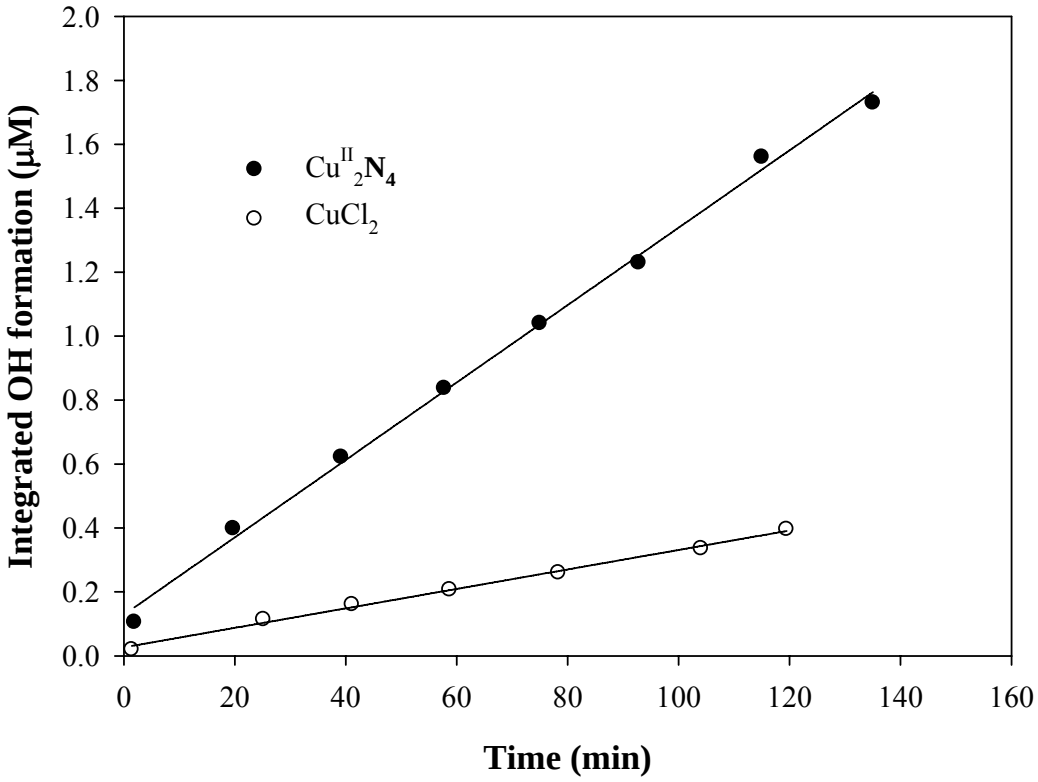


**Figure 2.32 Comparison of OH formation by $Cu^{II}_2N_4$ complex after complete ligand degradation and by $CuCl_2$**

$Cu^{II}_2\mathbf{N_4}$ (10 μM) was dissolved in phosphate buffer (pH 6.8, 10 mM) under aerobic condition. $H_2O_2$ (2.0 mM) was added to initiate the reaction. After 24 hours, benzoic acid (1.0 mM) was added to trap hydroxyl radicals. $CuCl_2$ (10 μM) and benzoic acid were dissolved in phosphate buffer (pH 6.8, 10 mM) under aerobic condition. $H_2O_2$ (2.0 mM) was added to start reaction. Reaction was terminated at different times by directly injection into the HPLC. Formation of the hydroxyl radical was approximated as three times of the concentration salicylic acid analyzed by HPLC.

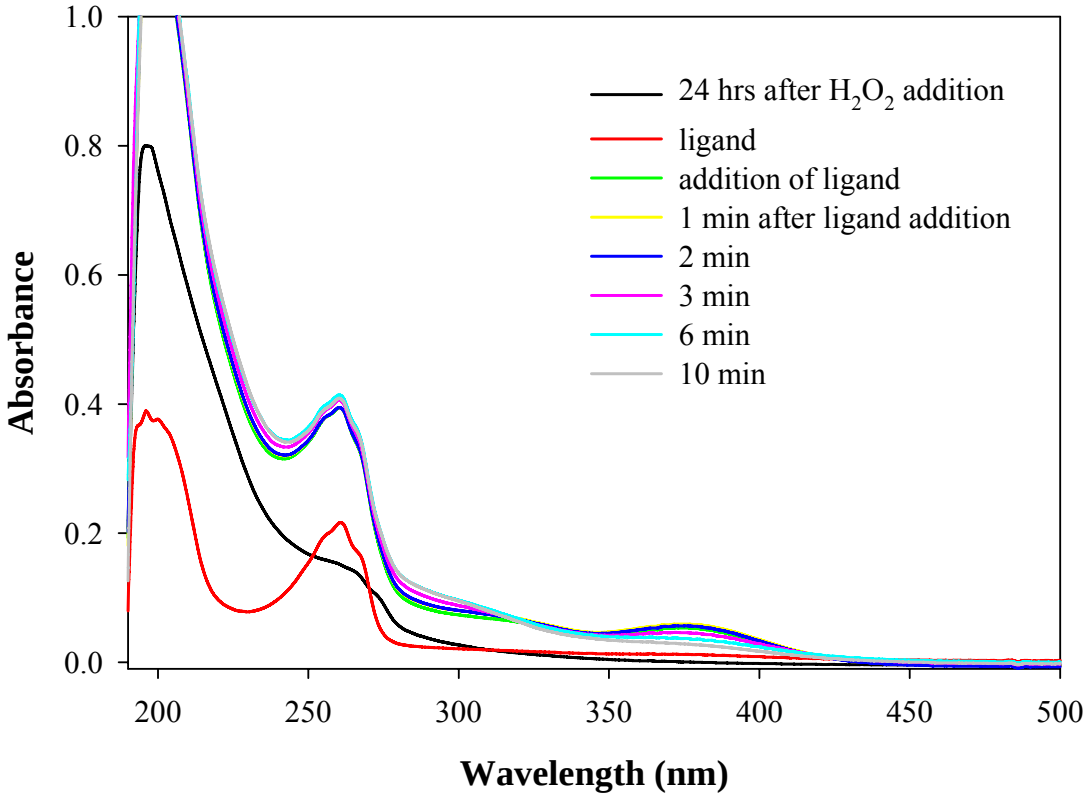


**Figure 2.33 Formation of the intermediate by addition of ligand after 24 hours of decomposition**

$Cu^{II}_2\mathbf{N_4}$ (10 μM) was dissolved in phosphate buffer (pH 6.8, 10 mM) under aerobic condition. $H_2O_2$ (2.0 mM) was added to initiate the reaction. After 24 hours, free ligand (40 μM) was added and the absorption sprectra were the recorded over time.

## 2.4 Summary and Conclusions

An intermediate with an absorption band at 376 nm is generated by the $Cu^{II}_2\mathbf{N_4}$ complex or $Cu^{II}_2\mathbf{N_5}$ complexes in the presence of $H_2O_2$ under both anaerobic and aerobic conditions. This intermediate is not formed with $Cu^{II}_2\mathbf{N_3}$, but is formed with mono-$Cu^{II}$ when high concentrations of $H_2O_2$ and the Cu(II) complex are used.

The intermediate generated from mono-$Cu^{II}$, $Cu^{II}_2\mathbf{N_4}$ and $Cu^{II}_2\mathbf{N_5}$ complexes possess very similar molar absorptivities based on the molarity of copper ion, 2690 $M^{-1}cm^{-1}$, 2630 $M^{-1}cm^{-1}$ and 2900 $M^{-1}cm^{-1}$, respectively. Formation of the intermediate from $Cu^{II}_2\mathbf{N_4}$ and $Cu^{II}_2\mathbf{N_5}$ complexes is first order with respect to both Cu(II) complex and $H_2O_2$ concentration, with rate constants of k= 250 ± 2 $M^{-1}s^{-1}$ and 110 ± 4 $M^{-1}s^{-1}$, respectively, at 26.5 $^oC$. However, a more complicated reaction scheme is followed by mono-$Cu^{II}$ to generate the intermediate.

The intermediate decays exponentially at room temperature. The decay of the intermediate is $H_2O_2$- and dioxygen-independent and not affected by catalase so long as the intermediate formation is complete prior to catalase addition, suggesting that the formation of the intermediate is irreversible. Very similar decay rate constants are obtained for mono-$Cu^{II}$, $Cu^{II}_2\mathbf{N_4}$ and $Cu^{II}_2\mathbf{N_5}$ complexes, 0.0077 $s^{-1}$, 0.0081 $s^{-1}$ and 0.0079 $s^{-1}$, respectively, at 26.5 $^oC$.

Chemical trapping experiments employing DMSO and methane unequivocally demonstrates that hydroxyl radical is generated during the intermediate decay. Based on the hydroxyl radical yield, the stoichiometry of hydroxyl radical formation with respect to the loss of the intermediate is 1 to 1. This stoichiometry and the similarities of molar absorptivities and decay rate constants for the $Cu^{II}_2\mathbf{N_4}$, $Cu^{II}_2\mathbf{N_5}$ and mono-$Cu^{II}$ suggest a

common structure of the intermediate, probably a (hydro)peroxo-bridged dinuclear copper(II) complex. This peroxide-bridged species is more readily formed with $Cu^{II}_2\mathbf{N_4}$ and $Cu^{II}_2\mathbf{N_5}$ presumably due to efficient intramolecular reaction. By contrast, an intermolecular reaction between two of mono-$Cu^{II}$ complexes and one of $H_2O_2$ is presumably required to generate this peroxide-bridged species, leading to a much slower reaction rate and more complicated mechanism of formation.

The intermediate is not formed with $Cu^{II}_2\mathbf{N_3}$ most likely due to a geometric constraint of the $(CH_2)_3$ bridge vs $(CH_2)_4$ and the $(CH_2)_5$ bridge of $Cu^{II}_2\mathbf{N_4}$ and $Cu^{II}_2\mathbf{N_5}$ complexes, limiting the formation of the (hydro)peroxo-bridged species.

The intermediate formed from $Cu^{II}_2\mathbf{N_4}$ complex or $Cu^{II}_2\mathbf{N_5}$ complex is unreactive or only weakly reactive with externally added electron donors. Its decay was either unaffected ($Cu^{II}_2\mathbf{N_4}$) or only slightly accelerated ($Cu^{II}_2\mathbf{N_5}$) by relatively high concentrations of electron donors, such as DMSO, 3-ap, DMA, glucose, benzoic acid, 3-MPA and guanine. The lack of reactivity of the intermediate with added electron donors and the stoichiometry of hydroxyl radical yield during intermediate decay suggests that the intermediate discharges through a rate-limiting intramolecular electron transfer from the ligand to the metal peroxo center, thereby producing a hydroxyl radical and a ligand-based radical.

Phosphate concentration and pH affect not only the absorption spectra of Cu(II) complex themselves but also intermediate formation. The intermediate is formed only at a pH between ~6 - 8 and at phosphate concentrations less than ~20 mM. At low or high pH, speciation of Cu(II) complex is changed so that the intermediate is not generated. Slow changes in the absorption spectra indicate that the reactions between $H_2O_2$ and the

dinuclear Cu(II) complexes are taking place, but through different pathways by which the intermediate is not involved. In contrast, the absorption spectrum of $Cu^{II}_2\mathbf{N_3}$ exhibits little change with pH or phosphate concentration.

Based on these results, the DNA cleavage caused by $Cu^{II}_2\mathbf{N_n}$ (n = 4-5) complex in the presence of $H_2O_2$ in aqueous solutions does not appear to be a result of direct reaction with a metal-peroxo intermediate, but instead arises from reaction with either a hydroxyl radical or a ligand-based radical. The reaction pathways followed by the Cu(II) complexes in the presence of $H_2O_2$ are proposed in Scheme 2.3.

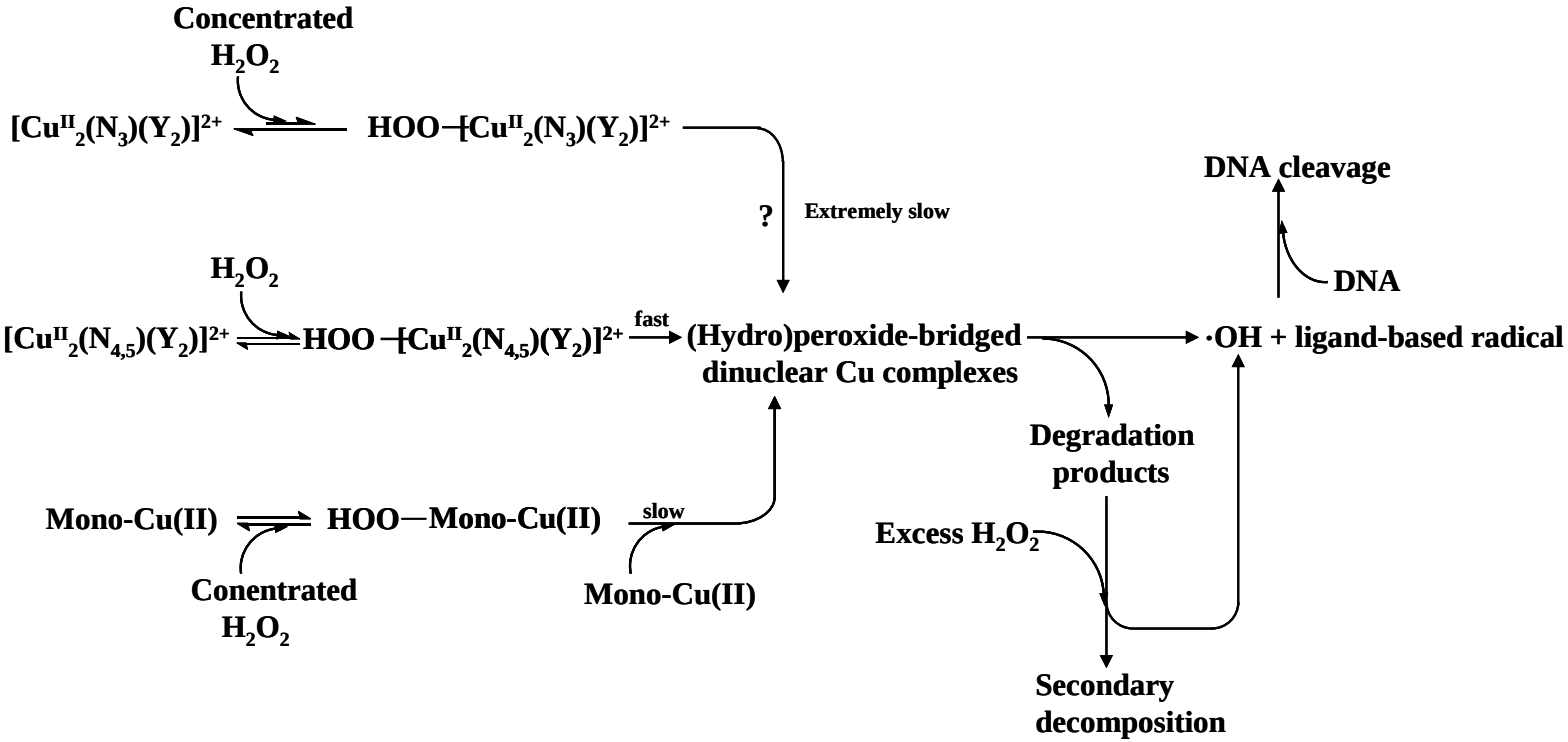


**Scheme 2.3 Proposed reactive intermediate generation by Cu(II) complexes in the presence of $H_2O_2$**

# Chapter III Metal-mediated Activation of $O_2$ by Binuclear and Mononuclear Cu(I) Complexes in Aqueous Solution

## 3.1 Introduction

Copper(II) complexes are known to degrade DNA in the presence of a reductant and $O_2$. This degradation can be inhibited by reagents that decrease the concentration of either the cuprous complex (eg. neocuproine) [106] or hydrogen peroxide (catalase),[106] suggesting that generation of the reactive species responsible for DNA oxidation is directly related to the reaction of the Cu(I) complex with $O_2$ (Scheme 3.1). It is commonly believed that the reactive species is either a direct adduct of Cu(I) complex with $O_2$ [24]or a reactive oxygen species (such as •OH).[19] Considerable effort has been directed to studying the interaction of dioxygen with copper (I) complexes, the spectroscopic features of the copper-dioxygen adducts, as well as their reactivity, but most of these experiments have performed using organic solvents.[123, 124] The reaction of Cu(I) complexes with $O_2$ and the oxidative properties of the resulting Cu(I)-dioxygen complexes in aqueous solution have not been systematically studied except for $Cu^{I}(OP)_2$ complex system.

Results presented in the previous chapter showed that an intermediate is formed from the reaction of $Cu^{II}_2\mathbf{N_4}$ and $Cu^{II}_2\mathbf{N_5}$ with low concentrations of $H_2O_2$, but is not generated from $Cu^{II}_2\mathbf{N_3}$ and mono-$Cu^{II}$ under identical conditions. In this chapter, the corresponding Cu(I) complexes were first generated in anaerobic aqueous solution. Air was then introduced to test whether the same intermediate could be generated by the reaction of the Cu(I) complex with $O_2$. Because the presence of excess reducing agent (RSH) could change the speciation of the copper complex by substituting from a ligand

on the copper centers (See appendix B), Cu(I) complexes were generated *in situ* by the stoichiometric reduction of the corresponding Cu(II) complexes with $Na_2S_2O_4$, thereby attempting to avoid interference from excess reductant. The intermediate obtained from the reaction of Cu(I) complex with $O_2$ was then compared with that obtained from the reaction of Cu(II) complex with $H_2O_2$.

Here, we find that $Cu^{I}\mathbf{N_4}$ and $Cu^{I}\mathbf{N_5}$ formed via the stoichiometric reduction of the Cu(II) complexes with $Na_2S_2O_4$, react with $O_2$ to form a species with an absorption spectrum and decay rate constant that is indistinguishable from that obtained through the reaction of the $Cu^{II}\mathbf{N_4}$ and $Cu^{II}\mathbf{N_5}$ with $H_2O_2$. Formation of this species was not affected by the presence of catalase, suggesting that $H_2O_2$ was not involved in the intermediate formation. Chemical trapping experiments indicate that hydroxyl radical is generated during the decay of the intermediate.

$$Cu^{2+} + RSH \longrightarrow Cu^{1+} + RS\bullet + H^+$$

$$RS\bullet + RS\bullet \longrightarrow RSSR$$

$$Cu^{1+} + O_2 \longrightarrow Cu^{2+} + O_2^{-\bullet}$$

$$2O_2^{-\bullet} + 2H^+ \longrightarrow H_2O_2 + O_2$$

$$Cu^{1+} + H_2O_2 \longrightarrow OH^- + Cu^{2+} + \bullet OH \xrightarrow{DNA} \text{Strand Scission}$$

$$Cu^{1+} + O_2 \xrightarrow{H^+} \text{Copper-dioxygen adduct} \xrightarrow{DNA} \text{Strand Scission}$$

**Scheme 3.1 Proposed mechanism for Cu-mediated DNA cleavage**

## 3.2 Experimental Sections

### 3.2.1 Reagents and Materials

Sodium dithionite (Tech. ~85%) was purchased from Sigma-Aldrich and used as received. The molar extinction coefficient of $Na_2S_2O_4$ was obtained from the literature (316 nm, $\varepsilon_{316} \sim 8000\ M^{-1}cm^{-1}$).[142]

Other chemicals used in this study were identical to those described in chapter II and were obtained from the same sources.

### 3.2.2 Apparatus

The HPLC set up was described in chapter II. The chromatographic conditions used to separate and quantify Me-3apf were identical to those described in chapter II. Other instruments employed were described in chapter II.

### 3.2.3 Experiment Preparations

A stock solution of sodium dithionite was prepared daily by first dissolving a precisely weighed amount of solid into 3 ml of nitrogen-purged phosphate buffer (10 mM) at pH 6.8. The resulting solution was then purged with $N_2$ for 20 minutes to ensure proper mixing. Forty microliters of the stock solution of sodium dithionite was transferred anaerobicaly to 2.5 ml of deaerated phosphate buffer (10 mM, pH 6.8) using a 100 µl air-tight syringe. Absorption at 316 nm of the diluted solution was then measured by UV-Vis spectrophotometer. Based on absorption at 316 nm and the dilution factor, the concentration of sodium dithionite in stock solutions was determined. The stock solution of sodium dithionite was continuously purged with $N_2$ during its use each day.

The concentration of the Cu(II) complexes and 3-ap were determined by UV-Vis spectroscopy using the molar extinction coefficients reported in the previous chapter.

### 3.2.4 Experiment Protocols

#### 3.2.4.1 Optical Absorption

A photometric titration was employed to determine the end point of the reduction of Cu(II) complex by $Na_2S_2O_4$. An appropriate volume of $Na_2S_2O_4$ stock solution was first transferred into 2.5 ml deaerated phosphate buffer (10 mM, pH 6.8) using a 100 µl air-tight syringe. Aliquots of a stock solution of the Cu(II) complex, previously deareated by purging with $N_2$ for 20 minutes, were then injected into the sodium dithionite solution. Absorption spectra were recorded after each addition of Cu(II) complex. Anaerobic conditions were maintained throughout the titration by continuously purging with $N_2$.

To test for a reaction between the Cu(I) complex and $O_2$, reactions were carried in a cuvette with a total reaction volume of 3 ml. An appropriate volume of phosphate buffer (10 mM, pH 6.8) and Cu (II) complex stock solution were added to the cuvette. The resulting mixture was then purged with $N_2$ for 20 minutes. An appropriate volume of $Na_2S_2O_4$ stock solution was transferred by a 100 µl gas-tight syringe and injected into the solution to reduce Cu(II) complex stoichiometrically. The concentrations of the Cu(II) complex and $Na_2S_2O_4$ are reported in the figure captions. Absorption spectra were recorded before and 15 seconds after each addition of $Na_2S_2O_4$. The reaction solution was then purged with air and the full absorption spectra recorded over time.

To test whether externally added electron donors such as DMSO, 3-ap and benzoic acid affected the decay of the intermediate, the protocol described above was

first employed to reduce the Cu(II) complex stoichiometrically. Air was then added to generate the intermediate. Appropriate electron donors were added when the absorption at 376 nm reached its maximum value. The kinetics of the absorption loss at 376 nm were then examined. As a control, deoxygenated phosphate buffer was added (100 μl) into the reaction mixture in place of the electron donors.

To test for an effect of catalase on formation of the intermediate, a known concentration of catalase, varying between 0.6 units/ml to 25 units/ml, was added to the Cu(I) complex at the same time that the solution was purged with pure $O_2$. Changes of absorption at 376 nm with time were then monitored.

To test whether the generation of the intermediate was reversible, $N_2$ was used to purge the reaction solution after the absorption at 376 nm reached its maximum. The full absorption spectra and absorption at 376 nm were then recorded as a function of time. As the control, the solution was purged with air after the maximum absorption at 376 nm was reached.

#### 3.2.4.2 Chemical Trapping Studies

Radical trapping experiments were carried out in a cuvette with a total reaction volume of 3 ml. A sample solution containing Cu(II) complex (40 μM) was prepared in 10 mM phosphate buffer at pH 6.8. The solution was deoxygenated by bubbling with ultra-high purity nitrogen gas for 20 minutes before an appropriate volume of deaerated $Na_2S_2O_4$ stock solution was added to stoichiometrically reduce the Cu(II) complex to the Cu(I) complex. DMSO (10 mM) and 3-ap (1.0 mM) were then added to the reaction solution at the same time that the solution was purged with air. The reaction solution was

continuously purged with air during course of the reaction. The reaction solution was withdrawn at different time intervals and derivatized with fluorescamine under aerobic conditions. The derivatized solution was injected onto HPLC for separation and quantification. The derivatization procedure was the same as that reported in chapter II.

Because $O_2$ competes with 3-ap for the methyl radical, thus reducing the efficiency of radical trapping, a second experimental protocol employed $N_2$ purging to reduce the concentration of $O_2$ following intermediate formation. When the absorption at 376 nm reached a maximum, the solution was purged with $N_2$ for one minute, with a deaerated solution DMSO (10 mM) and 3-ap (1.0 mM) then added. Aliquots were withdrawn at appropriate time intervals and immediately derivatized with fluoreacamine under aerobic conditions. The derivatized reaction mixture was then analyzed by HPLC. The absorption at 376 nm was further recorded at each time an aliquot was withdrawn.

## 3.3 Results and Discussion

### 3.3.1 Generation of Cu(I) Complexes

A photometric titration was carried out in phosphate buffer (10 mM, pH 6.8) to determine molar ratio between Cu(II) complex and $Na_2S_2O_4$ at the titration end-point so that a stoichiometric reduction of Cu(II) complex could be achieved. As shown in Figure 3.1, absorption of $Na_2S_2O_4$ at 316 nm first decreased with increasing volume of the Cu(II) complex due to the loss of $Na_2S_2O_4$ and formation of the Cu(I) complex. Following complete consumption of the $Na_2S_2O_4$, absorption at 316 nm increased with increasing volume of the Cu(II) complex, due to the accumulation of the excess Cu(II) complex. The end-point was obtained from the inflection point. Based on the reported extinction coefficient of $Na_2S_2O_4$[142] and the measured extinction coefficient of the Cu(II) complex, the molar ratio of $Na_2S_2O_4$ to the Cu(II) complex at the titration end-point was very close to 1, 1.1± 0.1, 1.1± 0.1, 1.2 ± 0.1 and 0.8 ± 0.1 for $Cu^{II}_2\mathbf{N_3}$, $Cu^{II}_2\mathbf{N_4}$, $Cu^{II}_2\mathbf{N_5}$ and mono-$Cu^{II}$ complex, respectively. The reported uncertainties represent ± one standard deviation about the mean of three independent experiments.

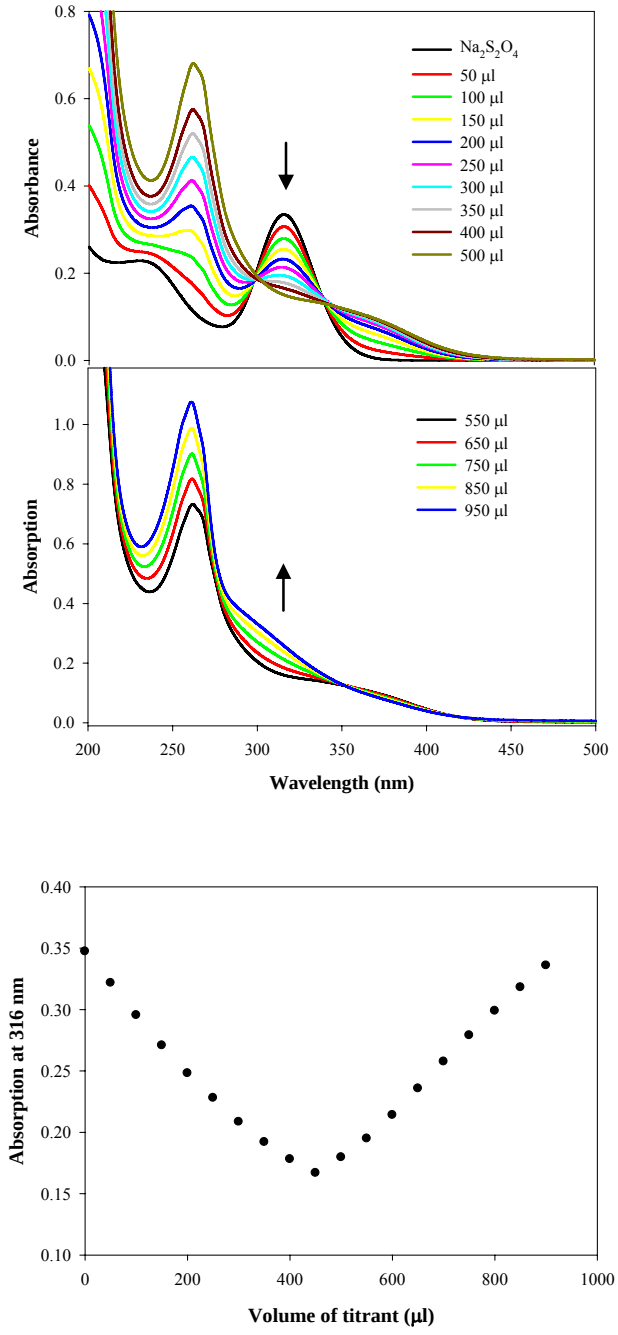


**Figure 3.1 Photometric titration of $Cu^{II}_2N_4$ complex**

$Na_2S_2O_4$ stock solution (~ 40 µM) was transferred into 2.5 ml nitrogen-purged phosphate buffer (10 mM, pH 6.8) by a 100 µl air-tight syringe. Deaerated $Cu^{II}_2\mathbf{N_4}$ complex stock solution (250 µM) was injected into sodium dithionite solution with a volume of 50 µl each time. Absorption spectra and absorption at 316 nm were then recorded as a function of the volume of Cu(II) complex.

### 3.3.2 Intermediate Generation by Reaction of the Cu(I) Complexes and $O_2$

When air was employed to purge the Cu(I) complex solution, a species with an absorption band at 376 nm was observed for the $Cu^{I}_{2}\mathbf{N_4}$ and $Cu^{I}_{2}\mathbf{N_5}$ complexes. However, this species was not observed in either $Cu^{I}_{2}\mathbf{N_3}$ or mono-$Cu^{I}$ complex system under similar conditions (Figure 3.2).

The intermediate formed with the $Cu^{I}_{2}\mathbf{N_4}$ and $Cu^{I}_{2}\mathbf{N_5}$ complexes in the presence of $O_2$ exhibited very similar absorption spectra and decay rate constants as compared with those obtained from $Cu^{II}_{2}\mathbf{N_4}$ and $Cu^{II}_{2}\mathbf{N_5}$ complexes in the presence of $H_2O_2$. The rate constants for the decay of the intermediate were 0.0073 $s^{-1}$ ($Cu^{I}_{2}\mathbf{N_4}$) and 0.0078 $s^{-1}$ ($Cu^{I}_{2}\mathbf{N_5}$) at 26.5 $^{o}$C (Figure 3.3), which were comparable to those obtained for $Cu^{II}_{2}\mathbf{N_4}$ (0.0083 $s^{-1}$) and $Cu^{II}_{2}\mathbf{N_5}$ (0.0079 $s^{-1}$) at same temperature. Very similar absorption spectra and decay rate constants suggest that the same intermediate was generated by either $Cu^{I}_{2}\mathbf{N_4}$ and $Cu^{I}_{2}\mathbf{N_5}$ complexes in the presence of $O_2$ or $Cu^{II}_{2}\mathbf{N_4}$ and $Cu^{II}_{2}\mathbf{N_5}$ complexes in the presence of $H_2O_2$.

However, the absorption spectrum of the product of intermediate decay obtained from reaction of $Cu^{I}_{2}\mathbf{N_4}$ and $Cu^{I}_{2}\mathbf{N_5}$ complexes with $O_2$ (Figure 3.3, left panels) was more similar to that obtained from reaction of $Cu^{II}_{2}\mathbf{N_4}$ and $Cu^{II}_{2}\mathbf{N_5}$ complexes with $H_2O_2$ in the presence of a radical scavenger. A possible explanation for this result is that oxidation products of $Na_2S_2O_4$ act as a radical scavenger. Additional work is needed to test this possibility.

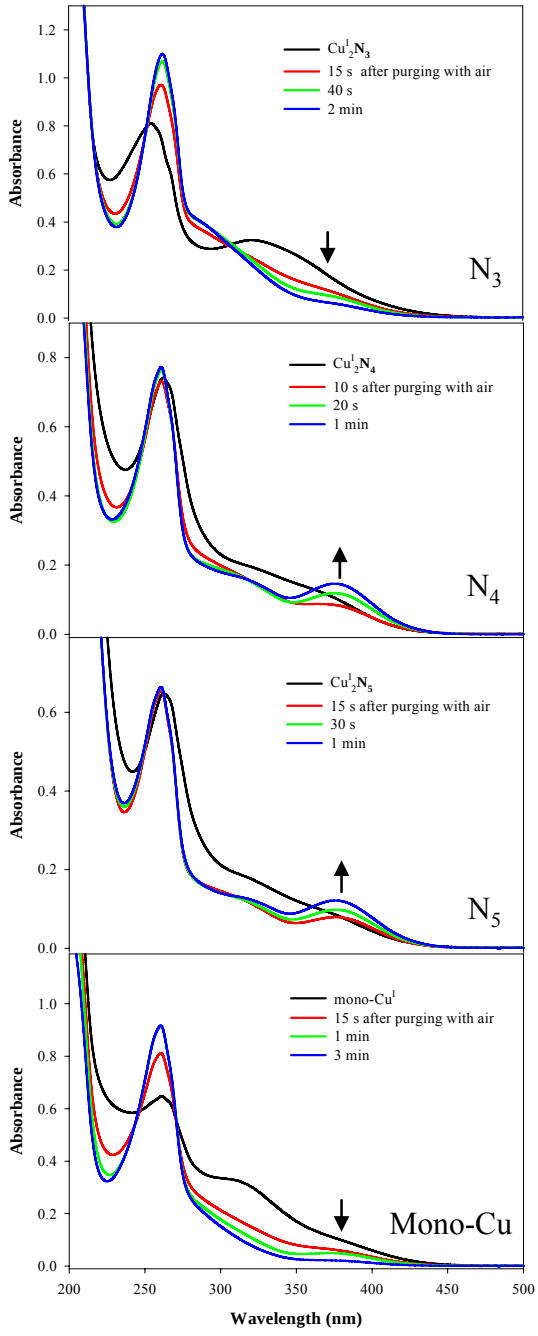


**Figure 3.2 Absorption spectra of Cu(I) complexes before and after purging with air**

$Cu^{II}\mathbf{N_3}$ (46 μM), $Cu^{II}\mathbf{N_4}$ (37 μM), $Cu^{II}\mathbf{N_5}$ (30 μM) or mono-$Cu^{I}$ Cu complex (66 μM) was dissolved in phosphate buffer (10 mM, pH 6.8). The resulting mixture was purged with $N_2$ for 20 minutes. $Na_2S_2O_4$ solution (50 μM, 40 μM, 36 μM, or 53 μM) was injected into the mixture to stoichiometrically reduce Cu(II) complex. The reaction solution was then purged with air and its absorption spectra recorded over time.

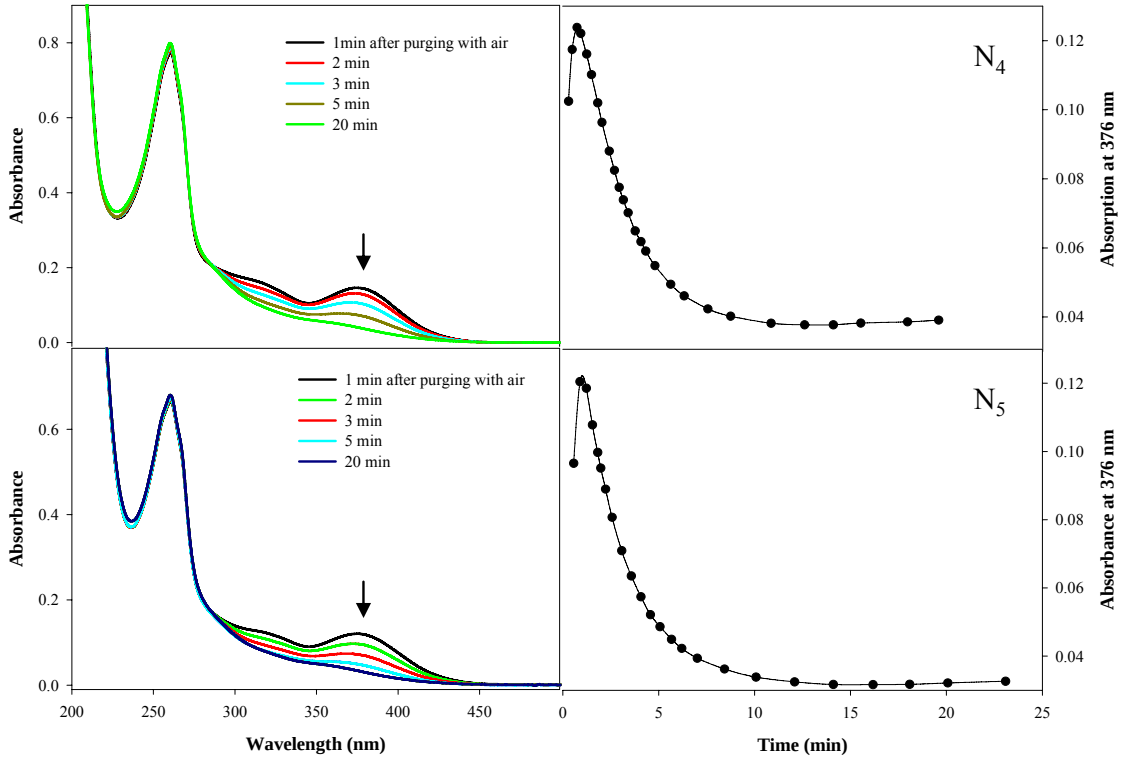


**Figure 3.3 Absorption spectra of the intermediate decay**

$Cu^{II}\mathbf{N_4}$ (40 μM) or $Cu^{II}\mathbf{N_5}$ ( 30 μM) was dissolved in phosphate buffer (10 mM, pH 6.8). The resulting mixture was purged with $N_2$ for 20 minutes. $Na_2S_2O_4$ solution (~44 μM or ~36 μM) was injected into the mixture to stoichiometrically reduce Cu(II) complex. The reaction solution was then purged by air. The absorption spectra (left panels) and absorption at 376 nm (right panels) were recorded over time.

To test whether the intermediate was generated by a direct addition reaction of $Cu^{I}_{2}\mathbf{N_4}$ or $Cu^{I}_{2}\mathbf{N_5}$ with $O_2$ or alternatively, through the reaction of $Cu^{II}_{2}\mathbf{N_4}$ or $Cu^{II}_{2}\mathbf{N_5}$ with $H_2O_2$ produced during oxidation of the Cu(I) complex (Scheme 3.2), catalase was added immediately before $O_2$ addition. The presence of catalase, from 0.6 units/ml to 25 units/ml, had no effect on the rate of the formation of the intermediate (Figure 3.4), thus indicating that the intermediate is formed through a direct reaction of $O_2$ with the Cu(I) complexes.

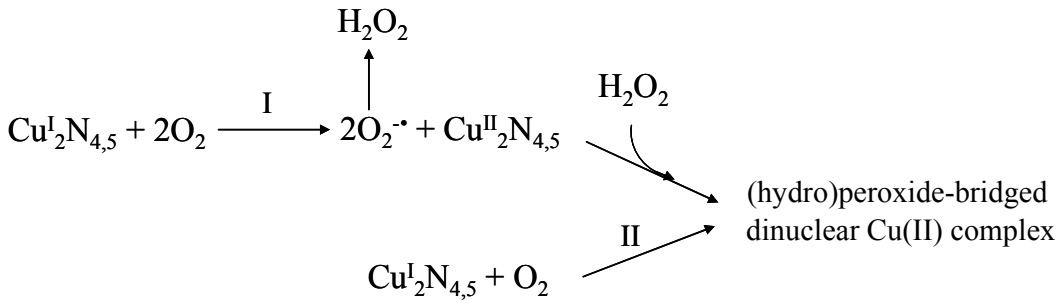


**Scheme 3.2 Possible pathways of the formation of the intermediate**

To further test whether the reaction of $O_2$ with the $Cu^{I}_{2}\mathbf{N_4}$ or $Cu^{I}_{2}\mathbf{N_5}$ complexes was reversible or irreversible, $N_2$ was employed to purge the reaction solution when the maximum absorption at 376 nm was reached in the presence of air. Compared with the control in which the reaction solution was purged with air during the reaction course, no difference in the decay rate of the intermediate was observed (0.39 $min^{-1}$ under air and 0.36 $min^{-1}$ under $N_2$), suggesting that the intermediate generation through reaction with $O_2$ is irreversible.

The effect of externally added electron donors (DMSO, 3-ap and benzoic acid) on the decay of the intermediate generated by $Cu^{I}_{2}\mathbf{N_4}$ was also investigated. As compared with the rate coefficient for decay obtained in the absence of electron donors (0.24 $min^{-1}$), the rate coefficients for the decay in the presence of DMSO (33 mM), 3-ap (2.0 mM) and

benzoic acid (1.0 mM) were 0.26 $min^{-1}$, 0.28 $min^{-1}$ and 0.23 $min^{-1}$, respectively, indicating that decay of the intermediate was not affected by the presence of electron donors.

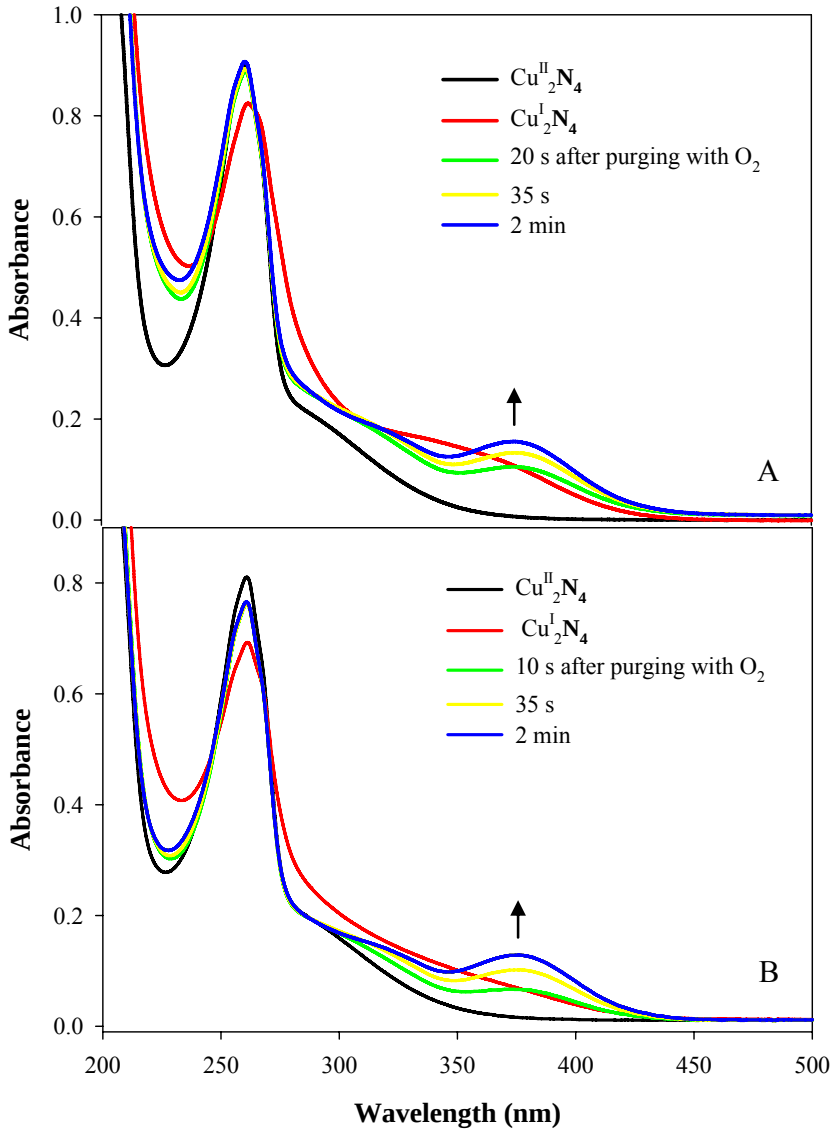


**Figure 3.4 Effect of the presence of catalase on the formation of the intermediate**

$Cu^{II}N_4$ (40 µM) was dissolved in phosphate buffer (10 mM, pH 6.8). The resulting mixture was purged with $N_2$ for 20 minutes. $Na_2S_2O_4$ solution (~ 40 µM) was injected into the mixture to stoichiometrically reduce the Cu(II) complex. Catalase (25 units/ml) 100 µl (panel A) or phosphate buffer100 µl (the control, panel B) was added to the reaction solution at the same time that the solution was purged with $O_2$. Absorption spectra were then recorded over time.

### 3.3.3 Chemical trapping experiment

To test whether the OH radical was generated during intermediate decay, the dependence of the yield of Me-3apf on DMSO and 3-ap was first examined so that appropriate concentrations for the chemical trapping experiments were obtained (Figure 3.5).

Me-3apf was detected during intermediate decay, indicating that the hydroxyl radical was formed, consistent with the results obtained with the Cu(II) and $H_2O_2$ system. However, unlike the Cu(II) and $H_2O_2$ system, only about half of Me-3apf was detected based on the concentration of Cu complex (Figure 3.6). The magnitude of the absorption at 376 nm indicated that the intermediate was not generated quantitatively under the experimental conditions. Based on the extinction coefficient obtained from the reaction of Cu(II) complex with $H_2O_2$, only ~70% of the intermediate was generated, suggesting that some unknown reactions occurs in this system.

Because $O_2$ competes with 3-ap for the methyl radical, thereby reducing the efficiency of Me-3apf formation, $N_2$ was employed to purge the reaction solution following intermediate formation. Aliquots were withdrawn at appropriate time intervals and immediately derivatized with fluorescamine under aerobic conditions. The derivatized reaction mixture was then analyzed by HPLC. The absorption at 376 nm was also recorded at each of the times. The results indicate that although the hydroxyl radical was generated simultaneously with the decay of the intermediate, yield was significantly lower than that expected (Figure 3.7) based on the results obtained with the Cu(II) plus $H_2O_2$ systems.

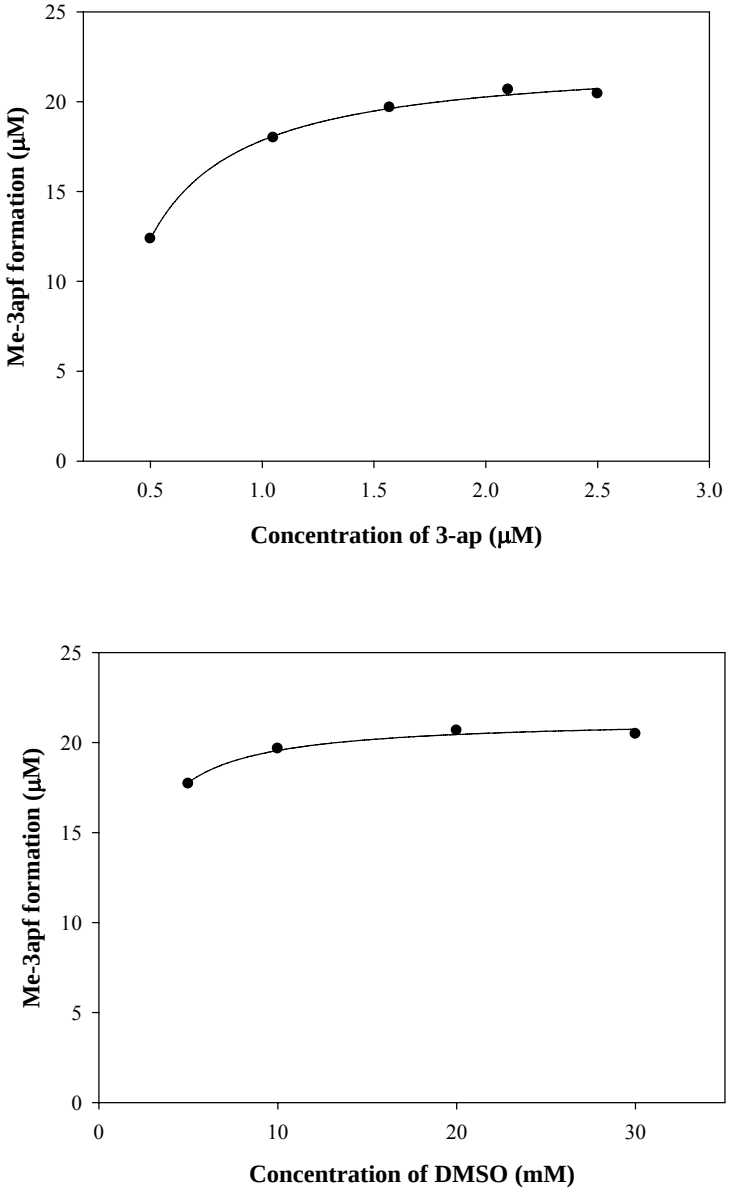


**Figure 3.5 3-ap and DMSO titration experiments**

$Cu^{II}_2\mathbf{N_4}$ complex (40 μM) was dissolved in phosphate buffer (10 mM, pH 6.8). The resulting solution was purged with $N_2$ for 20 minutes. Deaerated $Na_2S_2O_4$ (~ 46 μM) was injected into the solution to stoichiometrically reduce Cu(II) complex. The mixture of DMSO and 3-ap was added to the solution at the same time that the solution was purged with air. DMSO concentration (10 mM) or 3-ap concentration (2.0 mM) was kept constant in 3-ap titration experiments (upper panel) or in DMSO experiments (lower panel) respectively. After a 20 minute reaction, an aliquot was withdrawn and immediately derivatized by fluorescamine at different time intervals. The derivatized sample was then separated and analyzed by HPLC.

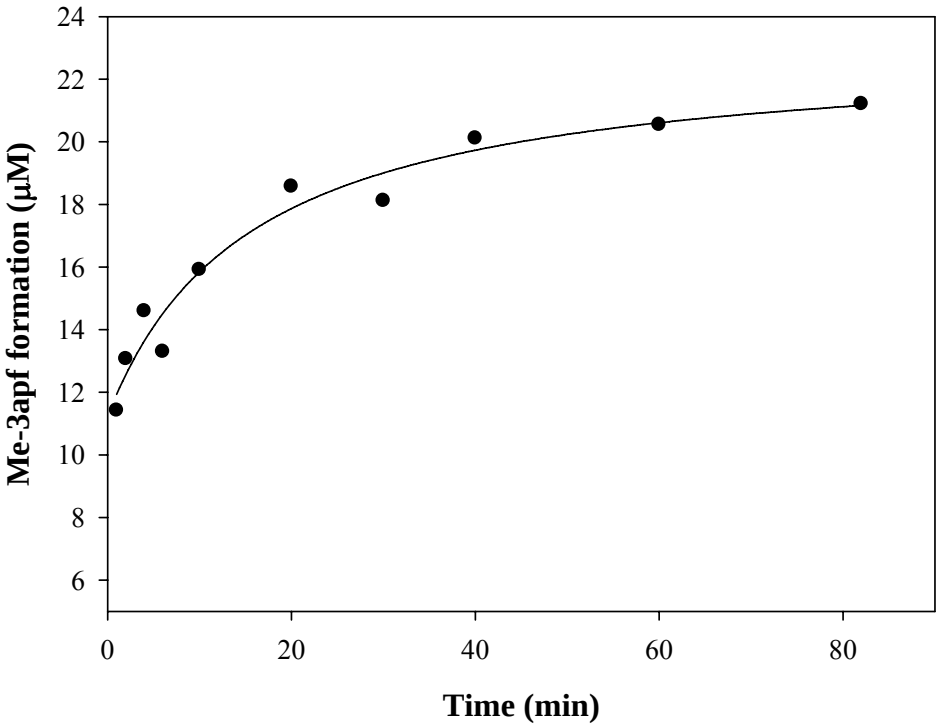


**Figure 3.6 Me-3apf generation during decay of the intermediate formed by $Cu^{I}_{2}N_4$ complex and $O_2$**

$Cu^{II}_{2}$**N4** complex (40 μM) was dissolved in phosphate buffer (10 mM, pH 6.8). The resulting solution was purged with $N_2$ for 20 minutes. Deaerated $Na_2S_2O_4$ (46 μM) was injected into the solution to stoichiometrically reduce Cu(II) complex. The mixture of DMSO (10 mM) and 3-ap (1.5 mM) was added to the solution at the same time that the solution was purged with air. The reaction solution was withdrawn at different times and immediately derivatized by fluorescamine. The derivatized sample was then separated and analyzed by HPLC. The line in this figure was obtained based on a fit to polynomial equation only so that the trend could be shown clearly.

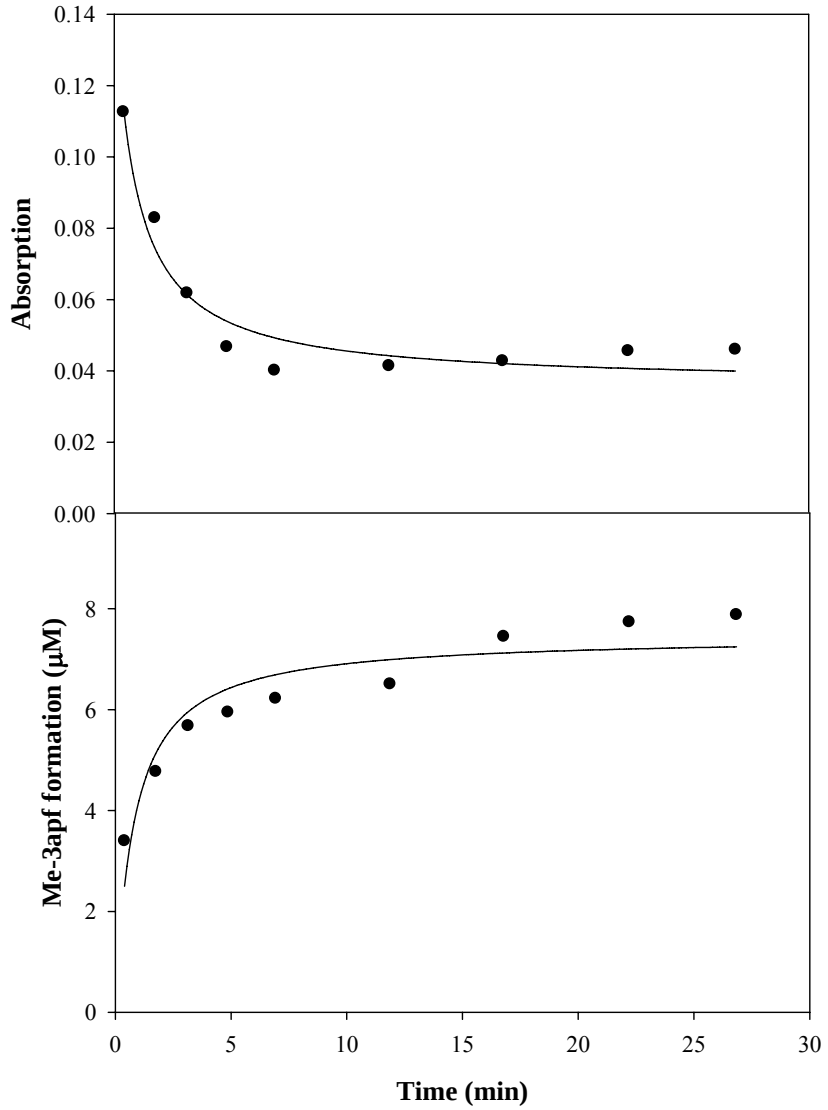


**Figure 3.7 Formation of Me-3apf and absorption at 376 nm during the decay of the intermediate formed by $Cu^{I}_{2}N_4$ complex and $O_2$**

$Cu^{II}_{2}\mathbf{N_4}$ complex (40 μM) was dissolved in phosphate buffer (10 mM, pH 6.8). The resulting solution was purged with $N_2$ for 20 minutes. Deaerated $Na_2S_2O_4$ (~ 46 μM) was injected into the solution to stiochiometrically reduce Cu(II) complex. The Cu(I) complex solution was then purged with air. When the maximum absorption at 376 nm was reached, $N_2$ was employed to purge the solution in place of air. Deaerated mixture of DMSO (10 mM) and 3-ap (1.5 mM) was added to the reaction solution after the solution had been purged with $N_2$ for one minute. The reaction solution was withdrawn at different times and immediately derivatized with fluorescamine. The derivatized sample was then separated and analyzed by HPLC. Lines in this figure were obtained based on a fit to polynomial equation only so that the trend could be shown clearly.

## 3.4 Summary and Conclusions

Based on these results, an intermediate with an absorption band at 376 nm is generated by either the $Cu^{I}_{2}\mathbf{N_4}$ or $Cu^{I}_{2}\mathbf{N_5}$ complex in the presence of $O_2$. This intermediate is not generated with the $Cu^{I}_{2}\mathbf{N_3}$ and mono-$Cu^{I}$ complex. The spectrum of this intermediate is indistinguishable from that generated from the $Cu^{II}_{2}\mathbf{N_4}$ or $Cu^{II}_{2}\mathbf{N_5}$ complexes in the presence of $H_2O_2$. The formation of the intermediate was not reversible; purging with $N_2$ following its complete formation did not accelerate its disappearance.

The intermediates formed from $Cu^{I}_{2}\mathbf{N_4}$ and $Cu^{I}_{2}\mathbf{N_5}$ complexes decay exponentially at 26.5 $^{o}$C, with decay rate constants of 0.0073 $s^{-1}$ ($Cu^{II}_{2}\mathbf{N_4}$) and 0.0078 $s^{-1}$ ($Cu^{II}_{2}\mathbf{N_5}$), which are very similar to those obtained from $Cu^{II}_{2}\mathbf{N_4}$ ( 0.0081 $s^{-1}$) and $Cu^{II}_{2}\mathbf{N_5}$ (0.0079 $s^{-1}$). These rate constants suggest that the same intermediate is generated via these two different reaction routes. The decay of the intermediates in Cu(I) plus $O_2$ system is not affected by the presence of externally added electron donors (DMSO, 3-ap and benzoic acid), mirroring the behavior of the intermediates generated from the Cu(II) complexes plus $H_2O_2$ system.

The addition of catalase did not inhibit the formation of the intermediate, suggesting that the intermediate is formed through a direct reaction between $O_2$ and the Cu(I) complex and not through a reaction of the Cu(II) complex with $H_2O_2$, formed through oxidation of the Cu(I) complex by $O_2$.

Chemical trapping experiments indicate that hydroxyl radical is produced during intermediate decay. The Origin of the lower yield of the intermediate, as well as the lower than expected yield of Me-3apf relative to the Cu(II) plus $H_2O_2$ system may be the result of several factors: 1) interference from the oxidation products of $Na_2S_2O_4$ 2)

interference from $O_2$ in radical trapping experiments 3) the decomposition of Cu(I) complex prior to reaction with $O_2$.

Combined with the results from the previous chapter, an overall mechanism of reactive intermediate generation by copper(II) complexes in the presence of $H_2O_2$ and Cu(I) complexes in the presence of $O_2$ is proposed and shown in Scheme 3.3.

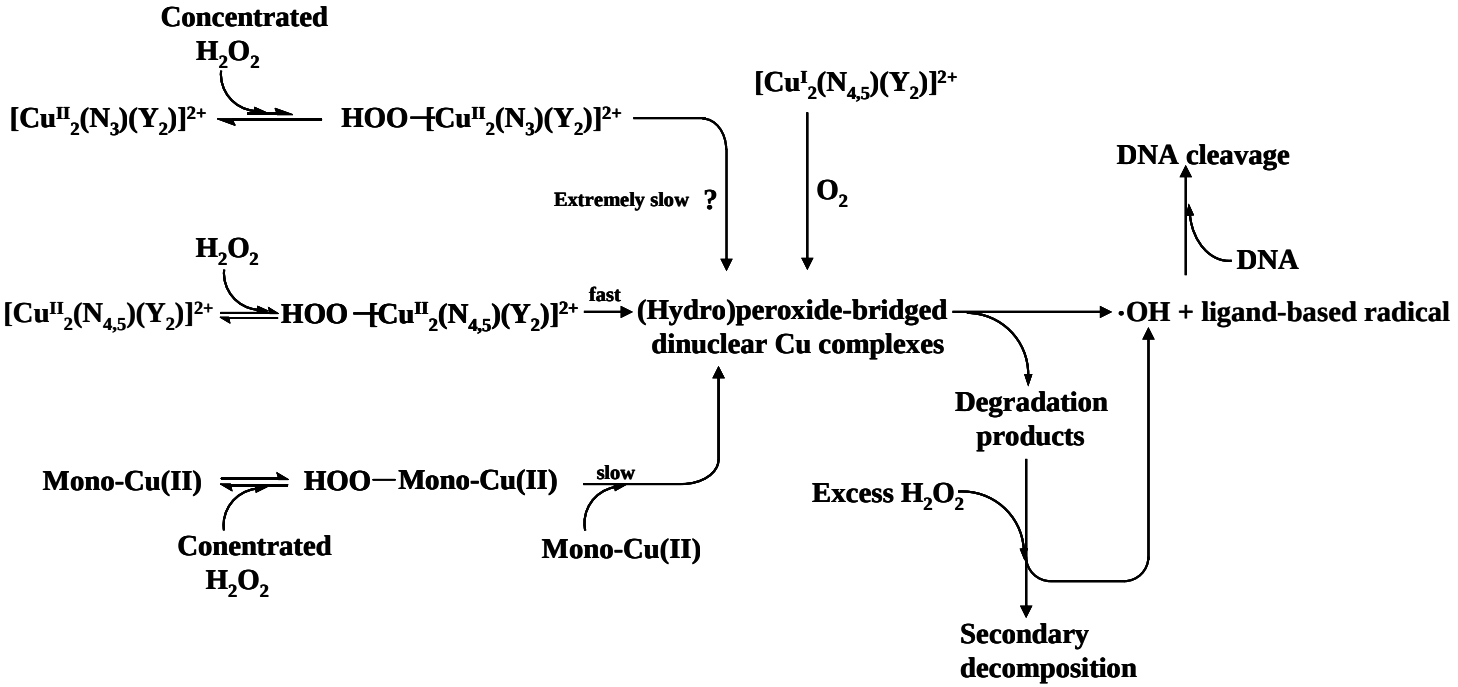


**Scheme 3.3 Proposed mechanism of reactive intermediate generation by Cu(II) complexes in the presence of $H_2O_2$ and Cu(I) complexes in the presence of $O_2$**

# Chapter IV Conclusions and Future Work

## 4.1 Conlusions

The objective of this work was to determine the nature of the reactive oxidizing intermediates generated from binuclear copper complexes and a mononuclear analogue in aqueous solutions, to learn how the copper ligand environment could affect the oxidative chemistry, as well as to provide insight into the mechanism of DNA cleavage mediated by these copper complexes. In this study, a copper-peroxo intermediate was observed in aqueous solutions for the first time and its reactivity was systematically studied. This work suggests that the DNA cleavage is not the result of direct reaction with a copper-based intermediate, but instead arises from reaction with either a hydroxyl radical or a ligand-based radical.

Although many previous studies have proposed that a metal-based intermediate is the reactive species responsible for DNA cleavage,[24, 36, 37] no clear evidence for formation of the intermediate in aqueous solutions have been presented, especially for multinuclear copper complex systems. This study clearly shows that this copper-based intermediate does not react with a series of compounds including guanine, suggesting it is not the reactive intermediate initiating DNA degradation, but is instead a precursor of the reactive intermediate. In most of earlier studies, hydroxyl radicals and high-valent metal species could not be differentiated because of limitations of the methodology employed. In this work, a highly sensitive and reliable technique was employed to discriminate between hydroxyl radical and a metal-based oxidizing species by reaction with DMSO and methane. The results provided strong evidence of hydroxyl radical formation during

the decomposition of the copper-based intermediate. Further, little prior work examined changes in speciation of mononuclear and dinuclear copper complex systems under different conditions. This study clearly shows the effect of phosphate concentration and pH on the speciation, which provides a good base for future work.

## 4.2 Future work

Although UV/visible spectroscopy clearly revealed the formation of an intermediate in the $Cu_2\mathbf{N_{4,5}}$ plus $H_2O_2$ system and the Cu(I) plus $O_2$ system, the structure(s) of the intermediate(s) is still unknown. The intermediates are reasonably stable at low temperature and under light (Appendix A), suggesting that resonance Raman spectroscopy could be employed at low temperature to obtain more exact structural information.

As mentioned in chapter II, the activation energy of the intermediate formation could not be obtained due to very fast reaction of $Cu^{II}_2\mathbf{N_4}$ with $H_2O_2$ at high temperatures. The more rapid kinetics could be examined by stopped-flow experiments.

The decomposition products of the intermediate in the presence and absence of a radical scavenger need to be identified to test further whether the intermediate decays via an intramolecular electron transfer from ligand to copper-peroxo center. Product analysis will also allow information about the site and mechanism of electron transfer from the ligand, as well as where hydroxyl radicals might attack the ligand.

Although this study has provided strong evidence that same intermediate is also generated by the reaction of $Cu^{I}_2\mathbf{N_{4,5}}$ complex with $O_2$, additional work is needed to confirm this finding, including a determination of the rate constant for formation, the

temperature dependence of the intermediate formation and decay, stoichiometry between hydroxyl radical generation and the loss of the intermediate, and structural studies by resonance Raman Spectroscopy, as one example. Because the oxidation products of $Na_2S_2O_4$ ($SO_2$, $HSO_3^-$) might interfere with the absorption spectra of the intermediate decay and the hydroxyl radical trapping, Cu(I) complexes need to be synthesized and directly employed to study the reaction with $O_2$. Electrochemical reduction of Cu(II) to Cu(I) complex is another possible way to obtain a clean reaction system. By these methods, the nature of intermediate formed by the reaction of $Cu^{I}_2\mathbf{N_{4,5}}$ complex with $O_2$ can be more fully understood, which will be very helpful for understanding the mechanism of copper-mediated DNA cleavage.

# Appendix A Study of Stability of the Intermediate Generated by $Cu^{II}_2N_4$ Complex in the Presence of $H_2O_2$

## A.1 Apparatus

The broad band irradiation system consisted of a 300W Xe arc lamp housed in an ILC technology R400-2 and powered by and ILC technology PS300-1 power supply.

The monochromatic irradiation system consisted of a 1000W Xenon-Mercury lamp and a Spectral Energy GM 252 monochromator. The band pass was set to10 nm.

## A.2 Experiment Proctocols

To test the stability of the intermediate at low temperature and under broad band irradiation, the standard reaction was carried out in a Micro-Vial (Kimble Knotes) with total reaction volume of 3 mL. $Cu^{II}_2\mathbf{N_4}$ complex (400 μM) was dissolved in appropriate volume of 10 mM phosphate buffer at pH 6.8 and purged with $N_2$ for 20 minutes. 100 μl of deoxygenated $H_2O_2$ stock solution was injected to initiate the reaction (final $[H_2O_2]$ = 4 mM) under anaerobic conditions. When the absorption at 376 reached its maximum, the solution was separated into two aliquots, of the first aliquot was recorded the absorption spectrum (control) while the second aliquot was immediately frozen in a liquid $N_2$ dewer. The second aliquot was stored in liquid $N_2$ for 1.5 - 2 hours in the presence of broad band radiation or in the absence of broad band radiation. The aliquot was thawed and its absorption spectrum recorded and compared to the first aliquot. A 1cm or 1 mm quartz cuvette was employed for the measurements.

To test the stability of the intermediate under monochromatic radiation at 376 nm at room temperature, $Cu^{II}_2\mathbf{N_4}$ complex (80 μM) was dissolved in appropriate volume of 10 mM phosphate buffer at pH 6.8 and purged with $N_2$ for 20 minutes. One-hundred microliter of deoxygenated $H_2O_2$ stock solution was injected to initiate the reaction (final $[H_2O_2]$ = 200 μM) under anaerobic conditions. When the absorption at 376 reached its maximum, the solution was exposed to monochromatic radiation at 376 nm for several minutes (shown in figure captions), absorption at 376 nm was then recorded and compared with the control in which the monochromatic radiation was absent.

## A.3 Results

The stability of the intermediate at low temperature was investigated in 10 mM phosphate buffer at pH 6.8. Immediately after the maximum absorbance at 376 nm was reached at room temperature, the resultant solution was frozen in liquid $N_2$ and kept under liquid $N_2$ for two hours. Absorption spectra were recorded and compared before and after sample freezing in liquid $N_2$ for two hours (Figure A.1). The results showed that the intermediate exhibited good stability at 77 $^{o}$K.

The stability of the intermediate under broad band radiation was also studied. The procedure was the same as the experiments described above except that the frozen sample was exposed to broad band radiation for 1.5 hours (Figure A.2). The result also indicated that the intermediate has good stability under broad band radiation.

The effect of monochromatic radiation at 376 nm on the intermediate decay was examined at room temperature. No significant differences were observed between the radiation experiments and the control experiments in which the monochromatic radiation

was absent. Moreover, the intermediate decay after radiation was not affected (Figure A.3).

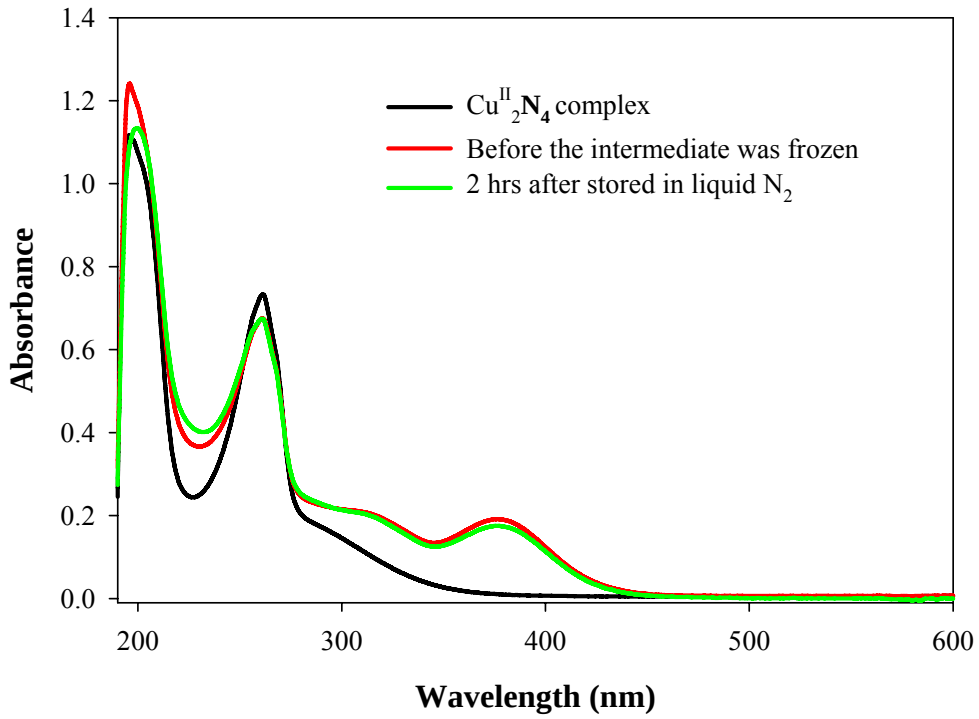


**Figure A.1 Stability of intermediate formed with Cu$^{II}_2$N$_4$ complex at low temperature**

Cu$^{II}_2$**N$_4$** complex (40 μM) was dissolve in phosphate buffer (10 mM, pH 6.8). $H_2O_2$ (400 μM) was added to initiate the reaction under anaerobic conditions. Absorption spectrum was recorded right after the intermediate generation was complete at room temperature. The sample solution was then frozen and stored in liquid $N_2$ for 2 hours. After the sample was thawed, absorption spectrum was recorded again.

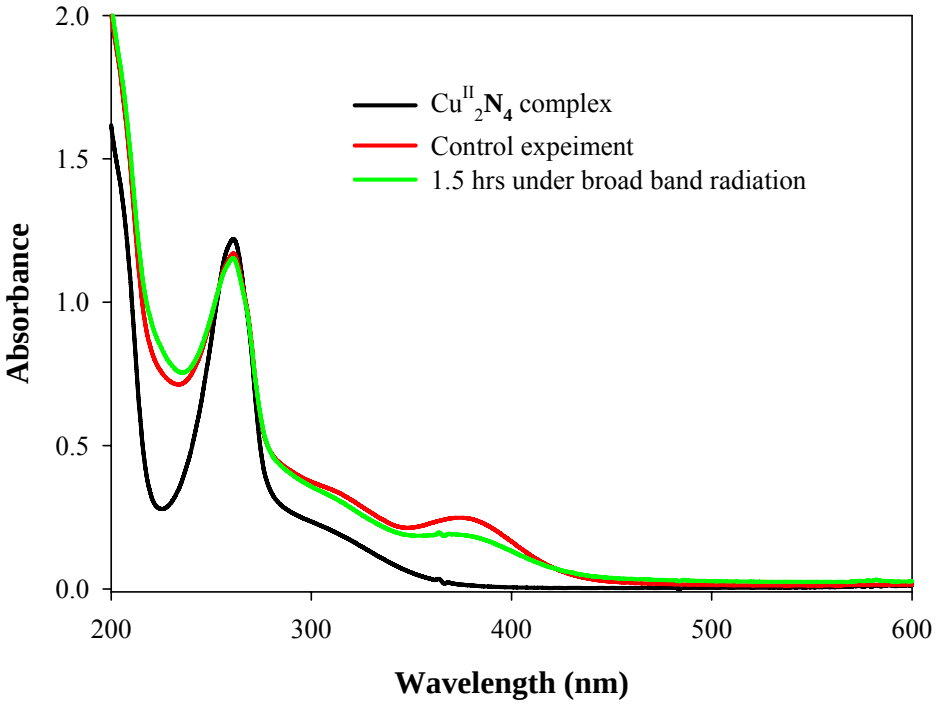


**Figure A.2 Stability of the intermediate under broad band radiation.**

$Cu^{II}_2$**N$_4$** complex (400 μM) was dissolved in phosphate buffer (10 mM, pH 6.8). $H_2O_2$ (4 mM) was added to initiate the reaction under anaerobic conditions. When the absorption at 376 reached its maximum, the solution was separated into two aliquots, of the first aliquot was recorded the absorption spectrum (control ) while the second aliquot was immediately frozen in a liquid $N_2$ dewer. The second aliquot was stored in liquid $N_2$ for for 1.5 - 2 hours in the presence of broad band radiation or in the absence of broad band radiation. After it was thawed, absorption spectrum was measured. 1 mm quartz cuvette was used for measurement in this experiment.

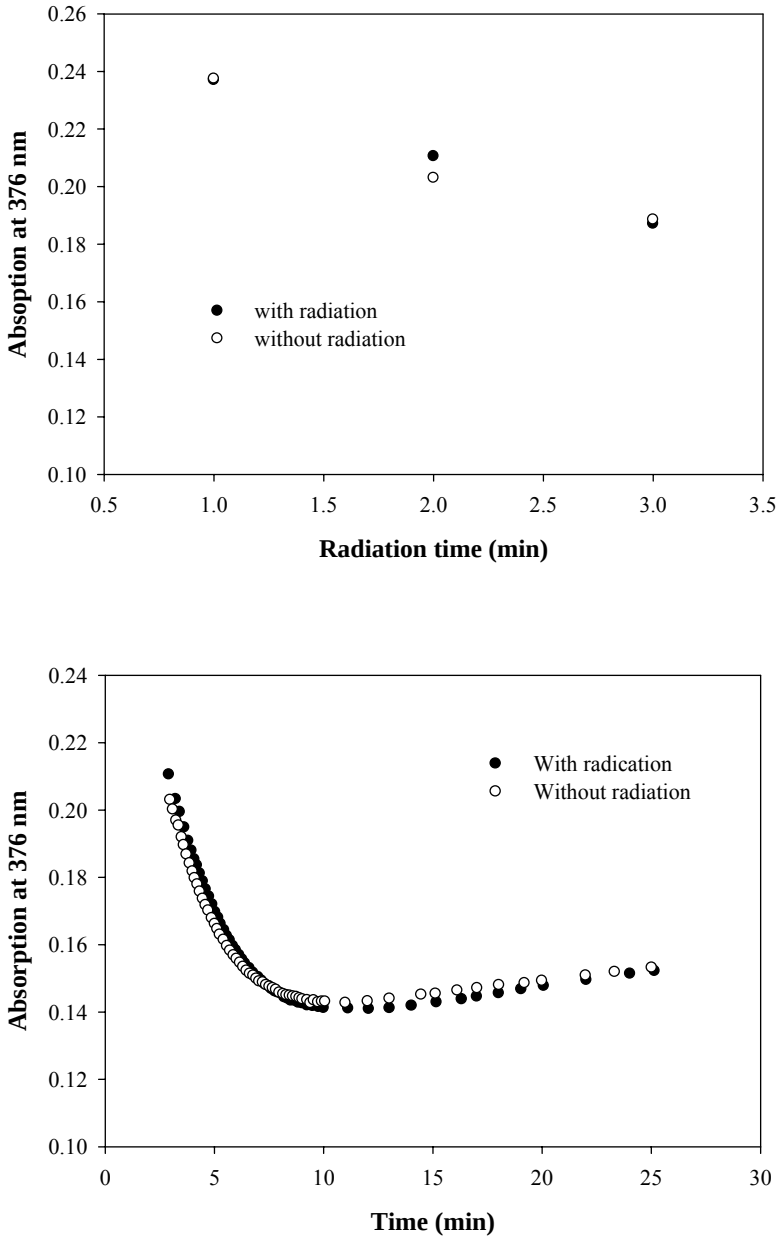


**Figure A.3 Effect of monochromatic radiation at 376 nm on the decay of the intermediate**

$Cu^{II}_2\mathbf{N_4}$ complex (80 μM) was dissolved phosphate buffer (10 mM, pH 6.8) and purged with $N_2$ for 20 minutes. Deoxygenated $H_2O_2$ solution (200 μM) was injected to initiate the reaction under anaerobic conditions. When the absorption at 376 reached its maximum, the solution was exposed under monochromatic radiation at 376 nm, absorption at 376 nm was then recorded and compared with the control in which the monochromatic radiation was absent.

# Appendix B Study of Hydroxyl Radical Generation by Cu(II) Complex in the Presence of a Reducing Reagent and $H_2O_2$

## B.1 Reagents and Materials

5,5'-dithiobis(2-nitrobenzoic acid) (DTNB) (99%), 1,10-phenanthroline monohydrate(OP) (99%) were purchased from Aldrich. Other chemicals used in this study were indentical to those described in chapter II and were obtained from the same sources.

## B.2 Experiment protocols

1,10-phenanthroline Cu(II) ($Cu(OP)_2$) stock solution was prepared by dissolving an appropriate amount of $CuCl_2$ in 1,10-phenanthroline monohydrate ligand (OP) solution at pH 2.0. pH of resulting solution was then carefully adjusted to 5.3. The molar ratio between Cu ion and OP was 1 to 2.

Concentration of 3-MPA in stock or in reaction mixture was determined by the reaction with DTNB at pH 8.0.[143] Since 3-MPA reacts with DTNB to quantitatively produce a highly colored 4-nitro-2-carboxyl-thiophenol anion (412 nm, $\varepsilon_{412}$ = 13600 $M^{-1}cm^{-1}$), this anion can be used to quantify the concentration of 3-MPA. An appropriate volume of 3-MPA was first dissolved in 2 ml phosphate buffer (30 mM, pH 8.0). Excess DNTB (at least seven fold excess than 3-MPA), prepared by dissolving appropriate amount of DNTB solid into phosphate buffer (100 mM, pH 7.0), was then added and fully mixed. After a one minute reaction, absorption at 412 nm was recorded.

Concentration of 3-MPA was then obtained based on absorption at 412 nm and dilution factors.

The standard reaction for optical absorption was carried out in a cuvette with total volume of 3 ml. An appropriate volume of $Cu(OP)_2$ solution (10 μM) was added to an given volume of phosphate buffer (10 mM, pH 6.8). The resultant solution was then purged with $N_2$ for 20 minutes. Deaerated 3-MPA solution (10 μM) was injected into the solution under anaerobic conditions. Absorption spectra before and after addition of 3-MPA were recorded.

The radical trapping experiments were carried out in a 5 ml Micro-Vial with total reaction volume of 3 ml. A sample solution containing Cu(II) complex, DMSO (10 mM), 3-ap (1.0 mM) and ligand with varying concentrations were prepared in 10 mM phosphate buffer at pH 6.8. The solution was purged with $N_2$ for 20 minutes. Deaerated $H_2O_2$ (1.0 mM) and 3-MPA (1.5 mM) were added to initiate the reaction under anaerobic conditions. After a 2 hour reaction, the reaction was terminated by derivatization with fluorescamine under aerobic conditions. The reaction solution was purged with $N_2$ during the entire reaction course.

## B.3 Results

As shown in Figure B.1, when 3-MPA was added to $Cu^{II}(OP)_2$ complex solution, an absorption band at ~ 450 nm was observed. Since neither the ligand nor 3-MPA has absorption at this wavelength, this band indicated that a new species was generated, suggesting an interaction between 3-MPA and Cu complex existed. To further test the effect of 3-MPA on the reactive speciation, hydroxyl radical generation was investigated in the presence of different concentration of ligand ranging from 0 μM to 800 μM at fixed 3-MPA concentration (Figure B.2). Different hydroxyl radical efficiency was obtained at different concentration of ligand, suggesting that different species were generated, probably due to competitive binding of ligand and 3-MPA to copper center. This result is consistent with the spectroscopic studies by Gilbelt and coworkers [51] which also suggests that a mixed complex is formed instead of $Cu^{I}(OP)_2$ in the presence of excess thiol.

Similar experiments were performed for mono-Cu(II) complex (Figure B.3). The result also suggested that the presence of excess 3-MPA might change the reactive speciation.

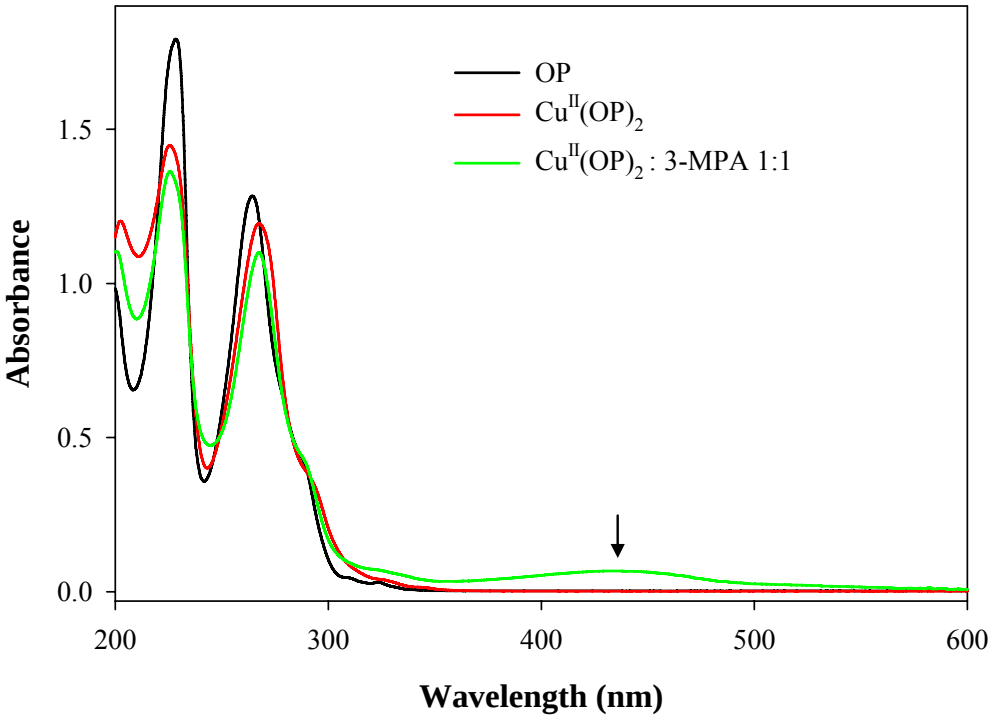


**Figure B.1 Absorption spectra of $Cu^{II}(OP)_2$ complex before and after addition of 3-MPA**

$Cu^{II}(OP)_2$ complex (10 μM) was dissolved in phosphate buffer (10 mM, pH 6.8). Deaerated 3-MPA (10 μM) was added to the solution under anaerobic conditions. Absorption spectra before and after addition of 3-MPA were recorded.

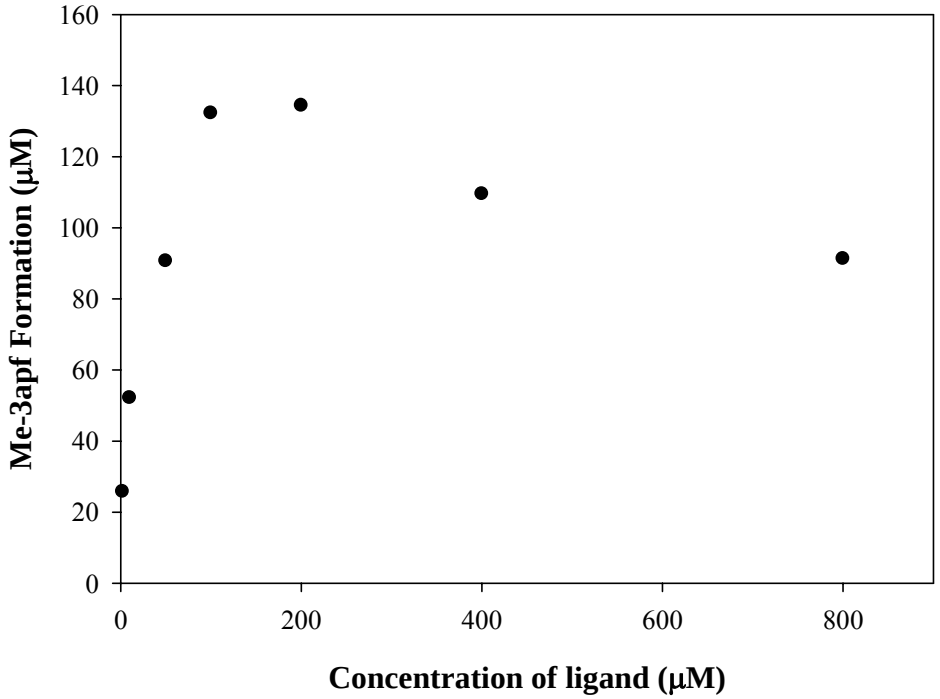


**Figure B.2 Me-3apf generation for $Cu^{II}(OP)_2$ complex at different concentration of ligand**

$Cu^{II}(OP)_2$ complex (1.0 μM), DMSO (10 mM), 3-ap (1.0 mM) and ligand (2 μM, 10 μM, 50 μM, 100 μM, 200 μM, 400 μM or 800 μM) were prepared in 10 mM phosphate buffer at pH 6.8. The solution was purged with $N_2$ for 20 minutes. Deaerated $H_2O_2$ (1.0 mM) and 3-MPA (1.5 mM) were added to initiate the reaction under anaerobic conditions. After a 2 hour reaction, the reaction was terminated by derivatization with fluorescamine under aerobic conditions. The derivatized sample was then separated and analyzed by HPLC.

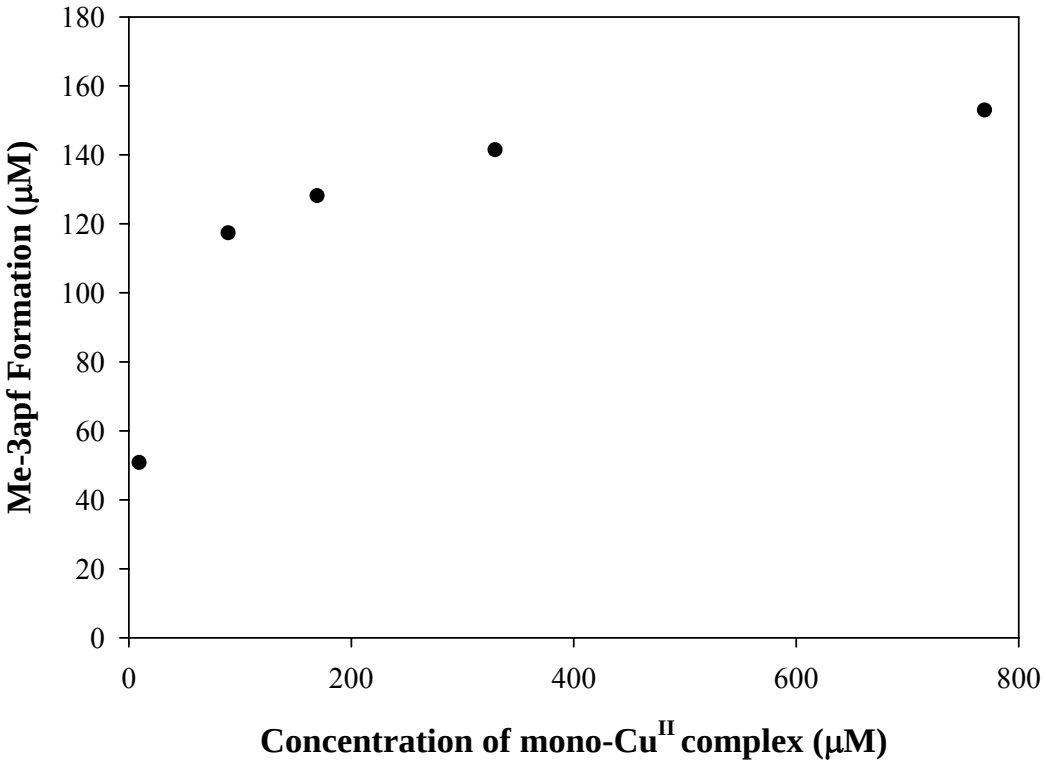


**Figure B.3 Me-3apf generation for mono-$Cu^{II}$ complex at different concentration of ligand**

Mono-$Cu^{II}$ complex (10.0 μM), DMSO (10 mM), 3-ap (1.0 mM) and ligand (10 μM, 90 μM, 170 μM, 330 μM or 770 μM) were prepared in 10 mM phosphate buffer at pH 6.8. The solution was purged with $N_2$ for 20 minutes. Deaerated $H_2O_2$ (1.0 mM) and 3-MPA (1.5 mM) were added to initiate the reaction under anaerobic conditions. After a 2 hour reaction, the reaction was terminated by derivatization with fluorescamine under aerobic conditions. The derivatized sample was then separated and analyzed by HPLC.

## References


1. Cadet, J.; Berger, M.; Decarroz, C.; Wagner, J. R.; van Lier, J. E.; Ginot, Y. M.; Vigny, P., *Biochimie* **1986,** *68*, (6), 813-34.
2. Von Sonntag, C., *The Chemical Basis of Radiation Biology*. 1987; pp 520.
3. Von Sonntag, C.; Schuchmann, H. P., *Methods in enzymology* **1994,** *233*, 47-56.
4. Urata, H.; Yamamoto, K.; Akagi, M.; Hiroaki, H.; Uesugi, S., *Biochemistry* **1989,** *28*, (25), 9566-9.
5. Piette, J., *Journal of photochemistry and photobiology. B, Biology* **1991,** *11*, (3-4), 241-60.
6. Kasai, H.; Yamaizumi, Z.; Berger, M.; Cadet, J., *Journal of the American Chemical Society* **1992,** *114*, (24), 9692-4.
7. Demple, B.; Halbrook, J., *Nature* **1983,** *304*, (5925), 466-8.
8. Mouret, J. F.; Odin, F.; Polverelli, M.; Cadet, J., *Chemical Research in Toxicology* **1990,** *3*, (2), 102-10.
9. Vieira, A. J. S. C.; Steenken, S., *Journal of the American Chemical Society* **1990,** *112*, (19), 6986-94.
10. Steenken, S., *Chemical Reviews* **1989,** *89*, (3), 503-20.
11. Grollman, A. P.; Moriya, M., *Trends in genetics: TIG* **1993,** *9*, (7), 246-9.
12. Sigman, D. S.; Mazumder, A.; Perrin, D. M., *Chemical Reviews* **1993,** *93*, (6), 2295-316.
13. Pyle, A. M.; Barton, J. K., *Progress in Inorganic Chemistry* **1990,** *38*, 413-75.
14. Dervan, P. B., *Science* **1986,** *232*, (4749), 464-71.

15. Pratviel, G.; Bernadou, J.; Meuminer, B., *Angewandte Chemie, International Edition in English* **1995,** *34*, (7), 746-69.

16. Pogozelski, W. K.; Tullius, T. D., *Chemical Reviews* **1998,** *98*, (3), 1089-1107.

17. Aruoma, O. I.; Halliwell, B.; Gajewski, E.; Dizdaroglu, M., *Journal of Biological Chemistry* **1989,** *264*, (34), 20509-12.

18. Smith, R. C.; Reed, V. D.; Hill, W. E., *Phosphorus, Sulfur and Silicon and the Related Elements* **1994,** *90*, (1-4), 147-54.

19. Tabbi, G.; Fry, S. C.; Bonomo, R. P., *Journal of Inorganic Biochemistry* **2001,** *84*, (3-4), 179-187.

20. Liu, C.; Zhou, J.; Li, Q.; Wang, L.; Liao, Z.; Xu, H., *Journal of Inorganic Biochemistry* **1999,** *75*, (3), 233-240.

21. Dizdaroglu, M.; Aruoma, O. I.; Halliwell, B., *Biochemistry* **1990,** *29*, (36), 8447-51.

22. Amine, A.; Atmani, Z.; El Hallaoui, A.; Giorgi, M.; Pierrot, M.; Reglier, M., *Bioorganic & Medicinal Chemistry Letters* **2001,** *12*, (1), 57-60.

23. Kobayashi, T.; Kunita, M.; Nishino, S.; Matsushima, H.; Tokii, T.; Masuda, H.; Einaga, H.; Nishida, Y., *Polyhedron* **2000,** *19*, (26-27), 2639-2648.

24. Masarwa, M.; Cohen, H.; Meyerstein, D.; Hickman, D. L.; Bakac, A.; Espenson, J. H., *Journal of the American Chemical Society* **1988,** *110*, (13), 4293-7.

25. Johnson, G. R. A.; Nazhat, N. B., *Journal of the American Chemical Society* **1987,** *109*, (7), 1990-4.

26. Meijler, M. M.; Zelenko, O.; Sigman, D. S., *Journal of the American Chemical Society* **1997,** *119*, (5), 1135-1136.

27. Goldstein, S.; Meyerstein, D., *Accounts of Chemical Research* **1999,** *32*, (7), 547-550.

28. Walling, C., *Accounts of Chemical Research* **1975,** *8*, (4), 125-31.

29. Kremer, M. L., *Physical Chemistry Chemical Physics* **1999,** *1*, (15), 3595-3605.

30. Sawyer, D. T.; Sobkowiak, A.; Matsushita, T., *Accounts of Chemical Research* **1996,** *29*, (9), 409-416.

31. Yamazaki, I.; Piette, L. H., *Journal of the American Chemical Society* **1991,** *113*, (20), 7588-93.

32. Rush, J. D.; Koppenol, W. H., *Journal of Biological Chemistry* **1986,** *261*, (15), 6730-3.

33. Sutton, H. C.; Vile, G. F.; Winterbourn, C. C., *Archives of biochemistry and biophysics* **1987,** *256*, (2), 462-71.

34. Yusa, K.; Shikama, K., *Biochemistry* **1987,** *26*, (21), 6684-8.

35. Gutteridge, J. M. C.; Maidt, L.; Poyer, L., *Biochemical Journal* **1990,** *269*, (1), 169-74.

36. Halliwell, B.; Gutteridge, J. M. C., *Methods in Enzymology* **1990,** *186*, (Oxygen Radicals Biol. Syst., Pt. B), 1-85.

37. Johnson, G. R. A.; Nazhat, N. B.; Saadalla-Nazhat, R. A., *Journal of the Chemical Society, Chemical Communications* **1985**, (7), 407-8.

38. Yamamoto, K.; Kawanishi, S., *Journal of Biological Chemistry* **1989,** *264*, (26), 15435-40.

39. Humphreys, K. J.; Karlin, K. D.; Rokita, S. E., *Journal of the American Chemical Society* **2001,** *123*, (23), 5588-5589.

40. Humphreys, K. J.; Karlin, K. D.; Rokita, S. E., *Journal of the American Chemical Society* **2002,** *124*, (27), 8055-8066.

41. Humphreys, K. J.; Karlin, K. D.; Rokita, S. E., *Journal of the American Chemical Society* **2002,** *124*, (21), 6009-6019.

42. Aruoma, O. I.; Halliwell, B.; Gajewski, E.; Dizdaroglu, M., *Biochemical Journal* **1991,** *273*, (3), 601-4.

43. Van Steveninck, J.; Van der Zee, J.; Dubbelman, T. M. A. R., *Biochemical Journal* **1985,** *232*, (1), 309-11.

44. Gilbert, B. C.; Silvester, S.; Walton, P. H.; Whitwood, A. C., *Journal of the Chemical Society, Perkin Transactions 2: Physical Organic Chemistry* **1999**, (9), 1891-1895.

45. Milligan, J. R.; Ward, J. F., *Radiation Research* **1994,** *137*, (3), 295-9.

46. Buettner, G. R., *Archives of Biochemistry and Biophysics* **1993,** *300*, (2), 535-43.

47. Halliwell, B.; Gutteridge, J. M. C., *Free radicals in biology and medicine*. 3rd ed.; Oxford university press Inc: 1999; pp 53.

48. John, D. C. A.; Douglas, K. T., *Biochemical Journal* **1993,** *289*, (2), 463-8.

49. John, D. C. A.; Douglas, K. T., *Biochemical and Biophysical Research Communications* **1989,** *165*, (3), 1235-42.

50. Veal, J. M.; Merchant, K.; Rill, R. L., *Nucleic acids research* **1991,** *19*, (12), 3383-8.

51. Gilbert, B. C.; Silvester, S.; Walton, P. H., *Journal of the Chemical Society, Perkin Transactions 2: Physical Organic Chemistry* **1999**, (6), 1115-1122.

52. Jain, A.; Alvi, N. K.; Parish, J. H.; Hadi, S. M., *Mutation Research* **1996,** *357*, (1,2), 83-88.

53. Kieber, D. J.; Blough, N. V., *Analytical Chemistry* **1990,** *62*, (21), 2275-83.

54. Samuni, A.; Krishna, C. M.; Riesz, P.; Finkelstein, E.; Russo, A., *Free radical biology & medicine* **1989,** *6*, (2), 141-8.

55. Samuni, A.; Samuni, A.; Swartz, H. M., *Free radical biology & medicine* **1989,** *6*, (2), 179-83.

56. Janzen, E. G.; Krygsman, P. H.; Lindsay, D. A.; Haire, D. L., *Journal of the American Chemical Society* **1990,** *112*, (23), 8279-84.

57. Gutteridge, J. M. C.; Stocks, J., *Critical Reviews in Clinical Laboratory Sciences* **1981,** *14*, (4), 257-329.

58. Ogihara, H.; Ogihara, T.; Miki, M.; Yasuda, H.; Mino, M. *Plasma copper and antioxidant status in Wilson's disease*; Department of Pediatrics, Osaka Medical College, Japan: United States, 1995; pp 219-26.

59. Kadiiska, M. B.; Burkitt, M. J.; Xiang, Q. H.; Mason, R. P., *The Journal of clinical investigation* **1995,** *96*, (3), 1653-7.

60. Young, I. S.; Trouton, T. G.; Torney, J. J.; McMaster, D.; Callender, M. E.; Trimble, E. R., *Free radical biology & medicine* **1994,** *16*, (3), 393-7.

61. Halliwell, B.; Gutteridge, J. M. C., *Free radicals in biology and medicine*. 3rd ed.; Oxford University Press Inc: 1999; pp 257.

62. Tullius, T. D., *Nature* **1988,** *332*, (6165), 663-4.

63. Hertzberg, R. P.; Hecht, S. M.; Reynolds, V. L.; Molineux, I. J.; Hurley, L. H., *Biochemistry* **1986,** *25*, (6), 1249-58.

64. Gunderson, S. I.; Chapman, K. A.; Burgess, R. R., *Biochemistry* **1987,** *26*, (6), 1539-46.

65. Celander, D. W.; Cech, T. R., *Biochemistry* **1990,** *29*, (6), 1355-61.

66. Prigodich, R. V.; Martin, C. T., *Biochemistry* **1990,** *29*, (35), 8017-9.

67. Pogozelski, W. K.; McNeese, T. J.; Tullius, T. D., *Journal of the American Chemical Society* **1995,** *117*, (24), 6428-33.

68. Hertzberg, R. P.; Dervan, P. B., *Journal of the American Chemical Society* **1982,** *104*, (1), 313-15.

69. Kennard, C. H. L., *Inorganica Chimica Acta* **1967,** *1*, (2), 347-54.

70. Hertzberg, R. P.; Dervan, P. B., *Biochemistry* **1984,** *23*, (17), 3934-45.

71. Lin, S. B.; Blake, K. R.; Miller, P. S.; Ts'o, P. O., *Biochemistry* **1989,** *28*, (3), 1054-61.

72. Youngquist, R. S.; Dervan, P. B., *Journal of the American Chemical Society* **1985,** *107*, (19), 5528-9.

73. Wade, W. S.; Dervan, P. B., *Journal of the American Chemical Society* **1987,** *109*, (5), 1574-5.

74. Youngquist, R. S.; Dervan, P. B., *Journal of the American Chemical Society* **1987,** *109*, (24), 7564-6.

75. Sluka, J. P.; Horvath, S. J.; Bruist, M. F.; Simon, M. I.; Dervan, P. B., *Science* **1987,** *238*, (4830), 1129-32.

76. Schultz, P. G.; Dervan, P. B., *Journal of the American Chemical Society* **1983,** *105*, (26), 7748-50.

77. Umezawa, H.; Suhara, Y.; Takita, T.; Maeda, K., *The Journal of antibiotics* **1966,** *19*, (5), 210-5.

78. Umezawa, H.; Maeda, K.; Takeuchi, T.; Okami, Y., *The Journal of antibiotics* **1966,** *19*, (5), 200-9.

79. Umezawa, H., *Biomedicine* **1973,** *18*, (6), 459-75.

80. Umezawa, H., *Lloydia* **1977,** *40*, (1), 67-81.

81. Umezawa, H., *Pure and applied chemistry* **1971,** *28*, (4), 665-80.

82. Suzuki, H.; Nagai, K.; Yamaki, H.; Tanaka, N.; Umezawa, H., *The Journal of antibiotics* **1969,** *22*, (9), 446-8.

83. Ishida, R.; Takahashi, T., *Biochemical and Biophysical Research Communications* **1975,** *66*, (4), 1432-8.

84. Onishi, T.; Iwata, H.; Takagi, Y., *Journal of biochemistry* **1975,** *77*, (4), 745-52.

85. Sausville, E. A.; Peisach, J.; Horwitz, S. B., *Biochemical and biophysical research communications* **1976,** *73*, (3), 814-22.

86. Steighner, R. J.; Povirk, L. F., *Proceedings of the National Academy of Sciences of the United States of America* **1990,** *87*, (21), 8350-4.

87. Worth, L., Jr.; Frank, B. L.; Christner, D. F.; Absalon, M. J.; Stubbe, J.; Kozarich, J. W., *Biochemistry* **1993,** *32*, (10), 2601-9.

88. Shepherd, R. E.; Lomis, T. J.; Koepsel, R. R., *Journal of the Chemical Society, Chemical Communications* **1992**, (3), 222-4.

89. Burger, R. M.; Peisach, J.; Horwitz, S. B., *Journal of Biological Chemistry* **1981,** *256*, (22), 11636-44.

90. Burger, R. M., *Chemical Reviews* **1998,** *98*, (3), 1153-1169.

91. Burger, R. M.; Kent, T. A.; Horwitz, S. B.; Munck, E.; Peisach, J., *The Journal of biological chemistry* **1983,** *258*, (3), 1559-64.

92. Burger, R. M.; Horwitz, S. B.; Peisach, J.; Wittenberg, J. B., *The Journal of biological chemistry* **1979,** *254*, (24), 12999-302.

93. Kuramochi, H.; Takahashi, K.; Takita, T.; Umezawa, H., *The Journal of antibiotics* **1981,** *34*, (5), 576-82.

94. Burger, R. M.; Blanchard, J. S.; Horwitz, S. B.; Peisach, J., *The Journal of biological chemistry* **1985,** *260*, (29), 15406-9.

95. Sam, J. W.; Tang, X.-J.; Peisach, J., *Journal of the American Chemical Society* **1994,** *116*, (12), 5250-6.

96. Bickers, D. R.; Dixit, R.; Mukhtar, H., *Biochimica et biophysica acta* **1984,** *781*, (3), 265-72.

97. Ciriolo, M. R.; Magliozzo, R. S.; Peisach, J., *Journal of Biological Chemistry* **1987,** *262*, (13), 6290-5.

98. Ciriolo, M. R.; Peisach, J.; Magliozzo, R. S., *The Journal of biological chemistry* **1989,** *264*, (3), 1443-9.

99. Burger, R. M.; Tian, G.; Drlica, K., *Journal of the American Chemical Society* **1995,** *117*, (3), 1167-8.

100. Natrajan, A.; Hecht, S. M.; Van der Marel, G. A.; Van Boom, J. H., *Journal of the American Chemical Society* **1990,** *112*, (11), 4532-8.

101. Sigman, D. S.; Graham, D. R.; D'Aurora, V.; Stern, A. M., *The Journal of biological chemistry* **1979,** *254*, (24), 12269-72.

102. Gallagher, J.; Zelenko, O.; Walts, A. D.; Sigman, D. S., *Biochemistry* **1998,** *37*, (8), 2096-104.

103. Zelenko, O.; Gallagher, J.; Xu, Y.; Sigman, D. S., *Inorganic Chemistry* **1998,** *37*, (9), 2198-2204.

104. Milne, L.; Xu, Y.; Perrin, D. M.; Sigman, D. S., *Proceedings of the National Academy of Sciences of the United States of America* **2000,** *97*, (7), 3136-41.

105. Chen, C. B.; Milne, L.; Landgraf, R.; Perrin, D. M.; Sigman, D. S., *Chembiochem: a European journal of chemical biology* **2001,** *2*, (10), 735-40.

106. Que, B. G.; Downey, K. M.; So, A. G., *Biochemistry* **1980,** *19*, (26), 5987-91.

107. Yoon, C.; Kuwabara, M. D.; Law, R.; Wall, R.; Sigman, D. S., *The Journal of biological chemistry* **1988,** *263*, (17), 8458-63.

108. Pope, L. M.; Reich, K. A.; Graham, D. R.; Sigman, D. S., *Journal of Biological Chemistry* **1982,** *257*, (20), 12121-8.

109. Marshall, L. E.; Graham, D. R.; Reich, K. A.; Sigman, D. S., *Biochemistry* **1981,** *20*, (2), 244-50.

110. Kuwabara, M.; Yoon, C.; Goyne, T.; Thederahn, T.; Sigman, D. S., *Biochemistry* **1986,** *25*, (23), 7401-8.

111. Thederahn, T. B.; Kuwabara, M. D.; Larsen, T. A.; Sigman, D. S., *Journal of the American Chemical Society* **1989,** *111*, (13), 4941-6.

112. Williams, L. D.; Thivierge, J.; Goldberg, I. H., *Nucleic acids research* **1988,** *16*, (24), 11607-15.

113. Frey, S. T.; Sun, H. H. J.; Murthy, N. N.; Karlin, K. D., *Inorganica Chimica Acta* **1996,** *242*, (1-2), 329-38.

114. Humphreys, K. J.; Johnson, A. E.; Karlin, K. D.; Rokita, S. E., *Journal of Biological Inorganic Chemistry* **2002,** *7*, (7-8), 835-842.

115. Suh, M. P.; Han, M. Y.; Lee, J. H.; Min, K. S.; Hyeon, C., *Journal of the American Chemical Society* **1998,** *120*, (15), 3819-3820.

116. Yoo, C. E.; Chae, P. S.; Kim, J. E.; Jeong, E. J.; Suh, J., *Journal of the American Chemical Society* **2003,** *125*, (47), 14580-14589.

117. Bencini, A.; Berni, E.; Bianchi, A.; Giorgi, C.; Valtancoli, B.; Chand, D. K.; Schneider, H.-J., *Dalton Transactions* **2003**, (5), 793-800.

118. Sigman, D. S.; Kuwabara, M. D.; Chen, C. H. B.; Bruice, T. W., *Methods in Enzymology* **1991,** *208*, (Protein-DNA Interact.), 414-33.

119. Tu, C.; Shao, Y.; Gan, N.; Xu, Q.; Guo, Z., *Inorganic Chemistry* **2004,** *43*, (15), 4761-4766.

120. Gonzalez-Alvarez, M.; Alzuet, G.; Borras, J.; Pitie, M.; Meunier, B., *JBIC, Journal of Biological Inorganic Chemistry* **2003,** *8*, (6), 644-652.

121. Kim, J. H.; Kim, S. H., *Chemistry Letters* **2003,** *32*, (6), 490-491.

122. Thyagarajan, S.; Murthy, N. N.; Sarjeant, A. A. N.; Karlin, K. D.; Rokita, S. E., *Journal of the American Chemical Society* **2006,** *128*, (21), 7003-7008.

123. Lewis, E. A.; Tolman, W. B., *Chemical Reviews* **2004,** *104*, (2), 1047-1076.

124. Mirica, L. M.; Ottenwaelder, X.; Stack, T. D. P., *Chemical Reviews* **2004,** *104*, (2), 1013-1045.

125. Liang, H.-C.; Karlin, K. D.; Dyson, R.; Kaderli, S.; Jung, B.; Zuberbuehler, A. D., *Inorganic Chemistry* **2000,** *39*, (26), 5884-5894.

126. Karlin, K. D.; Ghosh, P.; Cruse, R. W.; Farooq, A.; Gultneh, Y.; Jacobson, R. R.; Blackburn, N. J.; Strange, R. W.; Zubieta, J., *Journal of the American Chemical Society* **1988,** *110*, (20), 6769-80.

127. Frelon, S.; Douki, T.; Favier, A.; Cadet, J., *Chemical Research in Toxicology* **2003,** *16*, (2), 191-197.

128. Zhang, C. X.; Liang, H.-C.; Kim, E.-i.; Shearer, J.; Helton, M. E.; Kim, E.; Kaderli, S.; Incarvito, C. D.; Zuberbuehler, A. D.; Rheingold, A. L.; Karlin, K. D., *Journal of the American Chemical Society* **2003,** *125*, (3), 634-635.

129. Zhang, C. X.; Kaderli, S.; Costas, M.; Kim, E.-i.; Neuhold, Y.-M.; Karlin, K. D.; Zuberbuehler, A. D., *Inorganic Chemistry* **2003,** *42*, (6), 1807-1824.

130. Henson, M. J.; Vance, M. A.; Zhang, C. X.; Liang, H.-C.; Karlin, K. D.; Solomon, E. I., *Journal of the American Chemical Society* **2003,** *125*, (17), 5186-5192.

131. Karlin, K. D.; Kaderli, S.; Zueberbuehler, A. D., *Accounts of Chemical Research* **1997,** *30*, (3), 139-147.

132. Li, B.; Gutierrez, P. L.; Blough, N. V., *Analytical Chemistry* **1997,** *69*, (21), 4295-4302.

133. Li, B.; Gutierrez, P. L.; Blough, N. V., *Methods in Enzymology* **1999,** *300*, (Oxidants and Antioxidants, Part B), 202-216.

134. Eberhardt, M. K.; Colina, R., *Journal of Organic Chemistry* **1988,** *53*, (5), 1071-4.

135. Oturan, M. A.; Pinson, J., *Journal of Physical Chemistry* **1995,** *99*, (38), 13948-54.

136. Perrin, D. M.; Hoang, V. M.; Xu, Y.; Mazumder, A.; Sigman, D. S., *Biochemistry* **1996,** *35*, (16), 5318-26.

137. Morrow, J. R.; Iranzo, O., *Current Opinion in Chemical Biology* **2004,** *8*, (2), 192-200.

138. Park, G.; Tomlinson, J. T.; Melvin, M. S.; Wright, M. W.; Day, C. S.; Manderville, R. A., *Organic Letters* **2003,** *5*, (2), 113-116.

139. Rodiguin, N. M.; Rodiguina, E. N., *Consecutive Chemical Reactions - Mathematical Analysis and Development*. D. Van Nostrand Company, Inc.: 1964; pp 6.

140. Stevens, G. C.; Clarke, R. M.; Hart, E. J., *Journal of Physical Chemistry* **1972,** *76*, (25), 3863-7.

141. Buxton, G. V.; Greenstock, C. L.; Helman, W. P.; Ross, A. B., *Journal of Physical and Chemical Reference Data* **1988,** *17*, (2), 513-886.

142. Di Iorio, E. E., *Methods in Enzymology* **1981,** *76*, (Hemoglobins), 57-72.

143. Ellman, G. L., *Archives of biochemistry and biophysics* **1959,** *82*, (1), 70-7.